

CONNECTING EXPERIMENT WITH THEORY: A MODEL-INDEPENDENT  
PARAMETERIZATION OF NEUTRINO OSCILLATIONS

By

Doris Jeanne Wagner

Dissertation

Submitted to the Faculty of the  
Graduate School of Vanderbilt University  
in partial fulfillment of the requirements  
for the degree of

DOCTOR OF PHILOSOPHY  
in  
PHYSICS

December 2018

Nashville, Tennessee

Approved:

---

---

---

---

---

---

---

---

---

Date:

---

---

---

---

---

---

---

---

---

© Copyright by Doris Jeanne Wagner 2018  
All Rights Reserved

## ACKNOWLEDGEMENTS

This dissertation is not due solely to my efforts. Its beginnings lie in a high school physics class taught by Yvonne Waters, one of the most energetic and inspiring teachers I have encountered. Were it not for her obvious love and enthusiasm for the subject, I would never have enrolled in a physics course in college. As my interest in the subject grew, it was nurtured by the wonderful physics faculty at the College of William and Mary, in particular, my undergraduate advisor, Marc Sher. At Vanderbilt, my research has been shaped and guided by my advisor, Tom “Prof” Weiler, whose insight, advice, and “Seinfeld” watching helped bring this thesis to its present state. My graduate career has been greatly enriched by his support and guidance, and I am deeply appreciative of the assistance he has provided. I would also like to thank Professors Webster and Kephart for the many times they have helped me straighten out a perplexing problem. The rest of my committee members, Professors Greiner, Waters, and Ernst, have all supported me and my work in many different ways. I would like to thank each one of the six gentlemen on my committee for their guidance and the faith in me and my abilities which they have repeatedly displayed. Many other Vanderbilt faculty, including Tonnis ter Veldhuis and Professors Pinkston, Brau, Arenstorf, and Umar, have helped me professionally and personally, and I am quite grateful for the role each has played in bringing me to this point.

My wonderful friends who shared my graduate experience have helped me keep my sanity and sense of perspective. Katrina Wagner has stood by my side through ups and downs too numerous to count. I would like to thank her for keeping me honest while solving physics problems, eating chocolate with me when I got frustrated, giving me advice on oh so many papers and talks, and just being a fantastic friend. I would like to thank Alan Calder for his friendship, computer advice, company studying for the qualifier, and perspective on gun control laws. He too provided moral support during stressful situations, and I am very grateful. I appreciate greatly the assistance supplied by Russ Kegley. Russ was never too busy to help others with homework problems, computer problems, research problems, or personal problems, and many of us at Vanderbilt are indebted to him. I would like to thank all of my other friends who supported and encouraged me through my graduate career: Don Lamb, Jerri Tribble, Vijaya Sankaran, Tom Ginter, Lei Shan, Sung-Hye Park, Julie Wendt, and the members of the young adult Sunday School classes at Belmont United Methodist Church.

I have also received much encouragement from my home church family, namely the Sharing Group and the entire congregation of St. Luke’s United Methodist Church. I know I have been in their thoughts and prayers throughout my twenty-two years of school, and I have frequently been encouraged by that knowledge. God has blessed me with so much, and I thank God for all of the gifts I have received. In particular, I thank God for giving me the abilities and perseverance necessary

to complete this dissertation, as well as giving me all these friends to support and encourage my endeavors.

I wish to thank my brothers, their wives, and my grandparents for their love and encouragement. And I would like to give special thanks to my nephews and nieces: Frederick, Bethany, Megan, and Richard Wagner. Knowing that these children look up to me has encouraged me to reach my goals and be the best role model I can. I thank them not only for the sense of purpose they provide, but for the joy and love they constantly bring to me. Lastly, but certainly not leastly, I thank my parents. I would not be where, or who, I am were it not for my parents, two of the most intelligent, loving, and Christian people I know. I cannot express how much I appreciate their unconditional support for everything I have done. They wisely held their tongues, even when I thought I wanted to be an accountant, and let me choose my own course. I therefore dedicate my thesis to them in honor of the support and inspiration they constantly provide.

CONNECTING EXPERIMENT WITH THEORY: A MODEL-INDEPENDENT  
PARAMETERIZATION OF NEUTRINO OSCILLATIONS

DORIS JEANNE WAGNER

Dissertation under the direction of Professor Thomas J. Weiler

Many experiments are currently looking for evidence of neutrino mass in the form of neutrino oscillations. Oscillation probabilities are non-linear functions of the neutrino mixing matrix elements, so most comparisons of data to theory are based on simplifying models of the mixing matrix. We begin this dissertation with a review of neutrino interactions and a few of the popular models describing neutrino masses and mixing. Next we present our model-independent description of neutrino oscillations and derive the predictions of various models in terms of our new “box” parameterization. Finally, we use our boxes to find mixing matrices consistent with existing neutrino data. As more definitive data becomes available, these solutions will probably need to be adjusted; when such a need arises, our box notation will provide a convenient method for finding new solutions.

Approved \_\_\_\_\_ Date \_\_\_\_\_

## TABLE OF CONTENTS

	Page
ACKNOWLEDGEMENTS . . . . .	iii
I. INTRODUCTION . . . . .	1
1.1 Some History . . . . .	2
1.2 Whence We Start: A Review of the Standard Model . . . . .	4
1.3 Whither We Go: The Changes Wrought By Neutrino Oscillations . . . . .	12
II. GIVING NEUTRINOS MASS . . . . .	13
2.1 The Differences Between Majorana and Dirac Neutrinos . . . . .	13
2.2 The Dirac Mass Term . . . . .	16
2.3 The Majorana Triplet Mass Term . . . . .	17
2.3.1 The Triplet Higgs . . . . .	18
2.3.2 Radiative Mass Terms and the Zee Model . . . . .	18
2.4 The Majorana Singlet Mass Term . . . . .	21
2.5 Putting Them All Together . . . . .	21
2.6 The See-Saw Model . . . . .	23
2.7 Mass States vs. Flavor States . . . . .	24
III. OSCILLATIONS . . . . .	28
3.1 The Equations of Motion . . . . .	28
3.2 Vacuum Oscillations . . . . .	31
3.2.1 Two-Way Oscillations . . . . .	34
3.2.2 Three-Way Oscillations . . . . .	34
3.3 Matter Effects . . . . .	36
IV. A NEW PARAMETERIZATION . . . . .	40
4.1 The Unmeasurables . . . . .	40
4.2 The Measurables . . . . .	42
4.2.1 Mixing Matrix Elements and Boxes . . . . .	46
4.2.2 Using Unitarity to Reduce the Number of Independent Boxes . . . . .	50
4.3 More Unmeasurables . . . . .	69
4.4 More Measurables . . . . .	73
V. APPLICATIONS OF THE BOXES TO SPECIFIC PHENOMENOLOGICAL MODELS	77
5.1 Models of the Mixing Matrix . . . . .	77
5.1.1 The Standard KM Parameterization . . . . .	77
5.1.2 The Wolfenstein Parameterization . . . . .	79
5.1.3 The One-Angle Approximation . . . . .	80
5.1.4 The Dominant Mass Scale Approximation . . . . .	81
5.2 Models of the Mass Matrix . . . . .	83
5.2.1 Using a Fritzsch Mass Matrix . . . . .	83
5.2.2 Using a Democratic Mass Matrix . . . . .	91
5.2.3 Using a Zee Mass Matrix . . . . .	94
VI. THE CONNECTION TO EXPERIMENT . . . . .	98
6.1 The Data . . . . .	98
6.2 Interpreting the Data . . . . .	104

6.3	Finding Solutions . . . . .	108
6.4	How Do Specific Models Stack Up? . . . . .	111
VII.	OUTLOOK . . . . .	113
Appendix		
A.	NOTATION KEY . . . . .	115
B.	THE DIRAC EQUATION, WAVE FUNCTIONS, AND TRANSFORMATIONS . . .	117
B.1	Gamma Matrices . . . . .	117
B.2	Neutrino Wave Functions . . . . .	118
B.3	Helicity, Chirality, Parity, and Parity Violation . . . . .	120
B.3.1	A Review of Handedness . . . . .	120
B.3.2	Parity Transformations . . . . .	123
B.3.3	Parity Violation in Weak Interactions . . . . .	125
B.4	Charge Conjugation . . . . .	126
C.	A MORE REALISTIC TREATMENT OF NEUTRINO OSCILLATIONS . . . . .	129
C.1	Neutrinos as Wave-Packets . . . . .	130
C.2	Neutrinos in a Relativistically Correct Light . . . . .	131
D.	NEUTRINOLESS DOUBLE-BETA DECAY . . . . .	135
E.	A GRAPHICAL REPRESENTATION OF BOXES . . . . .	138
REFERENCES . . . . .		141

## CHAPTER I

### INTRODUCTION

*Neutrinos, they are very small.*

*They have no charge and have no mass*

*And do not interact at all.*

*The earth is just a silly ball*

*To them, through which they simply pass,*

*Like dustmaids down a drafty hall*

*Or photons through a sheet of glass.*

*They snub the most exquisite gas,*

*Ignore the most substantial wall,*

*Cold-shoulder steel and sounding brass,*

*Insult the stallion in his stall,*

*And, scorning barriers of class,*

*Infiltrate you and me! Like tall*

*And painless guillotines, they fall*

*Down through our heads into the grass.*

*At night, they enter at Nepal*

*And pierce the lover and his lass*

*From underneath the bed – you call*

*It wonderful; I call it crass.*

- COSMIC GALL by John Updike <sup>1</sup>

Updike's description of the neutrino, while quite poetic, could use a bit of updating to be scientifically accurate. Neutrinos do travel great distances through matter before interacting, but to say they "do not interact at all" is incorrect. Bernstein, the author of reference [1], also considers

---

<sup>1</sup>From COLLECTED POEMS (Alfred A. Knopf). Reprinted by permission; ©1960 John Updike. Originally in *The New Yorker*. All rights reserved.

Updike's poem and suggests "And do not interact a lot . . ." is better science but worse poetry." But it is the claim of the poem's previous line that neutrinos "have no mass" which is addressed by my research. Bernstein happens to agree here with the poet, claiming that "most physicists would be willing to give high betting odds that the mass is exactly zero." Bernstein and Updike, however, were writing in the 1960s, and a few decades can change the prevailing views in science. No concrete experimental evidence of non-zero mass has yet been found, but the existence of massive neutrinos is currently favored on theoretical and indirect experimental grounds. In view of the prevailing scientific opinion, I suggest the following replacement for the first three lines of Updike's poem:

*Neutrinos, they are very small.*

*They have no charge and not much mass*

*And barely interact at all.*

This dissertation will present some of the consequences of non-zero neutrino mass and will develop a mechanism to connect the theoretical models with the potential results of experiments.

### 1.1 Some History

The early 20th century was a time of great change for physics. Driving much of that change was the discovery and study of nuclear decays. Beta decay, in which an atom changes atomic number and emits an electron, provided some puzzling results. The decrease in the atom's energy should be equal to the energy carried away by the electron. But not only was the energy of the emitted electron in a particular reaction usually less than the expected amount, it was different for each occurrence of the same reaction. Energy seemed to be randomly vanishing in beta decay! In 1929, Pauli suggested the existence of an undetected particle which carried away the missing energy [2], [3]. In retrospect, Pauli's solution may seem obvious. But physicists in the 1920s were not yet in the habit of postulating the existence of new particles to explain surprising results. Only the proton, the electron, and the photon had been discovered. The prejudice against new particles was so strong, Bohr preferred to discard energy conservation. He suggested that individual reactions need not conserve energy as long as energy was conserved on the average. Pauli hesitantly proposed

his “neutron” as a possible solution in 1927, and Fermi renamed it the neutrino when Chadwick discovered what we now call the neutron [3].

The existence of a chargeless, weakly-interacting fermion was generally accepted by the mid-1930s, but experimental confirmation of the neutrino’s existence did not arrive until the 1950s [4], [3]. Reines eventually shared the 1995 Nobel Prize in physics for this innovative experiment. Yet these elusive particles have continued to raise questions in the decades following their detection. Some of the questions which intrigue researchers today, such as whether neutrinos and antineutrinos are distinct particles, have reemerged many years after they appeared resolved. Other questions, such as the number of neutrino flavors in nature, and whether the neutrinos are massless, have never really gone away.

According to Pauli’s proposal, the neutrino and the electron share the energy lost by an atom in beta decay. The minimum energy given to the electron is proportional to its mass, and the minimum energy carried off by the neutrino should yield a measurement of the neutrino mass. But in some of the decays, the electron seemed to carry off all of the energy, leaving none for the neutrino. Thus Perrin commented in 1933 “that the neutrino has *zero intrinsic mass*, like the photon” [5], [3]. Yet experiments cannot demonstrate that the mass of a particle (even the photon) is precisely zero. They may merely place upper bounds on the mass. The bounds on the mass of Pauli’s “neutron” (known now as the electron antineutrino) from beta decay currently require this mass to be more than 50000 times smaller than the mass of an electron, or less than 10 eV. Fifty thousand times smaller than the electron mass may sound negligibly small, but the existence of even a tiny non-zero neutrino mass has profound effects. Nevertheless, a prevailing belief in massless neutrinos continued well into the 1960s, when the Standard Model of particle physics was developed. This enormously successful theory describing particle interactions requires neutrino masses to be exactly zero.

Starting in 1968 with the Homestake solar neutrino experiment [6], evidence has been building in favor of non-zero neutrino masses. The Homestake experiment counts the neutrinos coming from the sun, and the number it detects is far smaller than the number predicted by solar theory. This “solar neutrino deficit” has since been confirmed by four other experiments [7]. In addition, experiments measuring neutrinos produced in our atmosphere find an “anomaly” in the ratio of muon-type to electron-type neutrinos [8]. Both of these results could be explained by neutrino mass

through its quantum-mechanical implications. As for the Standard Model, it is not the “Theory of Everything” physicists view as their Holy Grail. Adding masses to neutrinos is a natural extension to the theory, requiring merely additional particle fields, without significant formal changes. These minimal changes to the theory, however, have profound physical results. As will be discussed below, non-zero neutrino mass may lead to mixing between different flavors of neutrinos and to oscillations of neutrino flavor. The mixings and oscillations resulting from neutrino mass could explain the currently puzzling solar neutrino deficit and atmospheric anomaly. Large-scale neutrino experiments hope to address these issues, and my work provides a model-independent path between the data from such experiments and the answers to the mysteries surrounding neutrinos.

## 1.2 Whence We Start: A Review of the Standard Model

The Standard Model describes the interactions of quarks, leptons, gauge fields, and a Higgs scalar. Quarks come in three generations of two quarks each: up and down, strange and charm, and top and bottom. Leptons too come in three generations: electron, muon, and tau. Each generation contains a negatively charged lepton and its associated neutral neutrino. Each quark and lepton has an associated antiparticle as well. The gauge fields include the photon, carrier of the electromagnetic force, the three vector bosons ( $W^+, W^-, Z^0$ ), carriers of the weak nuclear force, and eight colored gluons, carriers of the strong nuclear force. Of these particles, only the Higgs scalar and the tau neutrino have yet to be detected by experiments.

Experiments show that only the left-handed particles and right-handed antiparticles are affected by the charged weak nuclear force (see Appendix B.3.1 for a discussion on handedness, or helicity). This “maximal parity violation” by the charged weak interaction was discovered in 1957 by Wu, *et. al.* [9], [10], and it necessitates an asymmetry between right-handed and left-handed particles in the Standard Model. Left-handed particles, which participate in charged weak interactions, are placed in “isospin doublets.” Right-handed particles, which do not experience the charged weak force, compose “isospin singlets.”

The Lagrangian of a theory provides information on particle interactions. Each term in the Lagrangian describes either a kinetic energy, a mass, or an interaction. Fermion terms contain

at least one field with Dirac conjugation  $\bar{\psi}$  (defined in Appendix A), and one without,  $\psi'$ . The conjugated fields represent outgoing particles or incoming antiparticles; the unconjugated fields represent incoming particles or outgoing antiparticles. Each term in the Lagrangian must follow the known conservation laws. For example, electric charge seems to be conserved in nature, so the total incoming charge of any term in the Lagrangian should equal the outgoing charge. Isospin and its component in a chosen direction ( $I_3$ ) must be conserved, so the field with the positive  $I_3$  in an incoming isospin doublet (isospin  $\frac{1}{2}$ ) must couple to the field with the positive  $I_3$  in an outgoing isospin doublet. Fields in an incoming triplet (isospin 1) can couple to fields of another triplet or to two doublet fields. Singlets have isospin 0 and thus can couple to any term without affecting the isospin of that term.

Many of the sources listed in the bibliography of this paper contain reviews of the Standard Model. References [10] and [11] treat the Model in great detail, while references [12], [13], and [14] consider only the aspects of the Model relevant to neutrinos. We will synthesize these treatments in the summary which follows.

Neutrinos do not interact by either the strong nuclear force or the electromagnetic force, so we will ignore the terms in the Lagrangian corresponding to those forces. The terms of the Standard Model Lagrangian that are of interest to neutrino physics may be represented as follows:

$$\begin{aligned}
\mathcal{L}_{SM}^\nu &= \sum_{\alpha} \overline{\nu_{\alpha L}} i \gamma^\mu \partial_\mu \nu_{\alpha L} + \sum_{\alpha} \overline{\alpha_L} i \gamma^\mu \partial_\mu \alpha_L + \sum_{\alpha} \overline{\alpha_R} i \gamma^\mu \partial_\mu \alpha_R - \sum_{\alpha} \overline{\alpha_L} m_{\alpha} \alpha_R - \sum_{\alpha} \overline{\alpha_R} m_{\alpha} \alpha_L \\
&\quad - \frac{e}{c_W s_W} \mathbf{Z}_\mu \mathcal{J}_{NC}^\mu - \frac{e}{\sqrt{2} s_W} \left( \mathbf{W}_\mu^+ \mathcal{J}_{CC}^\mu + \mathbf{W}_\mu^- \mathcal{J}_{CC}^{\mu\dagger} \right), \text{ where} \\
\mathcal{J}_{NC}^\mu &= \sum_{\alpha} \left[ \frac{1}{2} \overline{\nu_{\alpha L}} \gamma^\mu \nu_{\alpha L} - \frac{1}{2} \overline{\alpha_L} \gamma^\mu \alpha_L + \sin^2 \theta_W (\overline{\alpha_L} \gamma^\mu \alpha_L + \overline{\alpha_R} \gamma^\mu \alpha_R) \right] \\
&= \frac{1}{2} \overline{\nu_L} \gamma^\mu \nu_L - \left( \frac{1}{2} - \sin^2 \theta_W \right) \overline{l_L} \gamma^\mu l_L + \sin^2 \theta_W \overline{l_R} \gamma^\mu l_R, \text{ and} \\
\mathcal{J}_{CC}^\mu &= \sum_{\alpha} \overline{\nu_{\alpha L}} \gamma^\mu \alpha_L = \overline{\nu_L} \gamma^\mu l_L.
\end{aligned} \tag{1}$$

Here  $\alpha_L$  is the field operator spinor (expressed in full in Appendix B.2) for the charged lepton for the neutrino spinor  $\nu_{\alpha L}$ , and  $\nu_L$  and  $l_L$  are the vectors containing all  $\nu_{\alpha L}$  and  $\alpha_L$ , respectively. The subscripts  $R$  and  $L$  indicated left- and right-handed particles, respectively (defined in Appendix B.3.1).  $\mathbf{Z}_\mu$ ,  $\mathbf{W}_\mu^+$ , and  $\mathbf{W}_\mu^-$  are the fields of the vector bosons.  $e$  is the dimensionless charge of the electron,

which equals the square root of the fine structure constant, and  $\theta_W$  is the Weinberg angle:

$$\cos^2 \theta_W = \frac{m_W^2}{m_Z^2}. \quad (2)$$

Appendices A and B.1 contain a list of conventions used in this paper and descriptions of the gamma-matrices.

The Standard Model Lagrangian contains mass terms for the charged leptons, but not for the neutrinos. Mass terms occur when right-handed particles couple to their left-handed partners, giving rise to terms of the form

$$\overline{\psi}_L m_\psi \psi_R, \quad (3)$$

where  $m_\psi$  is the mass of the fermion field  $\psi = \psi_L + \psi_R$ . In such a term, the outgoing left-handed field has isospin  $\frac{1}{2}$ , and the incoming right-handed term has isospin 0. We know most fermions have a mass, so any physical theory must include mass terms for electrons, quarks, etc., but these terms seem to violate isospin conservation. Higgs [15], drawing from the work of Goldstone, Guralnik, Hagen, Kibble, Lange, and many others [16], finally came up with a solution to this apparent paradox. Higgs' work was incorporated into the Standard Model by Weinberg.

In the Standard Model's "Higgs mechanism," particles obtain masses by interacting with a Higgs field, introduced to conserve isospin:

$$\mathcal{L}_{\phi l} = \sum_{\alpha, \beta} g_{\alpha \beta}^D \overline{\psi}_{\alpha L} \phi_D \beta_R + h.c. \quad (4)$$

$\phi_D$  is the Higgs doublet, responsible for giving charged leptons and down-type quarks their masses:

$$\phi_D = \begin{pmatrix} \phi_D^- \\ \phi_D^0 \end{pmatrix}, \quad (5)$$

$\psi_{\alpha L}$  is the left-handed lepton doublet of flavor  $\alpha$ :

$$\psi_{\alpha L} = \begin{pmatrix} \nu_{\alpha L} \\ \alpha_L \end{pmatrix}, \quad (6)$$

$\beta_R$  is the right-handed charged lepton of flavor  $\beta$ , and the  $g_{\alpha\beta}^D$  are coupling constants. Up-type quarks obtain masses in the Standard Model by coupling with the conjugate Higgs doublet [14]

$$\tilde{\phi}_D \equiv i\sigma_2\phi_D^* = \begin{pmatrix} \phi_D^{0*} \\ -\phi_D^{+*} \end{pmatrix}, \quad (7)$$

where  $\sigma_2$  is the second Pauli matrix as given in Appendix B.1.

The neutral Higgs field has all the quantum numbers of the vacuum, so it may obtain a “vacuum expectation value,” or VEV:

$$\langle\phi_D^0\rangle = \langle 0|\phi_D^0|0\rangle. \quad (8)$$

The charged Higgs field cannot obtain a VEV since the vacuum is electrically neutral, so the ground state of the Higgs doublet is

$$\langle\phi_D\rangle = \begin{pmatrix} 0 \\ \langle\phi_D^0\rangle \end{pmatrix}. \quad (9)$$

The Higgs field is dynamical, so we include a term representing the deviation from the vacuum value and arrive at our final form for the Higgs doublet:

$$\phi_D^{SM} = \begin{pmatrix} 0 \\ \langle\phi_D^0\rangle + \frac{H^0(x)}{\sqrt{2}} \end{pmatrix}. \quad (10)$$

$H^0(x)$  is the massive Higgs scalar, and the VEV  $\langle\phi_D^0\rangle$  gives mass to particles through interactions such as

$$g_{\alpha\beta}^D \overline{\alpha_L} \langle\phi_D^0\rangle \beta_R \equiv \overline{\alpha_L} M_{\alpha\beta} \beta_R. \quad (11)$$

Because these terms involving the VEV do not conserve isospin, but the original interactions in equation (4) do, the Higgs mechanism *spontaneously breaks* the SU(2) symmetry in the ground state. The extra fields present in the original Higgs doublet (5) do not simply vanish in the symmetry breaking; they are transformed into extra spin states of the vector bosons. Such a discussion is irrelevant to the focus of this paper, but the interested reader can consult the sources [17] or [18] for more information.

In the Standard Model, the charged lepton mass matrix is diagonal,  $M_{\alpha\beta} = m_\alpha \delta_{\alpha\beta}$ , and mass terms for neutrinos do not arise because the Model has no right-handed singlet neutrino fields to participate in the coupling of equation (4). We will examine the consequences of the addition of a neutrino mass term in Chapter II.

The Lagrangian in equation (1) does not explicitly display terms involving the right-handed antineutrino fields  $\bar{\nu}_R \equiv C\bar{\nu}_L^T$ , where  $C$  is the charge-conjugation operator, discussed in Appendix B.4. These fields are CP-conjugates of the neutrino fields  $\nu_L$ .<sup>2</sup> The Lagrangian does, however, contain antiparticle fields implicitly.  $\mathcal{L}_{SM}^\nu$  above is CP-invariant, so if you replace the particles in equation (1) with their CP-conjugates, you get the same terms as you started with. Take, for example, a kinetic term for antineutrinos  $\bar{\nu}_R \gamma^\mu \partial_\mu \bar{\nu}_R$ :

$$\bar{\nu}_R \gamma^\mu \partial_\mu \bar{\nu}_R = \overline{C\bar{\nu}_L^T} \gamma^\mu \partial_\mu C\bar{\nu}_L^T = (\gamma^0 \nu_L)^T C^\dagger \gamma^0 \gamma^\mu C \partial_\mu \bar{\nu}_L^T. \quad (12)$$

The term in equation (12) is a number, so it is equal to its transpose:

$$(\gamma^0 \nu_L)^T C^\dagger \gamma^0 \gamma^\mu \partial_\mu C \bar{\nu}_L^T = -(\partial_\mu \bar{\nu}_L^T) C \gamma^{\mu T} \gamma^0 C^{-1} \gamma^0 \nu_L, \quad (13)$$

where we have added the minus sign because we switched the order of two fermion fields  $\nu_L$  and  $\nu_L^\dagger$ ,<sup>3</sup> and we have used the relations (421) from Appendix B.4. The operator  $C$  anticommutes with  $\gamma^0$ , and  $C\gamma^{\mu T}C^{-1} = -\gamma^\mu$ , so

$$\bar{\nu}_R \gamma^\mu \partial_\mu \bar{\nu}_R = -(\partial_\mu \bar{\nu}_L^T) \gamma^\mu \nu_L. \quad (14)$$

The last step is to bring the partial derivative  $\partial_\mu$  to the right of the spinor  $\bar{\nu}_L$ . We may do this by remembering that  $\mathcal{L}_{SM}^\nu$  is a Lagrangian *density* and thus always appears in an integral. We may

---

<sup>2</sup> The term antineutrino can be a bit confusing, since the charge-conjugate neutrino field is different from the physical CPT-conjugate antineutrino field. These subtleties are discussed in Appendix B.4

<sup>3</sup> When taking the transpose of a product of fermion fields, it is necessary to account for the anticommutation of those fields, so  $(\psi_1 \psi_2)^T = -\psi_2^T \psi_1^T$  if  $\psi_1$  and  $\psi_2$  are fermions. When taking the hermitian conjugate, however, no minus sign appears:  $(\psi_1 \psi_2)^\dagger = \psi_2^\dagger \psi_1^\dagger$ . The hermitian conjugate of a product is defined by the previous expression, and the anticommutator is never taken. Consider the number operator  $N = a^\dagger a$  from quantum mechanics, which must be hermitian since it is observable:  $N^\dagger = N$ , so  $(a^\dagger a)^\dagger$  must equal  $a^\dagger a$ , and not  $-a^\dagger a$ .

therefore use the technique of integrating by parts to obtain

$$-(\partial_\mu \bar{\nu}_L) \gamma^\mu \nu_L = -(\partial_\mu \bar{\nu}_L \gamma^\mu \nu_L) + \bar{\nu}_L \gamma^\mu \partial_\mu \nu_L, \quad (15)$$

where we have moved the partial derivative through the coordinate-independent  $\gamma^\mu$  in the second term. The first term on the right-hand side of equation (15) becomes a surface term and vanishes for integrals over all space-time. So we are left with

$$\bar{\nu}_R \gamma^\mu \partial_\mu \nu_R = -(\partial_\mu \bar{\nu}_L) \gamma^\mu \nu_L = \bar{\nu}_L \gamma^\mu \partial_\mu \nu_L, \quad (16)$$

which shows the kinetic term is invariant under CP-conjugation.

The CP-invariance of the weak current terms in  $\mathcal{L}_{SM}^\nu$  may be shown by a similar treatment, realizing that under a parity transformation, the vector field becomes its negative, so under CP,  $Z \rightarrow -Z$ , and  $W^\pm \rightarrow -W^\mp$ . The neutral current term, like the kinetic term, becomes itself. The  $W^+$  term becomes the  $W^-$  term, and vice versa:

$$\begin{aligned} (W_\mu^+ \bar{\nu}_L \gamma^\mu l_L + W_\mu^- \bar{l}_L \gamma^\mu \nu_L)^\dagger &= (W_\mu^{+\text{op}} \bar{\nu}_R \gamma^\mu l_R + (W_\mu^-)^{\text{op}} \bar{l}_R \gamma^\mu \nu_R) \\ &= -W_\mu^- (-\nu_L^T C^\dagger) \gamma^\mu C \bar{l}_L^T - W^+ (-l_L^T C^\dagger) \gamma^\mu C \bar{\nu}_L^T \\ &= -W_\mu^- \bar{l}_L^T C^T \gamma^{\mu T} C^{\dagger T} \nu_L - W_\mu^+ \bar{\nu}_L^T C^T \gamma^{\mu T} C^{\dagger T} l_L \\ &= W_\mu^- \bar{l}_L \gamma^\mu \nu_L + W_\mu^+ \bar{\nu}_L \gamma^\mu l_L. \end{aligned} \quad (17)$$

where we have used equation (426) from Appendix B.4 to substitute for  $\bar{\nu}_R$ , we have obtained a minus sign by switching the order of fermion fields in taking the transpose as before, and we have again used the properties of  $C$  given in equation (421) in the Appendix. The charged lepton mass terms also swap under CP,

$$\begin{aligned} \bar{\alpha}_R m_\alpha \delta_L + \bar{\alpha}_L m_\alpha \delta_R &= -\alpha_L^T C^\dagger m_\alpha C \bar{\alpha}_R^T - \alpha_R^T C^\dagger m_\alpha C \bar{\alpha}_L^T \\ &= \bar{\alpha}_R^T C^T C^{\dagger T} m_\alpha \alpha_L + \bar{\alpha}_L^T C^T C^{\dagger T} m_\alpha \alpha_R = \bar{\alpha}_R m_\alpha \alpha_L + \bar{\alpha}_L m_\alpha \alpha_R, \end{aligned} \quad (18)$$

so the entire  $\mathcal{L}_{SM}^\nu$  is invariant under a CP transformation; including separate terms for antiparticles would be redundant. In fact, the CP-invariance of the Lagrangian tells us that the antiparticle states are already contained in the particle spinors.

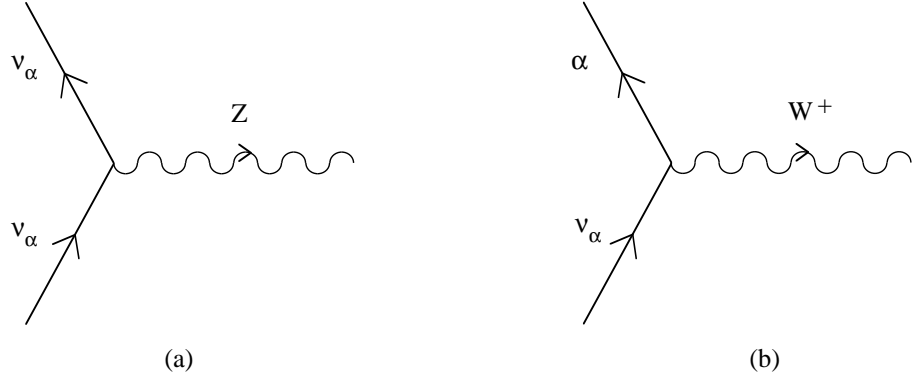


**Figure 1:** Feynman diagrams of neutrino vertices for the (a) neutral current, and (b) charged current.

Terms in the Lagrangian describe single vertices, such as those shown in Figure 1. But many physical processes, such as neutrino-electron scattering, consist of two vertices, as shown in Figure 2. So the matrix element for the charged current interaction shown in Figure 2a has the form [11]

$$\frac{e^2}{2 \sin^2 \theta_W} \mathbf{W}_\mu^+ \mathcal{J}_{CC}^\mu \mathbf{W}^{-\sigma} \mathcal{J}_{CC\sigma}^\dagger. \quad (19)$$

As before,  $e$  is defined in Appendix A and is only equal to the magnitude of the electron charge when  $\hbar = c = 1$ . A similar term occurs for the neutral current scattering in Figure 2b. If the momentum transferred by the W boson in Figure 2a is small compared to the mass of the boson, then the propagator for the boson collapses into  $\frac{-g_{\mu\nu}}{m_W^2}$  [11], and the interaction looks like Fermi's four-fermion coupling illustrated in Figure 3. The resulting matrix element displays the low-energy symmetries of a Lagrangian and provides the same analytic results for the S-matrix as the second order term in equation (19) when the momentum transferred by the boson is much less than the mass of the boson [11]. Together with the appropriate neutral-current terms, this matrix element is

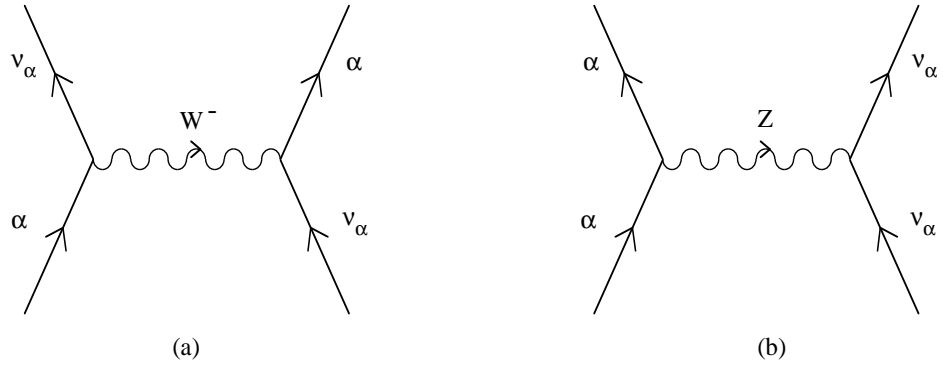


**Figure 2:** Feynman diagrams for (a) charged current  $\alpha - \nu_\alpha$  scattering, and (b) neutral current  $\alpha - \nu_\alpha$  scattering.

known as the “effective Lagrangian”:

$$\mathcal{L}_{eff} = -\frac{4G}{\sqrt{2}} \left( \mathcal{J}_{NC}^\mu \mathcal{J}_{NC\mu} + \mathcal{J}_{CC}^\mu \mathcal{J}_{CC\mu}^\dagger \right). \quad (20)$$

$G$  is the Fermi constant, and may be found by comparing equations (20) and (19) and substituting  $-\frac{1}{m_W^2} g_{\mu\sigma}$  for the product of  $\mathbf{W}$  fields:

$$G = \sqrt{2} \frac{e^2}{8m_W^2 \sin^2 \theta_W}. \quad (21)$$

The effective Lagrangian has the same form as Fermi’s four-fermion coupling; this particular effective

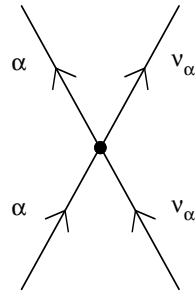


**Figure 3:** A Feynman diagram for the Fermi four-fermion neutrino scattering

Lagrangian for electron-neutrino scattering is responsible for matter-induced oscillations for massive neutrinos, as will be discussed in Section 3.3.

### 1.3 Whither We Go: The Changes Wrought By Neutrino Oscillations

The Standard Model contains only left-handed isospin  $\frac{1}{2}$  neutrinos and one Higgs doublet, so it allows no neutrino mass terms. As mentioned above, the neutrino mass was thought to be exactly zero in the 1960s, when Updike wrote his poem, and the Standard Model was developed during this same period. The Model, like the poem, reflects the prevailing views of its time and therefore yields a neutrino mass of zero. In the last thirty years, however, both the solar neutrino deficit and the atmospheric neutrino anomaly have surfaced. Experiments counting neutrinos from the sun see far fewer electron neutrinos than theory predicts, and experiments measuring neutrinos created in the atmosphere measure a muon-type-to-electron-type-neutrino ratio much smaller than expected. These surprising experimental results may be explained by making neutrino masses unequal and therefore not all zero. Non-zero neutrino mass is now preferred for symmetry reasons as well. Every fermion but the neutrino in the Standard Model has a right-handed singlet state and thus a mass, so the absence of right-handed neutrinos in the Standard Model seems unnatural and rather arbitrary to those who seek consistency in nature. Most extensions of the Standard Model, including Grand Unified Theories not based on an SU(5) symmetry, give the neutrinos mass. Some of the mechanisms by which neutrino mass may appear are discussed in Chapter II. The existence of mass terms in the neutrino Lagrangian may lead to neutrino oscillations between flavor states, as presented in Chapter III. Chapter IV develops a parameterization to describe neutrino oscillations which is independent of the model used to generate neutrino mass. This parameterization is then used to describe the predictions of many popular neutrino mass models (Chapter V) The predictions are compared to the existing neutrino oscillation data in Chapter VI. Chapter VII examines some of the implications of neutrino mass and oscillations and addresses the exciting future for this field of study.

## CHAPTER II

### GIVING NEUTRINOS MASS

The Lagrangian in equation (1) does not contain a neutrino mass term. Masses of fermions arise in the Standard Model through the coupling of the fermion with a Higgs scalar doublet, as described in Section 1.2. The Higgs doublet interacting with fermions such as the electron has isospin  $\frac{1}{2}$ , and it couples an isospin  $\frac{1}{2}$  state with an isospin singlet. Such interactions flip the helicity of the fermion involved, so both a right- and a left-handed state of each massive fermion are necessary in the Standard Model. This type of interaction is described by a Dirac mass term. Neutrinos may acquire a Dirac mass simply by adding a right-handed neutrino (and a left-handed antineutrino) to the Standard Model. Right-handed neutrinos do not participate in the charged weak interaction and are therefore dubbed “sterile”. In this work, sterile neutrinos will be denoted by  $N_R$  as in [19], while the active neutrinos will be represented by the traditional  $\nu_L$ . The associated helicity states of the CP-conjugate antineutrino will be given by  $\bar{\nu}_R$  and  $\bar{N}_L$ .<sup>1</sup>

Because neutrinos are neutral, they may obtain mass by an additional method. Unlike charged particles, whose particle and antiparticle states differ by the sign of the charge, neutrinos may be their own antiparticle, like the photon is. This type of fermion is known as a Majorana particle, after the physicist who first examined the possibility and ramifications of a self-conjugate fermion [20]. If neutrinos are Majorana particles, they could form a mass term from the left-handed  $\nu_L$  and the right-handed  $\bar{\nu}_R$ . Such a combination has isospin 1, so Majorana mass terms must be generated by a triplet Higgs interaction, which would be an addition to the Standard Model.

#### 2.1 The Differences Between Majorana and Dirac Neutrinos

Two different types of neutrino states have been experimentally observed:  $\nu_L$  and its CP-conjugate  $\bar{\nu}_R$ . The Dirac mass term introduces the right-handed neutrino  $N_R$  and its CP-conjugate

---

<sup>1</sup> I prefer  $N_R$  rather than the more apparent  $\nu_R$  to represent the right-handed component for two reasons: it clearly distinguishes active from sterile neutrinos, and it avoids confusion between  $\bar{\nu}_R$  and  $(\bar{\nu})_R = \bar{N}_L$ . In my notation, the former is denoted  $\bar{N}_R$ , which is clearly different from the latter.

$N_L$ , and has the form

$$\mathcal{L}_{Dirac} = - \left( \overline{\nu_L} M_D N_R + \overline{N_R} M_D^\dagger \nu_L \right). \quad (22)$$

As discussed in Section 1.2, terms with the antiparticles  $\nu_R$  and  $N_L$  are redundant and therefore not explicitly written. A Lorentz boost or spin flip will transform  $\nu_L$  to  $N_R$  and  $\nu_R$  to  $N_L$ , as shown in Figure 4a, which is adapted from reference [21]. CP conjugation, however, transforms  $\nu_L$  to  $\nu_R$  and  $N_R$  to  $N_L$ , as discussed in Appendix B.4, so four distinct neutrino states are necessary for Dirac mass terms.



**Figure 4:** A pictorial representation of the relationships between neutrino states for a) Dirac mass terms, and b) Majorana mass terms.

Majorana neutrinos, however, are self-conjugate, so the sterile states are not necessary [21], [14]:

$$\psi_{(maj)}(x) = C\gamma_0\psi_{(maj)}^*(x) = e^{i\theta}\psi_{(maj)}(x), \quad (23)$$

where  $C$  is the charge-conjugation operator. Acting on a Majorana field with CP only changes the phase of the field and takes one helicity state into the other, so it has the same effect as boosting the state, as illustrated in Figure 4b. Thus only two distinct neutrino states are necessary for Majorana mass terms.

Majorana mass terms have the general form

$$\overline{\psi_R} M_M \psi_L + \overline{\psi_L} M_M^\dagger \psi_R. \quad (24)$$

Because the Majorana field is self-conjugate, its mass matrix  $M_M$  is symmetric and so may be diagonalized by a transformation involving only one unitary matrix, as we will show. Following the

treatment found in reference [14], we set the Lagrangian in equation (24) equal to its transpose, which is allowed since the Lagrangian is a scalar:

$$\overline{\psi_R} M_M \psi_L + h.c. = (\overline{\psi_R} M_M \psi_L + h.c.)^T = - \left( \psi_L^T M_M^T \overline{\psi_R}^T \right) + h.c., \quad (25)$$

where the minus sign comes from swapping the order of fermion fields. Using the definitions of Dirac conjugates found in Appendix A, the Majorana condition (23), and the expression (425) for  $\overline{\psi_{L,R}}$  derived in Appendix B.4, we find

$$\overline{\psi_R} M_M \psi_L + h.c. = - \left( \psi_L^T M_M^T (-\psi_L^T C^\dagger)^T \right) + h.c. = \psi_L^T M_M^T C^{\dagger T} \psi_L + h.c. \quad (26)$$

$$= \psi_L^T (-C^\dagger) M_M^T \psi_L + h.c. = \overline{\psi_R} M_M^T \psi_L + h.c. \quad (27)$$

For the first expression to equal the last,  $M_M$  must be symmetric.

Still following the treatment of source [14], we remember that an arbitrary square matrix  $M$  is diagonalized by a biunitary rotation:

$$D = V^\dagger M U, \quad \text{or} \quad (28)$$

$$M = V D U^\dagger, \quad (29)$$

with  $D$  diagonal and  $V$  and  $U$  unitary. For a symmetric matrix,  $M_M = M_M^T$ , so

$$M_M M_M^\dagger = M_M^T M_M^{\dagger T}. \quad (30)$$

Using equation (29), we find

$$V D U^\dagger (V D U^\dagger)^\dagger = (V D U^\dagger)^T (V D U^\dagger)^{\dagger T}, \quad \text{so} \quad (31)$$

$$V D U^\dagger U D^\dagger V^\dagger = V D^2 V^\dagger = U^{\dagger T} D^T V^T V^{\dagger T} D^{\dagger T} U^T = U^{\dagger T} D^2 U^T. \quad (32)$$

Thus, multiplying by  $U^T$  on the left and  $V$  on the right,

$$U^T V D^2 = D^2 U^T V. \quad (33)$$

Since the matrix  $U^T V$  commutes with the matrix  $D^2$ , they must be simultaneously diagonalizable.  $D^2$  is already diagonalized, so  $U^T V$  must be diagonal too. A diagonal unitary matrix has the form of a diagonal matrix of phases,  $X$ , so

$$U^T V = X, \quad \text{with} \quad X_{ij} = \delta_{ij} e^{i\xi_i}. \quad (34)$$

We may define a new matrix  $V'$  which incorporates the phases of  $X$ :

$$V' = V X^\dagger, \quad (35)$$

giving  $U^T V' = \mathbb{1}$ . We may thus diagonalize  $M_M$  with the single matrix  $U$  and its transpose  $V'^\dagger = U^T$ :

$$D = V^\dagger M_M U = X^\dagger V'^\dagger M_M U, \quad \text{so} \quad (36)$$

$$U^T M_M U = X D, \quad (37)$$

which is diagonal, as claimed above.

## 2.2 The Dirac Mass Term

The Dirac mass term couples left-handed active neutrinos with their right-handed sterile partners through an interaction with the same Higgs doublet which gives mass to up-type quarks in the Standard Model.

$$\mathcal{L}_{Dirac} = - \sum_{\alpha, \beta} g_{\alpha\beta}^{D'} \overline{\psi_{\alpha L}} \tilde{\phi}_D N_{\beta R} + h.c., \quad (38)$$

with  $\psi_{\alpha L}$  and  $\tilde{\phi}_D$  defined in equations (6) and (7), respectively, and  $g_{\alpha\beta}^{D'}$  the Higgs-doublet coupling constants for the neutrino sector. Once the symmetry is broken, the Lagrangian term in equation

(38) contains a mass term of the form

$$\mathcal{L}_{Dirac} = - \sum_{\alpha, \beta} \overline{\nu_{\alpha L}} M_{\alpha \beta} N_{\beta R} + h.c. \quad (39)$$

The mass matrix  $M_D$  contains all of the coupling constants:

$$M_{D_{\alpha \beta}} = g_{\alpha \beta}^{D'} \langle \phi_D^0 \rangle. \quad (40)$$

This type of mass term is analogous to the quark mass terms and requires only the addition of sterile neutrinos to the Standard Model. Generating small neutrino masses by such a term would require the Yukawa coupling between the Higgs and the neutrinos to be many orders of magnitude smaller than the similar coupling between the Higgs and the quarks. While this difference of coupling constants may indeed exist, no ready explanation for the difference of scale has been suggested. This unexplained lack of symmetry is unattractive, so other mechanisms for generating neutrino masses have been proposed.

### 2.3 The Majorana Triplet Mass Term

If neutrinos possess a Majorana nature, no sterile neutrinos are necessary to produce a non-zero neutrino mass. The Majorana triplet mass term couples active left-handed neutrinos to their CP-conjugate right-handed partners as follows:

$$\mathcal{L}_{Triplet} = -\frac{1}{2} \left( \overline{\nu_L} M_T \nu_R + \overline{\nu_R} M_T^\dagger \nu_L \right). \quad (41)$$

Because both  $\nu_L$  and  $\nu_R$  have  $I_3$  of  $+\frac{1}{2}$ , the third component of isospin changes by one unit in such a term. An SU(2) triplet operator is therefore needed to conserve isospin. Such an operator may be a single object such as a Higgs triplet or a combination of objects yielding a single, isospin 1 “effective” operator.

### 2.3.1 The Triplet Higgs

Gelmini and Roncadelli [22] proposed a model using a triplet Higgs  $\phi_T$  with a Lagrangian given by

$$\mathcal{L}_{Triplet} = - \sum_{\alpha, \beta} g_{\alpha\beta}^{T'} \begin{pmatrix} \overline{\alpha}_R & \overline{\nu}_{\alpha R} \end{pmatrix} \begin{pmatrix} \phi_T^+ & \sqrt{2}\phi_T^{++} \\ -\sqrt{2}\phi_T^0 & \phi_T^+ \end{pmatrix} \begin{pmatrix} \nu_{\beta L} \\ \beta_L \end{pmatrix} + h.c. \quad (42)$$

The neutrino mass matrix in this model is

$$M_{T\alpha\beta}^\dagger = -2\sqrt{2}g_{\alpha\beta}^{T'} \langle \phi_T^0 \rangle, \quad (43)$$

and the charged leptons do not obtain any mass contribution from the triplet since they do not couple to the neutral Higgs triplet field. To conserve total lepton number before symmetry breaking, the Gelmini-Roncadelli model assigns a lepton charge of 2 to the Higgs triplet. When SU(2) symmetry is broken, lepton-number symmetry is broken as well, resulting in the formation of an additional Goldstone boson, the Majoron. This Majoron obtains a mass far smaller than the mass of the Z boson, so it provides new final states affecting the measured value of the Z-decay width. Such an effect contradicts experimental measurements of the width, so the Gelmini-Roncadelli triplet model with a lepton-number-conserving Lagrangian has been ruled out [14], [13].

All is not lost, however, for the Higgs triplet model. If lepton number is not conserved by the mass terms, the masses of the physical Higgs particles produced have no upper bound [14]. Thus the Higgs triplet remains a viable possibility for generation of Majorana neutrino masses without the addition of sterile neutrinos, but at the cost of introducing new Higgs particles and abandoning lepton number conservation entirely. We shall not concern ourself further with this model, but the interested reader may consult sources [14], [22], [23], and [13].

### 2.3.2 Radiative Mass Terms and the Zee Model

Additional mechanisms for generating neutrino masses exist at the one-loop level. Masses generated by such a mechanism are called “radiative masses.” One of the best-known radiative models using additional Higgs fields was proposed by Zee [24] (for discussions of the Zee model, see also [25], [26], [14], [27], and [12]). Zee’s model in its simplest form uses only two Higgs doublets,  $\phi_a$

and  $\phi_b$ , and a charged singlet Higgs field  $h$ . Such a singlet arises naturally from the simplest SU(5) theories, and it interacts with lepton doublets and Higgs doublets, but not quark fields [24]. The scalar  $h$  may be given lepton number  $-2$ , so its interactions with the lepton fields

$$\mathcal{L}_{h\psi_L} = f^{\alpha\beta} \left( \psi_{\alpha L}^i C \psi_{\beta L}^j \right) \epsilon_{ij} h + h.c. \quad (44)$$

conserves lepton number.<sup>2</sup> Here  $\psi_{\alpha L}$  is the left-handed lepton doublet of flavor  $\alpha$ , containing both neutrinos and charged leptons.  $i$  and  $j$  represent the SU(2) index:  $\psi_{\alpha L}^1 = \nu_{\alpha L}$ , and  $\psi_{\alpha L}^2 = \alpha_L$  [24].  $\epsilon_{ij}$  is of course the antisymmetric tensor, and  $C$  is the charge-conjugation operator. The coupling constant  $f^{\alpha\beta}$  must be antisymmetric because of Fermi statistics; interchanging two fermion spinors must change the overall sign of any fermion coupling, so

$$f^{\alpha\beta} \left( \psi_{\alpha L}^i C \psi_{\beta L}^j \right) \epsilon_{ij} h = -f^{\beta\alpha} \left( \psi_{\beta L}^j C \psi_{\alpha L}^i \right) \epsilon_{ji} h. \quad (45)$$

Obtaining the left-hand side from the right-hand side involves swapping the order of two fermion fields, which provides one sign change; swapping the indices of the antisymmetric tensor, thereby providing a second sign change; and swapping the order of the indices of the coupling  $f^{\alpha\beta}$ . The coupling must therefore be antisymmetric in its indices to arrive at the required overall sign change.

The coupling between the charged scalar  $h$  and the doublets  $\phi_n$  takes the form [24]

$$\mathcal{L}_{h\phi} = M_{ab} \epsilon_{ij} \phi_a^i \phi_b^j h + h.c. \quad (46)$$

The  $\epsilon_{ij}$  couples the doublets to conserve  $I_3$ . This interaction violates lepton number by  $-2$ . Most treatments of the Zee model [12], [14], [25], [27], treat only the simplest case, in which only one of the Higgs doublets  $\phi_a$  couples to leptons, and then only diagonally in isospin space:

$$\mathcal{L}_{\phi\beta} = \sum_{\beta} g_{\alpha\beta}^{D'} \overline{\psi_{\beta L}^i} \beta_R \phi_a^i + h.c. \quad (47)$$

---

<sup>2</sup>Reference [24] incorrectly states that individual lepton numbers  $L_e$ ,  $L_{\mu}$ , and  $L_{\tau}$  are conserved by this term. Only the total lepton number  $L = L_e + L_{\mu} + L_{\tau}$  is conserved by the Zee interaction. Zee corrects this misstatement in his later work [28].

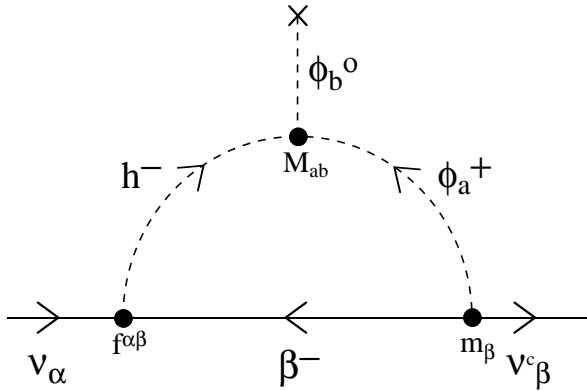


**Figure 5:** A Feynman diagram for the Zee model. The arrows denote the direction of the flow of the quantum numbers associated with the given particle. Charge is conserved at each vertex, but lepton number is not conserved at the top Higgs-Higgs interaction vertex.

None of the interactions (44), (46), or (47) alone will give the neutrino a mass, but the combination of these three terms at the one-loop level as shown in Figure 5 produces a Majorana mass term for the neutrino. The neutrino mass term under this Zee model ultimately has the form of equation (41) [27]:

$$-\mathcal{L}_\nu^{eff} = \frac{1}{2} \sum_{\alpha, \beta} \overline{\nu}_{R\alpha} M_{\alpha\beta}^{Zee} \nu_{L\beta} + h.c., \quad \text{with} \quad (48)$$

$$M_{\alpha\beta}^{Zee} = 2g_{\alpha\beta}^{Zee} (m_\alpha^2 - m_\beta^2). \quad (49)$$

$g_{\alpha\beta}^{Zee}$  is a complicated function of Higgs masses and Standard Model parameters. An expression for it may be found in reference [27], but it is not necessary for our purposes. Because the mass term in equation (48) is a Majorana term, the matrix  $M_{\alpha\beta}$  in equation (49) must be symmetric, so  $g_{\alpha\beta}^{Zee} = -g_{\beta\alpha}^{Zee}$ . The observant reader may note that the diagonal entries  $M_{\alpha\alpha}$  are therefore equal to zero.

As mentioned above, the assumption that the lepton-Higgs doublet coupling has the diagonal form (47) is generally, but not always, made. Zee himself did not make this simplification in reference [24], and the authors of [29] have chosen a different Zee model to present. The mass matrix in reference [29] is “motivated by the empirical hierarchy in the [quark mixing] matrix,” and has the

approximate form

$$M_{\alpha\beta} \approx \frac{m_\tau}{m_h} A \begin{pmatrix} \epsilon^3 & \epsilon^2 & \epsilon \\ \epsilon^2 & \epsilon & 1 \\ \epsilon & 1 & 0 \end{pmatrix}. \quad (50)$$

This alternative form has its virtues, but for the rest of this paper we will consider only the form (49), remembering that it is merely the simplest, rather than the only, possibility for a mass term generated according to the Zee model.

#### 2.4 The Majorana Singlet Mass Term

The sterile neutrinos  $N_R$ , being isospin singlets, may obtain a Majorana mass without Higgs fields. Such a “bare mass” term has the form

$$\mathcal{L}_{Singlet} = -\frac{1}{2} \left( \overline{N_L} M_S N_R + \overline{N_R} M_S^\dagger N_L \right). \quad (51)$$

This term is explicitly SU(2)-invariant, so it may be included in the overall Lagrangian before symmetry breaking. Such a term may also be generated by interactions with a Higgs singlet, but the use of such an extra Higgs is not necessary. The singlet mass term does not generate any type of mass for the active neutrinos and thus is somewhat uninteresting on its own, but it is possible in models with right-handed neutrinos and so it must be included in any full treatment of neutrino mass possibilities.

#### 2.5 Putting Them All Together

Dirac terms and Majorana terms are not mutually exclusive, and mass terms of all three types (22), (41), and (51) may occur simultaneously. We may also add additional sterile neutrinos  $\chi_{\eta R}$  which do not have active counterparts. These additional neutrinos may be Majorana or Dirac particles. In the most general case, we can have  $n_L$  flavors of active neutrinos  $\nu_{\alpha L}$ ,  $n_R$  flavors of their right-handed sterile partners  $N_{\beta R}$ , and  $n_\chi$  flavors of additional sterile neutrinos  $\chi_\eta$ . Most reasonable scenarios set  $n_L = n_R$ , but one can imagine other scenarios, so we will not *a priori* set

them equal. The neutrino mass terms of (22), (41), and (51) may be combined with the mass terms involving the additional sterile neutrinos in the matrix equation

$$\mathcal{L}_{mass} = -\frac{1}{2} (\bar{\nu}_L \bar{N}_L \bar{\chi}_L) M_\nu \begin{pmatrix} \bar{\nu}_R \\ N_R \\ \chi_R \end{pmatrix} + h.c. \quad (52)$$

$M_\nu$  is the  $n \times n$  neutrino mass matrix, where  $n = n_L + n_R + n_\chi$ ,  $\nu$  contains all  $n_L$  active neutrino spinors,  $N_R$  contains the  $n_R$  Dirac counterparts, and  $\chi$  contains all  $n_\chi$  sterile neutrino spinors.  $M_\nu$  may be broken into block form:

$$M_\nu = \begin{pmatrix} M_T & M_D & M_{\nu\chi} \\ M_D^T & M_S & M_{N\chi} \\ M_{\nu\chi}^T & M_{N\chi}^T & M_\chi \end{pmatrix}, \quad (53)$$

where  $M_T$  is  $n_L \times n_L$ ,  $M_D$  is  $n_L \times n_R$ , *et cetera*.

The singlet and triplet Majorana terms fall directly out of equations (52) and (53) when the other couplings are set to zero, but the Dirac term requires a bit of algebra. For pure Dirac neutrinos, the matrices  $M_T$ ,  $M_S$ , and all  $M_\chi$  are zero. We are left with the Lagrangian

$$\begin{aligned} \mathcal{L}_{Dirac} &= -\frac{1}{2} (\bar{\nu}_L \bar{N}_L \bar{\chi}_L) \begin{pmatrix} 0 & M_D & 0 \\ M_D^T & 0 & 0 \\ 0 & 0 & 0 \end{pmatrix} \begin{pmatrix} \bar{\nu}_R \\ N_R \\ \chi_R \end{pmatrix} + h.c. \\ &= -\frac{1}{2} [\bar{\nu}_L M_D N_R + \bar{N}_L M_D^T \bar{\nu}_R] + h.c. \end{aligned} \quad (54)$$

Using the relations (425) and (420) from Appendix B.4, we see that the two terms in the brackets are identical:

$$\bar{N}_L M_D^T \bar{\nu}_R = -N_R^T C^\dagger M_D^T C \bar{\nu}_L^T = \bar{\nu}_L C^T M_D C^\dagger N_R = \bar{\nu}_L M_D N_R. \quad (55)$$

The Dirac mass Lagrangian becomes

$$\mathcal{L}_{Dirac} = -\overline{\nu_L} M_D N_R + h.c., \quad (56)$$

in agreement with the definition of a Dirac term (22). The extra  $\frac{1}{2}$  in the definition of the Majorana terms (41) and (51) does not appear in Dirac terms because the particle and antiparticle Dirac mass terms sum when we use the general notation (52). This factor is also consistent with what one expects for the equation of motion resulting from variation of  $\mathcal{L}$  with respect to the neutrino fields. For Dirac fields,  $\psi$  and  $\psi^\dagger$  are varied independently, whereas for Majorana fields the two are not independent and their variation consequently returns a factor of 2.

## 2.6 The See-Saw Model

A popular class of neutrino mass models which includes both Majorana and Dirac mass terms is that of seesaw models. Seesaw models have achieved their popularity because they naturally give rise to small neutrino masses with minimum additions to the Standard Model. In such models, active neutrinos compose Dirac mass terms with their sterile counterparts, and the sterile neutrinos also form a bare Majorana mass term. Equation (52) becomes

$$\mathcal{L}_{mass} = -\frac{1}{2} (\overline{\nu_L} \overline{N_L}) \begin{pmatrix} 0 & M_D \\ M_D^T & M_S \end{pmatrix} \begin{pmatrix} \nu_R \\ N_R \end{pmatrix}. \quad (57)$$

In see-saw models, the elements of  $M_D$ , which arise from coupling to the Higgs doublet and the standard  $SU(2) \times U(1)$  symmetry breaking, are on the order of lepton masses, while the  $SU(2) \times U(1)$ -invariant elements of  $M_S$  are on the order of a larger scale, perhaps the scale of grand unified theories. Thus we may expand to leading order in  $M_S^{-1}$ . Roughly following the treatment in [19], we find that  $U_\nu$  has the form

$$U_\nu = \begin{pmatrix} A & M_D M_S^{-1} B \\ -M_S^{-1\dagger} M_D^\dagger A & B \end{pmatrix}, \quad (58)$$

where  $A$  and  $B$  diagonalize the “light” and “heavy” mass matrices:

$$-A^\dagger M_D M_S^{-1} M_D^T A^{T\dagger} = D_{light}, \quad \text{and} \quad B^\dagger M_S B^{T\dagger} = D_{heavy}. \quad (59)$$

The mass eigenstates are

$$\begin{pmatrix} \nu^m \\ N^m \end{pmatrix}_L = \begin{pmatrix} A^\dagger (\nu_L - M_D M_S^{-1} N_L) \\ B^\dagger (M_S^{-1\dagger} M_D^\dagger \nu_L + N_L) \end{pmatrix}. \quad (60)$$

These are Majorana states, so the right-handed component is also the charge-conjugate of the left-handed state:

$$\begin{pmatrix} \nu^m \\ N^m \end{pmatrix}_R = \left[ \begin{pmatrix} \nu^m \\ N^m \end{pmatrix}_L \right]^c = \begin{pmatrix} A^T (\nu_R - M_D^{T\dagger} M_S^{-1\dagger} N_R) \\ B^T (M_S^{-1} M_D^T \nu_R + N_R) \end{pmatrix}. \quad (61)$$

The seesaw model is so-named because it naturally gives small masses to the states  $\nu^m$ , which are composed mainly of active neutrinos, while giving large masses to the states  $N^M$ , which are largely made up of sterile neutrinos.

In the above treatment,  $M_T$  has been set to zero. The seesaw model still works for non-zero  $M_T$ , provided the elements of  $M_T$  are still much smaller than the elements of  $M_S$ . Such an inclusion of  $M_T$  has negligible effects on the heavy mass states, and changes the light mass matrix from  $-M_D M_S^{-1} M_D^T$  to  $M_T - M_D M_S^{-1} M_D^T$  [19].

## 2.7 Mass States vs. Flavor States

Any mass term, regardless of the origin of the term, has the form  $\overline{\psi_L} M \psi_R$ , where  $\psi$  is a  $n$ -dimensional vector and  $M$  is an  $n \times n$  matrix.  $\psi$  can contain the active  $\nu_\alpha$ , the sterile  $N_\alpha$ , the additional  $\chi_\eta$ , or all three. As is the case for quarks, the mass matrix  $M$  for neutrinos is not necessarily diagonal. Neutrino states of definite mass correspond to eigenvectors of the mass matrix, which are generally distinct from the states of definite flavor. Adding neutrino masses, the lepton

Lagrangian of equation (1) in matrix form is

$$\begin{aligned}\mathcal{L}^\nu &= \overline{\psi} i\partial_\mu \gamma^\mu \psi + \overline{l} i\partial_\mu \gamma^\mu l - c_1 Z_\mu (\overline{\nu_L} \gamma^\mu \nu_L - (1 - 2 \sin^2 \theta_W) \overline{l}_L \gamma^\mu l_L + 2 \sin^2 \theta_W \overline{l}_R \gamma^\mu l_R) \quad (62) \\ &\quad - c_2 (W_\mu^+ \overline{\nu_L} \gamma^\mu l_L + W_\mu^- \overline{l} \gamma^\mu \nu_L) + \overline{l}_L M_l l_R + \overline{l}_R M_l^\dagger l_L + \overline{\psi_L} M_\nu \psi_R + \overline{\psi_R} M_\nu^\dagger \psi_L.\end{aligned}$$

The subscripts on the mass matrices  $\nu$  and  $l$  label a matrix by the type of particle for which it provides mass; they do not denote flavor indices. The lepton spinors in equation (62) correspond to states of definite *flavor*. States of definite mass (to be denoted by the superscript  $m$ ) are achieved by diagonalizing the mass matrix, thereby rotating from the flavor basis to the mass basis. The diagonal mass matrices,  $D_l$  and  $D_\nu$ , are given by

$$D_l = U_{l_L}^{-1} M_l U_{l_R}, \quad \text{and} \quad D_\nu = U_{\nu_L}^{-1} M_\nu U_{\nu_R}. \quad (63)$$

As discussed in Section 2.1, when  $\psi$  represents a Majorana spinor,  $M_\nu$  is symmetric and we may take  $U_{\nu_R} = U_{\nu_L}^{\dagger T}$ . At this point, however, we will consider a three-generation case without Majorana terms. The following treatment is extended to allow higher generations in Section 4.3.

The rotation from flavor states to mass states leaves the kinetic and neutral current terms unchanged, but the charged current is not invariant under the transformation:

$$\begin{aligned}\mathcal{L}^\nu &= \overline{\nu_L} U_{\nu_L} U_{\nu_L}^{-1} i\partial_\mu \gamma^\mu U_{\nu_L} U_{\nu_L}^{-1} \nu_L + \overline{N_R} U_{N_R} U_{N_R}^{-1} i\partial_\mu \gamma^\mu U_{N_R} U_{N_R}^{-1} N_R \\ &\quad + \overline{l}_L U_{l_L} U_{l_L}^{-1} i\partial_\mu \gamma^\mu U_{l_L} U_{l_L}^{-1} l_L + \overline{l}_R U_{l_R} U_{l_R}^{-1} i\partial_\mu \gamma^\mu U_{l_R} U_{l_R}^{-1} l_R \\ &\quad - c_1 Z_\mu (\overline{\nu_L} U_{\nu_L} U_{\nu_L}^{-1} \gamma^\mu U_{\nu_L}^{-1} U_{\nu_L} \nu_L - (1 - 2 \sin^2 \theta_W) \overline{l}_L U_{l_L} U_{l_L}^{-1} \gamma^\mu U_{l_L} U_{l_L}^{-1} l_L \\ &\quad + 2 \sin^2 \theta_W \overline{l}_R U_{l_R} U_{l_R}^{-1} \gamma^\mu U_{l_R} U_{l_R}^{-1} l_R) \\ &\quad - c_2 (W_\mu^+ \overline{\nu_L} U_{\nu_L} U_{\nu_L}^{-1} \gamma^\mu U_{l_L} U_{l_L}^{-1} l_L + W_\mu^- \overline{l}_L U_{l_L} U_{l_L}^{-1} \gamma^\mu U_{\nu_L} U_{\nu_L}^{-1} \nu_L) + \overline{l}_L U_{l_L} U_{l_L}^{-1} M_l U_{l_R} U_{l_R}^{-1} l_R \\ &\quad + \overline{l}_R U_{l_R} U_{l_R}^{-1} M_l^\dagger U_{l_L} U_{l_L}^{-1} l_L + \overline{\nu_L} U_{\nu_L} U_{\nu_L}^{-1} M_\nu U_{N_R} U_{N_R}^{-1} N_R + \overline{N_R} U_{N_R} U_{N_R}^{-1} M_\nu^\dagger U_{\nu_L} U_{\nu_L}^{-1} \nu_L \\ &= \overline{\nu_L^m} U_{\nu_L}^{-1} U_{\nu_L} i\partial_\mu \gamma^\mu \nu_L^m + \overline{N_R^m} U_{N_R}^{-1} U_{N_R} i\partial_\mu \gamma^\mu N_R^m \\ &\quad + \overline{l}_L^m U_{l_L}^{-1} U_{l_L} i\partial_\mu \gamma^\mu l_L^m + \overline{l}_R^m U_{l_R}^{-1} U_{l_R} i\partial_\mu \gamma^\mu l_R^m \\ &\quad - c_1 Z_\mu (\overline{\nu_L^m} U_{\nu_L}^{-1} U_{\nu_L} \gamma^\mu \nu_L^m - (1 - 2 \sin^2 \theta_W) \overline{l}_L^m U_{l_L}^{-1} U_{l_L} \gamma^\mu l_L^m + 2 \sin^2 \theta_W \overline{l}_R^m U_{l_R}^{-1} U_{l_R} \gamma^\mu l_R^m)\end{aligned}$$

$$\begin{aligned}
& - c_2 (W_\mu^+ \overline{\nu_L^m} U_{\nu_L}^{-1} U_{l_L} \gamma^\mu l_L^m + W_\mu^- \overline{l_L^m} U_{l_L}^{-1} U_{\nu_L} \gamma^\mu \nu_L^m) + \overline{l_L^m} D_l l_R^m + \overline{l_R^m} D_l^\dagger l_L^m \\
& + \overline{\nu_L^m} D_\nu N_R^m + \overline{N_R^m} D_\nu^\dagger \nu_L^m \\
= & \overline{\nu_L^m} i \partial_\mu \gamma^\mu \nu_L^m + \overline{N_R^m} i \partial_\mu \gamma^\mu N_R^m + \overline{l_L^m} i \partial_\mu \gamma^\mu l_L^m + \overline{l_R^m} i \partial_\mu \gamma^\mu l_R^m \\
& - c_1 Z_\mu \left( \overline{\nu_L^m} \gamma^\mu \nu_L^m - (1 - 2 \sin^2 \theta_W) \overline{l_L^m} \gamma^\mu l_L^m + 2 \sin^2 \theta_W \overline{l_R^m} \gamma^\mu l_R^m \right) \\
& - c_2 (W_\mu^+ \overline{\nu_L^m} U_{\nu_L}^{-1} U_{l_L} \gamma^\mu l_L^m + W_\mu^- \overline{l_L^m} U_{l_L}^{-1} U_{\nu_L} \gamma^\mu \nu_L^m) \\
& + \overline{l_L^m} D_l l_R^m + \overline{l_R^m} D_l^\dagger l_L^m + \overline{\nu_L^m} D_\nu N_R^m + \overline{N_R^m} D_\nu^\dagger \nu_L^m. \tag{64}
\end{aligned}$$

The charged current term in equation (64) is not simultaneously diagonalizable in both the flavor basis and mass basis; upon rotation to the mass basis, it acquires a mixing matrix,  $V = U_{l_L}^{-1} U_{\nu_L}$ . For Dirac neutrinos, the lepton mixing matrix  $V$  has the same properties as the CKM matrix in the quark sector. If the Lagrangian does not contain a neutrino mass term, as in the Standard Model, or if the neutrino mass eigenvalues are degenerate, the neutrino states may undergo an arbitrary rotation, so we may set  $U_{\nu_L} = U_{l_L}$ , which yields  $V = \mathbb{1}$ . In such models, flavor states and mass states are indistinguishable, so we may assume a diagonal charged lepton mass matrix for the Standard Model, as we did in Section 1.2, with no loss of generality.

Even when neutrino mass terms are present, the matrices  $U_{\nu_L}$  and  $U_{l_L}$  are not unique. Multiplying each by any unitary matrix  $R$  leaves

$$V = (R U_{l_L})^\dagger (R U_{\nu_L}) = U_{l_L}^\dagger U_{\nu_L} \tag{65}$$

invariant. In the quark sector, an implicit choice  $R = U_{upL}^\dagger$  is made so that quark mixing is constrained to the down-type quarks, with the up-type flavor states assumed identical to mass states. Mixing in the lepton sector is typically similarly restricted to neutrinos. Under this implicit assumption, the neutrino flavor states are connected to the neutrino mass states by the mixing matrix  $V$  which appears in the weak charged current term:

$$\nu_{\alpha L} = \sum_{i=1}^n V_{\alpha i} \nu_{i L}, \text{ with} \tag{66}$$

$$\mathcal{J}_{CC} = \sum_{\alpha=flavors} \overline{\nu_{\alpha L}} \gamma^{\mu} l_{\alpha L} + h.c. = \sum_{i,j=1}^n \overline{\nu_{i L}} V_{ij}^{-1} \gamma^{\mu} l_{j L} + h.c. \quad (67)$$

The mixing matrix occurring in the charged current term has two mass indices, since it couples the neutrino mass states to the lepton mass states. Under the assumption that charged leptons have a diagonal mass matrix, the lepton mass state  $l_{iL}$  is equivalent to the lepton flavor state  $l_{\alpha L}$ , and the mixing matrix may be given a mass index and a flavor index and identified with the neutrino rotation matrix  $U_{\nu L}$ . In the following Chapters, we will assume the lepton matrix is diagonal and give the mixing matrix one mass index and one flavor index.

## CHAPTER III

### OSCILLATIONS

If the eigenvalues of the neutrino mass matrix are non-degenerate, then neutrinos may change flavors as they propagate. We will show that the flavor of a neutrino changes in a cyclic fashion, so the neutrino flavor *oscillates* with distance traveled. To see how these oscillations arise, let us consider the neutrino Lagrangian and derive the appropriate equations of motion.

#### 3.1 The Equations of Motion

For simplicity, we will consider a Dirac mass term as in equation (22). The neutrino Lagrangian in vacuum is then given by

$$\mathcal{L}^\nu = \sum_{\alpha=flavors} \left[ \overline{\nu_{\alpha L}} i\partial_\mu \gamma^\mu \nu_{\alpha L} + \overline{N_{\alpha R}} i\partial_\mu \gamma^\mu N_{\alpha R} - \sum_{\beta=flavors} \left( \overline{\nu_{\alpha L}} M_{D\alpha\beta} N_{\beta R} + \overline{N_{\alpha R}} M_{D\alpha\beta}^\dagger \nu_{\beta L} \right) \right] \quad (68)$$

Varying (68) with respect to  $\overline{\nu_{\alpha L}}$  and then with respect to  $\overline{N_{\alpha R}}$  yields the following equations of motion:

$$\frac{\delta \mathcal{L}^\nu}{\delta \overline{\nu_{\alpha L}}} = i\partial_\mu \gamma^\mu \nu_{\alpha L} - \sum_{\beta} M_{D\alpha\beta} N_{\beta R} = 0, \text{ and} \quad (69)$$

$$\frac{\delta \mathcal{L}^\nu}{\delta \overline{N_{\alpha R}}} = i\partial_\mu \gamma^\mu N_{\alpha R} - \sum_{\beta} M_{D\alpha\beta}^\dagger \nu_{\beta L} = 0. \quad (70)$$

Solving for  $N_{\alpha R}$  in the first equation and then substituting into the second, we obtain an equation involving only the active neutrino  $\nu_{\gamma L}$ :

$$i\partial_\mu \gamma^\mu N_{\alpha R} = i\partial_\mu \gamma^\mu \sum_{\gamma} M_{D\alpha\gamma}^{-1} (i\partial_\nu \gamma^\nu \nu_{\gamma L}) = \sum_{\gamma} M_{D\alpha\gamma}^\dagger \nu_{\gamma L}. \quad (71)$$

Following the treatment of Kuo and Pantaleone in [30], we make the following simplification using the properties of the gamma matrices:

$$\partial_\mu \gamma^\mu \partial_\nu \gamma^\nu = \frac{1}{2} [\partial_\mu \partial_\nu \gamma^\mu \gamma^\nu + \partial_\nu \partial_\mu \gamma^\nu \gamma^\mu] = \partial_\mu \partial_\nu g^{\mu\nu} = \partial_\mu \partial^\mu. \quad (72)$$

With this substitution, equation (71) may be written as

$$\partial_\mu \partial^\mu \nu_{\beta L} + \sum_\gamma (M_D M_D^\dagger)_{\beta\gamma} \nu_{\gamma L} = 0. \quad (73)$$

This has the same form as a Klein-Gordon equation. Following the traditional treatment of a Klein-Gordon equation, we assume a plane wave solution of the form

$$\nu_{\alpha L}(x_\mu) = \sum_\beta e^{-ip_{\alpha\beta}^\mu x_\mu} \nu_\beta. \quad (74)$$

$\nu_\beta$  is a  $\beta$ -flavor neutrino spinor, with no time or spatial dependence. The 4-momentum is represented by a matrix because it is not diagonal in flavor space. Eventually, we will diagonalize the 4-momentum and move into the mass basis, but first a word about the plane wave assumption.

As mentioned above, a given flavor of neutrino created at a source does not necessarily have a definite mass, and therefore the 4-momentum is not diagonal in flavor space. Most discussions of neutrino oscillations, such as those found in [12] and [14], treat the neutrino of definite flavor as a particle with definite momentum, composed of a superposition of energy states corresponding to the different mass states. Reference [31] shows that this treatment yields the same results as a treatment using a definite energy and a superposition of momentum states, and that both yield results consistent with a more rigorous treatment of the problem using wave packets, provided the neutrinos are relativistic. Appendix C.1 summarizes the wave-packet approach and the validity of its approximation by the plane wave solution (74). The energy-momentum assumptions of the standard oscillation treatment are examined in reference [32], and we present those arguments in Appendix C.2. In what follows, we will use the plane wave solution (74) rather than wave packets for simplicity, but we will use the relativistic results of Appendix C.2 to conserve both energy and momentum.

Examining the plane wave  $\nu_{\alpha L}$  in equation (74), we find

$$\partial_0 \partial^0 \nu_{\alpha L} = - \sum_{\beta=flavors} (E_{\alpha\beta})^2 \nu_{\beta L}, \text{ and} \quad (75)$$

$$\partial_a \partial^a \nu_{\alpha L} = - \sum_{a=1}^3 \sum_{\beta=flavors} p_{\alpha\beta a} p_{\alpha\beta}^a \nu_{\beta L} \equiv - \sum_{\beta} (|\vec{p}|^2)_{\alpha\beta} \nu_{\beta L}. \quad (76)$$

Note that the index  $\alpha$  is not summed over in equations (76) and (75), but  $a$  is. As usual,  $\alpha$  and  $\beta$  are flavor indices, and  $a$  is a spatial Lorentz index. The conventions we use for summing and indices are described in Appendix A. Using the plane wave solution in (73), we obtain an equation for the matrix  $p_{\alpha\beta}^\mu p_{\alpha\beta\mu}$ .

$$\partial_\mu \partial^\mu \nu_{\alpha L} = \sum_{\beta} (E_{\alpha\beta}^2 - |\vec{p}|_{\alpha\beta}^2) \nu_{\beta L} = \sum_{\beta} (M_D M_D^\dagger)_{\alpha\beta} \nu_{\beta L}. \quad (77)$$

Neutrinos propagate in *mass* states, not flavor states, so we must diagonalize the mass matrix in (77) to find an equation of motion for the mass states. The same mixing matrix  $V$  diagonalizes both the mass matrix and the four-momentum matrix, leaving us with an expression for the four-momentum of the  $i$ th mass state  $\nu_{iL}$ :

$$\begin{aligned} \sum_{\alpha, \beta, \gamma} V_{j\alpha}^\dagger (E^2 - |\vec{p}|^2)_{\alpha\gamma} (VV^\dagger)_{\gamma\beta} \nu_{\beta L} &= \sum_{\alpha, \beta, \gamma} V_{j\alpha}^\dagger (M_D M_D^\dagger)_{\alpha\gamma} (VV^\dagger)_{\gamma\beta} \nu_{\beta L}, \text{ so} \\ \sum_{\alpha, \gamma} \sum_i \left[ V_{j\alpha}^\dagger (E^2 - |\vec{p}|^2)_{\alpha\gamma} V_{\gamma i} \right] \sum_{\beta} V_{i\beta}^\dagger \nu_{\beta L} &= \sum_{\alpha, \gamma} \sum_i \left[ V_{j\alpha}^\dagger (M_D M_D^\dagger)_{\alpha\gamma} V_{\gamma i} \right] \sum_{\beta} V_{i\beta}^\dagger \nu_{\beta L} \\ &= \sum_i m_i \delta_{ij} \nu_{iL}, \end{aligned} \quad (78)$$

with

$$\nu_{iL} \equiv \sum_{\beta} V_{i\beta}^\dagger \nu_{\beta L} \quad (79)$$

and

$$\sum_{\alpha\gamma} V_{i\alpha}^\dagger (M_D M_D^\dagger)_{\alpha\gamma} V_{\gamma j} = m_i^2 \delta_{ij}. \quad (80)$$

The matrix on the right-hand side of equation (78) is diagonal, so the matrix on the left-hand side must be diagonal too. Consider first the rest frame of the neutrino. The three momentum is zero,

so the left-hand side of equation (78) is

$$\sum_{\alpha, \gamma} \left[ V_{j\alpha}^\dagger (E_{\alpha\gamma}^2) V_{\gamma i} \right] \nu_{iL} \equiv E_i \delta_{ij}. \quad (81)$$

Making a Lorentz boost back into the moving frame only changes Lorentz indices, not flavor indices, so equation (81) remains valid in the frames with non-zero momentum. Since the left-hand side of equation (78) must be diagonal and the first term is diagonal by equation (81), the second term must be diagonal too:

$$\sum_{\alpha, \gamma} \left[ V_{j\alpha}^\dagger (|\vec{p}|_{\alpha\gamma}^2) V_{\gamma i} \right] \equiv |\vec{p}_i|^2 \delta_{ij}. \quad (82)$$

Comparison of equations (78) through (82) yield the familiar energy-momentum relationship

$$(E_i^2 - |\vec{p}_i|^2) \nu_{iL} = m_i^2 \nu_{iL}. \quad (83)$$

Having rotated into mass states of definite energy and momentum, we may now describe the propagation of the neutrino mass eigenstates through space:

$$\nu_{iL}(t_i, \mathbf{x}_i) = e^{i(E_i t_i - \mathbf{p}_i \cdot \mathbf{x}_i)} \nu_i. \quad (84)$$

We have placed mass indices on the time and position, since the propagation of the state in space and time depends on the mass. (Different mass states will travel the same distance in different times or different distances in the same time). An equation similar to (84) may be derived for the sterile neutrino  $N_R$ , and the two may be combined in vacuum to describe the behavior of a Dirac neutrino  $\nu$ .

### 3.2 Vacuum Oscillations

Weak interactions at a neutrino source produce neutrinos of a definite flavor,  $\nu_\alpha$ , so the wavefunction of a neutrino when it is produced is

$$\nu_L(t = 0, x = 0) = \nu_{\alpha L} = \sum_i V_{\alpha i} \nu_{iL}, \quad (85)$$

The wavefunction a distance  $x$  from the source, and a time  $t$  after emission, (taking the x-axis along the momentum direction) is

$$\nu_L(t, x) = \sum_{i=1}^n V_{\alpha i} \nu_i e^{-i(E_i t_i - p_i x_i)} \equiv \sum_{i=1}^n V_{\alpha i} \nu_i e^{-i\phi_i}, \quad (86)$$

where  $\phi_i \equiv E_i t_i - p_i x_i$  is the *kinematic phase* of the propagating mass state  $\nu_i$ . Although neutrinos travel in mass states, they are detected in flavor states, so we must rotate back to the flavor basis to compare with experiment:

$$\nu_L(t, x) = \sum_{\beta=\text{flavors}} \left[ \sum_{i=1}^n V_{\alpha i} V_{\beta i}^* e^{-i\phi_i} \right] \nu_\beta \equiv \sum_{\beta} a_{\beta\alpha} \nu_\beta. \quad (87)$$

$a_{\beta\alpha}$  is the amplitude for the transformation  $\nu_\alpha \rightarrow \nu_\beta$ , and the probability of the transformation is

$$P_{\nu_\alpha \rightarrow \nu_\beta}(x) = |a_{\beta\alpha}|^2 = \sum_{i=1}^n \sum_{j=1}^n (V_{\alpha i} V_{\beta i}^* V_{\alpha j}^* V_{\beta j}) e^{-i(\phi_i - \phi_j)}. \quad (88)$$

We call the phase difference the *relative phase*

$$\Phi_{ij} \equiv \frac{1}{2} (\phi_i - \phi_j), \quad (89)$$

where the factor of  $\frac{1}{2}$  is included for future convenience.

Because the mixing matrix is unitary,

$$\sum_{i=1}^n \sum_{j=1}^n (V_{\alpha i} V_{\beta i}^* V_{\alpha j}^* V_{\beta j}) = \delta_{\alpha\beta}, \quad (90)$$

and (88) may be written as

$$P_{\nu_\alpha \rightarrow \nu_\beta}(x) = \sum_{i=1}^n \sum_{j=1}^n (V_{\alpha i} V_{\beta i}^* V_{\alpha j}^* V_{\beta j}) (e^{-i2\Phi_{ij}} - 1) + \delta_{\alpha\beta}. \quad (91)$$

Terms antisymmetric under the interchange  $i \leftrightarrow j$  will cancel in the double sum, leaving only symmetric terms. The product of matrix elements in equation (91) becomes its complex conjugate under this interchange, so the real part is symmetric and the imaginary part antisymmetric. The

exponential may also be broken into its symmetric cosine and antisymmetric sine contributions.

Keeping only the symmetric products, equation (91) becomes

$$\begin{aligned}
P_{\nu_\alpha \rightarrow \nu_\beta}(x) &= \sum_{i=1}^n \sum_{j=1}^n [\operatorname{Re}(V_{\alpha i} V_{\beta i}^* V_{\alpha j}^* V_{\beta j}) (\cos(2\Phi_{ij}) - 1) \\
&\quad + \operatorname{Im}(V_{\alpha i} V_{\beta i}^* V_{\alpha j}^* V_{\beta j}) \sin(2\Phi_{ij})] + \delta_{\alpha\beta} \\
&= - \sum_{i=1}^n \sum_{j=1}^n [\operatorname{Re}(V_{\alpha i} V_{\beta i}^* V_{\alpha j}^* V_{\beta j}) 2 \sin^2(\Phi_{ij}) \\
&\quad - \operatorname{Im}(V_{\alpha i} V_{\beta i}^* V_{\alpha j}^* V_{\beta j}) \sin(2\Phi_{ij})] + \delta_{\alpha\beta}.
\end{aligned} \tag{92}$$

The terms for which  $i = j$  do not contribute since  $\Phi_{ii} = 0$ , so we remove them to arrive at our final form for the neutrino oscillation probability:

$$\begin{aligned}
P_{\nu_\alpha \rightarrow \nu_\beta}(x) &= -2 \sum_i \sum_{j \neq i} \operatorname{Re}(V_{\alpha i} V_{\beta i}^* V_{\alpha j}^* V_{\beta j}) \sin^2(\Phi_{ij}) \\
&\quad + \sum_i \sum_{j \neq i} \operatorname{Im}(V_{\alpha i} V_{\beta i}^* V_{\alpha j}^* V_{\beta j}) \sin(2\Phi_{ij}) + \delta_{\alpha\beta}
\end{aligned} \tag{93}$$

For relativistic neutrinos,  $\Phi_{ij}$  is derived in Appendix C.2 to be

$$\Phi_{ij} \approx \frac{m_i^2 - m_j^2}{4p} x, \tag{94}$$

which is linear in  $x$ , the distance traveled. As a neutrino propagates, its transition probability thus oscillates in distance as the square of a sine function with an oscillation length

$$L_{ij} \equiv \frac{\pi x}{\Phi_{ij}} = \frac{4\pi p}{m_i^2 - m_j^2} \equiv \frac{4\pi p}{\Delta m_{ij}^2}. \tag{95}$$

$\Delta m_{ij}^2 \equiv m_i^2 - m_j^2$  is called the *mass-squared difference* for mass states  $i$  and  $j$ .

We see upon examination of equations (93) and (94) that the oscillation probability when all  $m_i = m_j$  is  $\delta_{\alpha\beta}$ . Thus if the neutrino masses are all zero, the probability for a neutrino to change flavors is 0 and the probability for the neutrino to stay the same flavor is 1. Detection of neutrino oscillations would therefore be proof of non-zero neutrino masses and potentially the first contradiction of the Standard Model.

### 3.2.1 Two-Way Oscillations

Consider the simplified case of two neutrino flavors,  $n = 2$ . An arbitrary  $2 \times 2$  unitary matrix will have one angle parameterizing the real degree of freedom, and three phases corresponding to the three imaginary degrees of freedom. But all three phases may be absorbed into the definitions of Dirac fermion fields (or cancel in oscillation probabilities for Majorana neutrinos as described later in Section 4.2.2), so a  $2 \times 2$  mixing matrix has only one (real) degree of freedom, which we will describe by the angle  $\theta$ . The mixing matrix  $V$  then has the form

$$V = \begin{pmatrix} \cos \theta & -\sin \theta \\ \sin \theta & \cos \theta \end{pmatrix}. \quad (96)$$

Since the matrix is explicitly real, the term in equation (93) involving imaginary matrix elements disappears, and the oscillation probability in the two flavor case is simply

$$\begin{aligned} P_{\nu_\alpha \xrightarrow{\nu_\beta}} (x) &= +4 \cos^2 \theta \sin^2 \theta \sin^2 \left( \frac{\Delta m_{12}^2}{4p} x \right) + \delta_{\alpha\beta} \\ &= \sin^2 2\theta \sin^2 \left( \frac{\Delta m_{12}^2}{4p} x \right) + \delta_{\alpha\beta} \end{aligned} \quad (97)$$

### 3.2.2 Three-Way Oscillations

The three-generation case provides a bit of freedom in parameterizing the mixing matrix. An arbitrary  $3 \times 3$  unitary matrix has three real degrees of freedom, and six phases. As will be shown in Section 4.2.2,  $2n - 1 = 5$  relative phases are not observable, so the three-generation mixing matrix needs three mixing angles and one phase to describe it. The quark sector contains such a matrix, called the CKM matrix after Cabibbo, Kobayashi, and Maskawa, who developed the theory of quark mixing. The original choice of these four parameters, by Kobayashi and Maskawa, is perhaps the best known parameterization. Their choice of  $V$  is [11]

$$\begin{pmatrix} c_1 & s_1 c_3 & s_1 s_3 \\ -s_1 c_2 & c_1 c_2 c_3 - s_2 s_3 e^{i\delta} & c_1 c_2 s_3 + s_2 c_3 e^{i\delta} \\ -s_1 s_2 & c_1 s_2 c_3 + c_2 s_3 e^{i\delta} & c_1 s_2 s_3 - c_2 c_3 e^{i\delta} \end{pmatrix}, \quad (98)$$

where  $c_a \equiv \cos \theta_a$ , and  $s_a \equiv \sin \theta_a$ . We will refer to this particular choice of angles as the “standard” or “KM” parameterization, while the name “CKM matrix” refers to any three-generation mixing matrix parameterization.

In the standard KM parameterization, the phase only appears in the lower right-hand “corner” of the matrix. The placement of the phase is somewhat arbitrary, since we absorb five relative phases into the field definitions. Choosing to absorb a different set of relative phases repositions the remaining phase in the mixing matrix. Clearly the location of the phase cannot be measurable! Indeed, as discussed in the next chapter, individual mixing matrix elements cannot be measured independently, and the measurable probabilities include a single function of the phase, called  $\mathcal{J}$ , not the phase itself. In the standard KM parameterization, the invariant  $\mathcal{J}$  has the form

$$\mathcal{J} = c_1 s_1^2 c_2 s_2 c_3 s_3 \sin \delta. \quad (99)$$

This function has a maximum value of  $\frac{1}{6\sqrt{3}}$  [33]:

$$\mathcal{J}_{max} = (\cos \theta_1 - \cos \theta_1^3)_{max} \left( \frac{1}{2} \sin 2\theta_2 \right)_{max} \left( \frac{1}{2} \sin 2\theta_3 \right)_{max} (\sin \delta)_{max} = \frac{2}{3\sqrt{3}} \frac{1}{2} \frac{1}{2} (1) = \frac{1}{6\sqrt{3}}. \quad (100)$$

Another popular parameterization chooses slightly different mixing angles and places the phases elsewhere in the mixing matrix [34], [33]:

$$\begin{pmatrix} c_{12}c_{13} & s_{12}c_{13} & s_{13}e^{-i\delta'} \\ -c_{23}s_{12} - c_{12}s_{23}s_{13}e^{i\delta'} & c_{12}c_{23} - s_{12}s_{23}s_{13}e^{i\delta'} & c_{13}s_{23} \\ s_{12}s_{23} - c_{12}c_{23}s_{13}e^{i\delta'} & -c_{12}s_{23} - c_{23}s_{12}s_{13}e^{i\delta'} & c_{13}c_{23} \end{pmatrix}. \quad (101)$$

Both of these parameterizations (98) and (101) are equally valid, but they are not equivalent. In addition, we will demonstrate in Chapter V how complicated the observables are in terms of the standard KM parameterization. Our development of a model-independent parameterization has been motivated by the arbitrariness and complexity of the traditional approach.

### 3.3 Matter Effects

When neutrinos travel through matter, they may interact with the electrons, protons, and neutrons contained in the matter. Once these interactions are averaged, the resulting terms in the effective Lagrangian resemble mass terms, as shown below. All flavors of neutrinos will scatter off of electrons, protons, and neutrons by the neutral current interaction, so the mass matrix receives a contribution proportional to the identity matrix which does not affect the mixing matrix. (Rotating this identity term by the mixing matrix leaves it diagonal while diagonalizing the mass terms. Thus the same mixing matrix that diagonalizes the vacuum Lagrangian will diagonalize the Lagrangian with neutral-current terms added.) However, only electron-type neutrinos and electrons may scatter via the charged current. This type of interaction produces a non-trivial contribution to the mass matrix, affecting the mixing matrix and oscillation parameters.

As discussed in Section 1.2, neutrino-electron charged current scattering may be represented by the effective Lagrangian of equation (20). Substituting for  $\mathcal{J}^{CC}$ , we obtain

$$\mathcal{L}_{eff}^{CC} = \frac{-4G}{\sqrt{2}} [\bar{\nu}_{eL} \gamma^\mu e_L] [\bar{e}_L \gamma_\mu \nu_{eL}]. \quad (102)$$

The order of the spinors may be changed by a *Fierz transformation* (see, for example, Appendix F of reference [11] or Exercise 2.12 of reference [10] for details on these transformations), resulting in

$$\mathcal{L}_{eff}^{CC} = -\frac{4G}{\sqrt{2}} [\bar{\nu}_{eL} \gamma^\mu \nu_{eL}] [\bar{e}_L \gamma_\mu e_L]. \quad (103)$$

The electron factor may be reduced by averaging over the electron field and assuming non-relativistic electrons [12] to give

$$\langle \bar{e}_L \gamma^\mu e_L \rangle \approx \langle \bar{e}_L \gamma^0 e_L \rangle = \langle e_L^\dagger e_L \rangle = n_{eL} \approx \frac{1}{2} n_e, \quad (104)$$

where  $n_e$  is the electron number density in the medium interacting with the neutrinos, and we assume that the medium contains equal numbers of left- and right-handed electrons. Thus the contribution to the Lagrangian from the charged current neutrino-electron scattering is

$$\mathcal{L}_{eff}^{CC} = -\sqrt{2} G n_e \bar{\nu}_{eL} \gamma_0 \nu_{eL}. \quad (105)$$

A similar treatment may be applied to the neutral current contribution to the effective Lagrangian, resulting in

$$\mathcal{L}_{eff}^{NC} = \sum_{\alpha} \frac{\sqrt{2}G}{2} (n_n + n_p - n_e) \overline{\nu_{\alpha L}} \gamma_0 \nu_{\alpha L} = \sum_{\alpha} \frac{1}{\sqrt{2}} G n_n \overline{\nu_{\alpha L}} \gamma_0 \nu_{\alpha L}, \quad (106)$$

where the factor of  $\frac{1}{2}$  comes from the difference between charged and neutral currents, and we have set  $n_e = n_p$  for electrically neutral matter. As we shall see, this neutral current term does not affect neutrino oscillations since it is uniform in flavor.

Because these effective Lagrangian terms contain only the spinor products  $\overline{\nu}\nu$ , they are similar to mass terms and affect the diagonalization of the mass matrix. When these interaction terms are added to the vacuum neutrino Lagrangian (68), equation (69) becomes

$$\frac{\delta \mathcal{L}}{\delta \overline{\nu_{\alpha L}}} = i \partial_{\mu} \gamma^{\mu} \nu_{\alpha L} - \sum_{\beta} M_{D\alpha\beta} N_{\beta R} + \frac{1}{\sqrt{2}} G n_n \gamma_0 \nu_{\alpha L} - \sqrt{2} G n_e \delta_{\alpha e} \gamma_0 \nu_{\alpha L} = 0, \quad (107)$$

while equation (70) remains unchanged:

$$\frac{\delta \mathcal{L}'}{\delta \overline{N_{\alpha R}}} = i \partial_{\mu} \gamma^{\mu} N_{\alpha R} - \sum_{\beta} M_{D\alpha\beta}^{\dagger} \nu_{\beta L} = 0. \quad (70)$$

The equation of motion for the active neutrino (71) becomes

$$\begin{aligned} i \partial_{\mu} \gamma^{\mu} N_{\alpha R} &= \sum_{\gamma} M_{D\alpha\gamma}^{-1} i \partial_{\mu} \gamma^{\mu} \left[ \left( i \partial_{\nu} \gamma^{\nu} + \frac{1}{\sqrt{2}} G n_n \gamma_0 - \sqrt{2} G n_e \delta_{\gamma e} \gamma_0 \right) \nu_{\gamma L} \right] \\ &= \sum_{\gamma} M_{D\alpha\gamma}^{\dagger} \nu_{\gamma L}. \end{aligned} \quad (108)$$

If the densities  $n_e$  and  $n_n$  do not fluctuate quickly in space or time, we may approximate

$$i \partial_{\mu} n_{e,n} \approx n_{e,n} i \partial_{\mu}. \quad (109)$$

This approximation is valid if  $\frac{1}{nE} \frac{dn}{dt} \ll 1$  [30].

From the Dirac equation we know

$$\partial_{\mu} \gamma^{\mu} \nu_{\alpha L} \approx m_{\nu} \nu_{\alpha L} \approx 0. \quad (110)$$

The flavor states don't have definite mass, but we can assume  $m_\nu$ , the effective mass of a flavor state, to be on the order of the individual masses  $m_i$ , and therefore small. From this approximation, we find

$$\partial_0 \gamma^0 \nu_{\alpha L} \approx \partial_a \gamma^a \nu_{\alpha L}, \quad \text{so} \quad (111)$$

$$\partial_\mu \gamma^\mu \gamma_0 \nu_{\alpha L} = \gamma_0 (\partial_0 \gamma^0 + \partial_a \gamma^a) \nu_{\alpha L} \approx \gamma_0 (2 \partial_0 \gamma^0) \nu_{\alpha L} = 2 \partial_0 \nu_{\alpha L}. \quad (112)$$

With these substitutions and the simplification of equation (72), equation (108) becomes

$$\partial_\mu \partial^\mu \nu_{\alpha L} + \sum_\beta (M_D M_D^\dagger)_{\alpha\beta} \nu_{\beta L} + iG\sqrt{2} (2n_e \delta_{\alpha e} - n_n) \partial_0 \nu_{\alpha L} = 0. \quad (113)$$

This looks like the Klein-Gordon equation (73) with an amount  $G\sqrt{2}\partial_0(2n_e \delta_{\alpha e} - n_n)$  added to the diagonal elements of the mass matrix. Again we try a plane-wave solution of the form (74). The energy-momentum relationship, however, is affected by the matter, becoming

$$\sum_\beta (E_{\alpha\beta}^2 - |\vec{p}|_{\alpha\beta}^2) \nu_{\beta L} = \sum_\beta \left[ (M_D M_D^\dagger)_{\alpha\beta} + iG\sqrt{2} (2n_e \delta_{\alpha e} - n_n) (-iE_{\alpha\beta}) \right] \nu_{\beta L}. \quad (114)$$

The neutral current term will automatically be diagonalized by the same mixing matrix which diagonalizes  $E_{\alpha\beta}$ , but the charged current term will affect the diagonalization. We may define a new mass matrix  $M^M$  which includes this charged current term and is diagonalized by the matter mixing matrix,  $V^M$ :

$$V_{i\alpha}^{M\dagger} \left[ (M_D M_D^\dagger)_{\alpha\beta} + 2E_{\alpha\beta} \sqrt{2} G n_e \delta_{\alpha e} \right] V_{\beta j}^M \equiv V_{i\alpha}^{M\dagger} (M^M M^{M\dagger})_{\alpha\beta} V_{\beta j}^M = (m_i^M)^2 \delta_{ij}, \quad (115)$$

where  $m_i^M$  are the effective neutrino masses in matter. The mixing matrix is independent of the neutral current term, as predicted before. As for the vacuum case, the momentum and energy are also diagonalized by the mixing matrix:

$$V_{i\alpha}^{M\dagger} |\vec{p}|_{\alpha\beta}^2 V_{\beta j}^M = |\vec{p}_i|^2 \delta_{ij}, \quad \text{and} \quad (116)$$

$$V_{i\alpha}^{M\dagger} E_{\alpha\beta}^2 V_{\beta j}^M = E_i^2 \delta_{ij}. \quad (117)$$

The oscillation equations in matter are the same as they were for neutrinos traveling through a vacuum, provided the mixing matrix  $V$  is replaced with  $V^M$ , and the masses  $m_i^2$  are also replaced with their corresponding  $(m_i^M)^2$ . For example, equation (93) would become

$$\begin{aligned}
 P_{\nu_\alpha \rightarrow \nu_\beta}^M(x) = & -2 \sum_i \sum_{j \neq i} \operatorname{Re}(V_{\alpha i}^M V_{\beta i}^{M*} V_{\alpha j}^{M*} V_{\beta j}^M) \sin^2 \left( \frac{(m_i^M)^2 - (m_j^M)^2}{4p} \right) \\
 & + \sum_i \sum_{j \neq i} \operatorname{Im}(V_{\alpha i}^M V_{\beta i}^{M*} V_{\alpha j}^{M*} V_{\beta j}^M) \sin \left( \frac{(m_i^M)^2 - (m_j^M)^2}{2p} \right) + \delta_{\alpha\beta}.
 \end{aligned} \tag{118}$$

## CHAPTER IV

### A NEW PARAMETERIZATION

#### 4.1 The Unmeasurables

The individual elements of the mixing matrix  $V$  which appear in the Lagrangian are unmeasurable. Consider the two different parameterizations of the three-generation mixing matrix presented in equations (98) and (101) of Section 3.2.2. The freedom to absorb phases into the definitions of fermion fields produces a freedom in the placement of the remaining phase. For a Dirac mass term, we may absorb  $2n$  phases into the definitions of the  $n$  left-handed neutrino fields and  $n$  left-handed fields of the charged leptons. Such an absorption removes  $2n - 1$  relative phases from the mixing matrix without changing any other terms in the Lagrangian, provided we absorb conjugate phases in the right-handed fields:

$$\begin{aligned}
\mathcal{L} &= \overline{\nu_L} M_\nu N_R + \overline{l_L} M_l l_R + c_2 W_\mu^+ \overline{\nu_L} \gamma^\mu l_L + h.c. \\
&= \overline{\nu_L^m} D_\nu N_R^m + \overline{l_L^m} M_l l_R^m + c_2 W_\mu^+ \overline{\nu_L^m} V \gamma^\mu l_L^m + h.c. \\
&= \overline{\nu_L^m} X_\nu X_\nu^{-1} D_\nu X_N X_N^{-1} N_R^m + \overline{l_L^m} X_{l_L} X_{l_L}^{-1} M_l X_{l_R} X_{l_R}^{-1} l_R^m \\
&\quad + c_2 W_\mu^+ \overline{\nu_L^m} X_\nu X_\nu^{-1} V X_{l_L} X_{l_L}^{-1} \gamma^\mu l_L^m + h.c.,
\end{aligned} \tag{119}$$

with

$$(X_\psi)_{ij} = \delta_{ij} e^{-i(\xi_\psi)_i} \tag{120}$$

Setting  $X_N = X_\nu$  and  $X_{l_R} = X_{l_L}$ , which leaves the diagonalized matrices  $D_\nu$  and  $M_l$  unchanged, and redefining  $\psi' = X_\psi^{-1} \psi^m$ , we get

$$\overline{\nu_L'} D_\nu N_R' + \overline{l_L'} M_l l_R' + c_2 W_\mu^+ \overline{\nu_L'} [X_\nu^{-1} V X_{l_L}] \gamma^\mu l_L' + h.c. \tag{121}$$

So we may absorb  $n$  phases through  $X_\nu$  and  $n$  phases through  $X_{l_L}$  in the field definitions, thereby removing  $2n - 1$  relative phases from the mixing matrix, without changing the rest of the Dirac

neutrino Lagrangian. Note that it is the phase *differences* between  $X_\nu^{-1}$  and  $X_l$  that enter into the new mixing matrix, and so  $2n - 1$ , rather than  $2n$ , phases are removed from  $V$ .

If the neutrinos are Majorana particles, however, we do not have the freedom to set the phase matrix  $X_N$  independently of  $X_\nu$  [14]. The Majorana mass term has the form

$$\overline{\nu_L} M_\nu \nu_R, \quad \text{with} \quad \nu_R = C \overline{\nu_L}^T. \quad (122)$$

Making the transformation  $\nu_L \rightarrow \nu_L' = X_\nu^{-1} \nu_L^m$  results in the transformation  $\nu_R \rightarrow \nu_R' = X_\nu^{-1*} \nu_R^m = X_\nu \nu_R^m$ ; the phase matrices in the mass term do not cancel, but combine, and the Lagrangian is not invariant under such a transformation:

$$\overline{\nu_L} M_\nu \nu_R \neq \overline{\nu_L'} D_\nu \nu_R'. \quad (123)$$

Therefore phases may be absorbed only in the charged lepton fields, and just  $n_l$  (which may be different from  $n = n_\nu$  in models with sterile neutrinos) phases may be removed from a Majorana mixing matrix.

These  $2n - 1 - n_l$  extra phases in a mixing matrix for Majorana neutrinos are not, however, observable in oscillation experiments [14]. Each row and each column of  $V$  may be multiplied by an arbitrary phase; *id est*, any mixing matrix element  $V_{\alpha i}$  may be replaced with  $e^{i\xi_\alpha} V_{\alpha i} e^{-i\xi_i}$  without changing the product of four matrix elements found in the oscillation equations:

$$V_{\alpha i} V_{\alpha j}^* V_{\beta i}^* V_{\beta j} = e^{i\xi_\alpha} V_{\alpha i} e^{-i\xi_i} e^{-i\xi_\alpha} V_{\alpha j}^* e^{i\xi_j} e^{-i\xi_\beta} V_{\beta i}^* e^{i\xi_i} e^{i\xi_\beta} V_{\beta j} e^{-i\xi_j}. \quad (124)$$

Thus whether the mass matrix is Majorana or Dirac,  $2n - 1$  relative phases will not appear in the oscillation probabilities even if the number of neutrinos is greater than the number of charged leptons. Processes sensitive to the “extra” Majorana phases include double-beta decay and the radiative decay of unstable neutrinos contained in some models; in these processes the *same* vertex occurs twice (as opposed to a vertex and its hermitian conjugate) in the relevant Feynman diagrams. A discussion of neutrinoless double-beta decay and its relation to Majorana masses is contained in Appendix D.

## 4.2 The Measurables

The immeasurability of the mixing matrix elements in the quark sector has been addressed by numerous authors, such as those of references [35], [36], [37], and [38]. Measurable quantities include only the magnitudes of mixing matrix elements, the products of four mixing matrix elements appearing in the oscillation equation (93), and particular higher-order functions of mixing matrix elements [36]. Neutrino oscillation probabilities depend linearly on the fourth-order objects,

$${}^{\alpha i} \square_{\beta j} \equiv V_{\alpha i} V_{i\beta}^\dagger V_{\beta j} V_{j\alpha}^\dagger = V_{\alpha i} V_{\alpha j}^* V_{\beta i}^* V_{\beta j}, \quad (125)$$

which we will call “boxes” since each contains as factors the corners of a submatrix, or “box,” of the mixing matrix. For example,

$${}^{11} \square_{22} = V_{11} V_{12}^* V_{21}^* V_{22}. \quad (126)$$

These boxes are the neutrino equivalent of the “plaques” used by Bjorken and Dunietz for another purpose in the quark sector in reference [37]. In this work, we will examine the applications of using boxes to describe neutrino oscillations.

We have developed a graphical representation (discussed in detail in Appendix E) which proves useful when considering relationships between boxes. Figure 6 illustrates the representation of  ${}^{11} \square_{22}$ . This representation will be used throughout this Chapter to illustrate various relationships.

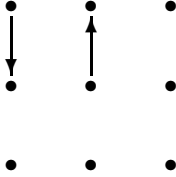


**Figure 6:** The graphical representation for the box  ${}^{11} \square_{22}$  in three generations. Vertical arrows point from the matrix elements which are not complex conjugated in the box to the complex-conjugated elements.

In general, each of the box indices  $i$ ,  $j$ ,  $\alpha$ , and  $\beta$  may be any number between 1 and  $n$ , the number of neutrino flavors. We therefore initially have  $n^4$  possible boxes. Examination of equation (125),

however, reveals a few symmetries in the indexing:

$${}^{\alpha i} \square_{\beta j} = {}^{\beta j} \square_{\alpha i} = {}^{\beta i} \square_{\alpha j}^* = {}^{\alpha j} \square_{\beta i}^*. \quad (127)$$

If the order of either set of indices is reversed (*id est*,  $j \leftrightarrow i$  or  $\beta \leftrightarrow \alpha$ ), the box turns into its complex conjugate; if both sets of indices are reversed, the box returns to its original value. Equation (127) demonstrates that boxes with  $\alpha = \beta$  or  $i = j$ , are real. Indeed, these are given from equation (125) as

$${}^{\alpha i} \square_{\alpha j} = |V_{\alpha i}|^2 |V_{\alpha j}|^2, \text{ and} \quad (128)$$

$${}^{\alpha i} \square_{\beta i} = |V_{\alpha i}|^2 |V_{\beta i}|^2. \quad (129)$$

Those boxes with both sets of indices equal are

$${}^{\alpha i} \square_{\alpha i} = |V_{\alpha i}|^4. \quad (130)$$

We call boxes with one or two repeated indices “singly-degenerate” and “doubly-degenerate,” respectively. As can be seen from equation (93), singly-degenerate boxes with repeated flavor indices enter into the formulae for flavor-conserving survival probabilities, but not for flavor-changing transition probabilities. Degenerate boxes with repeated mass indices (including the doubly-degenerate boxes) do not appear in any oscillation formula. Degenerate boxes may be expressed in terms of the nondegenerate boxes with  $\alpha \neq \beta$  and  $i \neq j$ , as will be shown shortly. This possibility and the symmetries expressed in equation (127) allow us to express combinations of boxes in terms of only the nondegenerate “ordered” boxes for which  $\alpha < \beta$  and  $i < j$ .

The number of flavor-index pairs satisfying  $\alpha < \beta$  ordering is  $N \equiv \binom{n}{2} = \frac{n(n-1)}{2}$ .  $N$  mass-index pairs similarly satisfy  $i < j$  ordering. Thus, the number of ordered nondegenerate boxes is  $N^2$ . The number of flavor-degenerate boxes is  $n^3$ , and that of mass-degenerate boxes is also  $n^3$ . The  $n^2$  doubly-degenerate boxes appear in both these counts, so the total number of degenerate boxes is  $2n^3 - n^2 = n^2(2n-1)$ , implying  $n^2(n-1)^2$  nondegenerate boxes. From the nondegenerate boxes,

we want to select only the ordered ones for which  $j > i$  and  $\beta > \alpha$ , which comprise one fourth of the nondegenerate boxes. The number of nondegenerate ordered boxes is therefore  $\left(\frac{n(n-1)}{2}\right)^2$ , as argued above. Applying ordering to the singly-degenerate boxes gives a count of  $\frac{1}{2}n^2(n-1) = nN$  for flavor-degenerate boxes, and the same for mass-degenerate boxes, yielding  $2nN$  total singly-degenerate ordered boxes. For  $n = 3$ ,  $N = 3$  too, and we have nine ordered nondegenerate boxes, nine ordered singly-degenerate boxes, and nine doubly-degenerate boxes. These counts are recapped later in Table 1, along with other box counts.

Using the symmetries expressed in equation (127), equation (93) becomes

$$\begin{aligned}
P_{\nu_\alpha \rightarrow \nu_\beta}(x) &= -\sum_{i=1}^n \sum_{j>i} [2\text{Re}(\alpha^i \square_{\beta j}) \sin^2 \Phi_{ij} - \text{Im}(\alpha^i \square_{\beta j}) \sin 2\Phi_{ij}] \\
&\quad - \sum_{i=1}^n \sum_{j< i} [2\text{Re}(\alpha^i \square_{\beta j}) \sin^2 \Phi_{ij} - \text{Im}(\alpha^i \square_{\beta j}) \sin 2\Phi_{ij}] \\
&= -\sum_{i=1}^n \sum_{j>i} [2\text{Re}(\alpha^i \square_{\beta j} + \alpha^i \square_{\beta j}^*) \sin^2 \Phi_{ij} - \text{Im}(\alpha^i \square_{\beta j} - \alpha^i \square_{\beta j}^*) \sin 2\Phi_{ij}] + \delta_{\alpha\beta} \\
&= -2 \sum_{i=1}^n \sum_{j>i} [2\text{Re}(\alpha^i \square_{\beta j}) \sin^2 \Phi_{ij} - \text{Im}(\alpha^i \square_{\beta j}) \sin 2\Phi_{ij}] + \delta_{\alpha\beta},
\end{aligned} \tag{131}$$

with  $\Phi_{ij}$  defined in equation (94). The survival probabilities  $P_{\nu_\alpha \rightarrow \nu_\alpha}(x)$  may be found from the transition probabilities  $P_{\nu_\alpha \rightarrow \nu_\beta}(x)$  by

$$P_{\nu_\alpha \rightarrow \nu_\alpha}(x) = 1 - \sum_{\beta \neq \alpha} P_{\nu_\alpha \rightarrow \nu_\beta}(x). \tag{132}$$

Interchanging  $\alpha \leftrightarrow \beta$  in equation (131) gives the time-reversed reactions  $P_{\nu_\beta \rightarrow \nu_\alpha}(x)$ :

$$P_{\nu_\beta \rightarrow \nu_\alpha}(x) = -2 \sum_{i=1}^n \sum_{j>i} [2\text{Re}(\alpha^i \square_{\beta j}) \sin^2 \Phi_{ij} + \text{Im}(\alpha^i \square_{\beta j}) \sin 2\Phi_{ij}] + \delta_{\alpha\beta}, \tag{133}$$

so a measure of T-violation, or equivalently CP-violation, in the neutrino sector is

$$P_{\nu_\alpha \rightarrow \nu_\beta}(x) - P_{\nu_\beta \rightarrow \nu_\alpha}(x) = 4 \sum_{i=1}^n \sum_{j>i} \text{Im}(\alpha^i \square_{\beta j}) \sin 2\Phi_{ij}. \tag{134}$$

Equation (131) may be expressed in matrix form. For three flavors, we find

$$\mathcal{P}(n=3) \equiv \begin{pmatrix} P_{\nu_e \rightarrow \nu_\mu}(x) \\ P_{\nu_\mu \rightarrow \nu_\tau}(x) \\ P_{\nu_e \rightarrow \nu_\tau}(x) \end{pmatrix} = -4 \operatorname{Re}(\mathcal{B}) S^2(\Phi) + 2 \operatorname{Im}(\mathcal{B}) S(2\Phi), \quad (135)$$

where

$$\mathcal{B} \equiv \begin{pmatrix} 11 \square_{22} & 12 \square_{23} & 11 \square_{23} \\ 21 \square_{32} & 22 \square_{33} & 21 \square_{33} \\ 11 \square_{32} & 12 \square_{33} & 11 \square_{33} \end{pmatrix}, \quad \text{and} \quad S^k(\Phi) \equiv \begin{pmatrix} \sin^k \Phi_{12} \\ \sin^k \Phi_{23} \\ \sin^k \Phi_{13} \end{pmatrix}. \quad (136)$$

Here the operation  $\operatorname{Re}(\mathcal{B})$  is defined so that  $[\operatorname{Re}(\mathcal{B})]_{kl} \equiv \operatorname{Re}(\mathcal{B}_{kl})$ ;  $\operatorname{Im}(\mathcal{B})$  is defined in a similar manner.  $\mathcal{B}$  and  $S^k(\Phi)$  are defined for three flavors in equation (136), and these definitions may be extended to any number of flavors. This extension, however, rapidly becomes difficult to manage. Adding a fourth, perhaps sterile, neutrino flavor increases the number of boxes from nine to thirty-six, since there are now six independent transition probabilities and six mass differences. For the six flavors of neutrinos in the see-saw mechanism,  $\mathcal{B}$  is a fifteen-by-fifteen matrix, and we have two hundred twenty-five boxes!

If CP is conserved, the boxes are real. CP conservation also implies time-reversal symmetry if CPT is a good symmetry, so  $P_{\nu_\alpha \rightarrow \nu_\beta}(x) = P_{\nu_\beta \rightarrow \nu_\alpha}(x)$ . These symmetries leave us with just three independent probabilities (assuming three flavors):

$$\begin{pmatrix} P_{\nu_e \rightarrow \nu_\mu}(x) \\ P_{\nu_\mu \rightarrow \nu_\tau}(x) \\ P_{\nu_e \rightarrow \nu_\tau}(x) \end{pmatrix} = -4 \begin{pmatrix} 11 \square_{22} & 12 \square_{23} & 11 \square_{23} \\ 21 \square_{32} & 22 \square_{33} & 21 \square_{33} \\ 11 \square_{32} & 12 \square_{33} & 11 \square_{33} \end{pmatrix} \begin{pmatrix} \sin^2 \Phi_{12} \\ \sin^2 \Phi_{23} \\ \sin^2 \Phi_{13} \end{pmatrix}. \quad (137)$$

Our three probabilities are, however, still functions of  $E$  and  $x$ , so different experiments may not measure the same values for a given oscillation probability, regardless of whether CP is conserved.

### 4.2.1 Mixing Matrix Elements and Boxes

Neutrino oscillation experiments will measure the boxes in equation (131), not the individual mixing matrix elements,  $V_{\alpha i}$ . But one would like to obtain the fundamental  $V_{\alpha i}$  from the measured boxes. Some tautologous relationships between the degenerate and nondegenerate boxes are easily confirmed using equation (125); they hold for any number of generations:

$$|V_{\alpha i}|^2 |V_{\alpha j}|^2 = {}^{\alpha i} \square_{\alpha j} = \frac{{}^{\alpha i} \square_{\eta j}^* {}^{\alpha i} \square_{\lambda j}}{{}^{\eta i} \square_{\lambda j}}, \quad (\eta \neq \lambda \neq \alpha), \quad (138)$$

$$|V_{\alpha i}|^2 |V_{\beta i}|^2 = {}^{\alpha i} \square_{\beta i} = \frac{{}^{\alpha i} \square_{\beta x}^* {}^{\alpha i} \square_{\beta y}}{{}^{\alpha x} \square_{\beta y}}, \quad (x \neq y \neq i), \quad \text{and} \quad (139)$$

$$\frac{|V_{\alpha i}|^2}{|V_{\beta j}|^2} = \frac{{}^{\alpha i} \square_{\eta j}^* {}^{\alpha i} \square_{\beta x}}{{}^{\alpha j} \square_{\beta x} {}^{\beta i} \square_{\eta j}^*}, \quad (\eta \neq \alpha \neq \beta, \text{ and } x \neq i \neq j). \quad (140)$$

In these equations and what follows,  $\alpha, \beta, \gamma, i, j$ , and  $k$  will usually be reserved for indices that are chosen at the start of a calculation, while other indices such as  $x, y, \eta$ , and  $\lambda$  primarily represent “dummy” indices which are chosen arbitrarily except to respect the inequality constraints following equations such as equation (140).

The tautologies (138) to (140) become evident not only by algebraically using the definitions of the boxes, but also by considering the graphical representation described in Appendix E. For example, the degenerate box  ${}^{12} \square_{13}$  is “created” when one uncanceled vertical arrow enters and another leaves each of the matrix elements  $V_{12}$  and  $V_{13}$ , while arrows at all other points cancel. This is illustrated in Figure 7a. Those arrows are the result of the combination of ordered boxes given in (138), as shown in Figure 7b.

Equations (138) and (139) are themselves special cases of the more general

$$\begin{aligned} {}^{\alpha i} \square_{\beta j} {}^{\gamma i} \square_{\delta j} &= [V_{\alpha i} V_{\alpha j}^* V_{\beta j} V_{\beta i}^*] [V_{\gamma i} V_{\gamma j}^* V_{\delta j} V_{\delta i}^*] \\ &= [V_{\alpha i} V_{\alpha j}^* V_{\delta j} V_{\delta i}^*] [V_{\gamma i} V_{\gamma j}^* V_{\beta j} V_{\beta i}^*] = {}^{\alpha i} \square_{\delta j} {}^{\gamma i} \square_{\beta j}, \end{aligned} \quad (141)$$

and the analogous relation

$${}^{\alpha i} \square_{\beta j} {}^{\alpha k} \square_{\beta l} = {}^{\alpha i} \square_{\beta l} {}^{\alpha k} \square_{\beta j}. \quad (142)$$

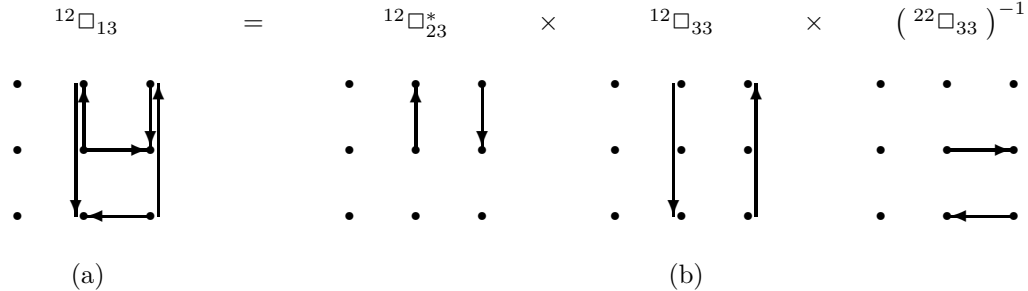


**Figure 7:** The graphical representation in three generations for (a) the degenerate box  ${}^{12}\square_{13}$ , and (b) the combination of nondegenerate boxes which “create” it.

These relations hold for both degenerate boxes and nondegenerate boxes. Including disordered boxes adds no new information, so we will as usual consider only ordered boxes on one side of the equation. (Swapping indices to produce the other side of the equation may lead to disordered boxes on that side, but that can quickly be remedied by using equations (127)). If  $\alpha = \gamma$  or  $\beta = \delta$  for equation (141), or if  $i = k$  or  $j = l$  for equation (142), the relationships are trivial. Ordering of these pairs, however, should not be imposed.

Consider the second relation, (142). Each of the  $\frac{1}{2}n(n+1)$  ordered plus degenerate pairings of  $(\alpha, \beta)$  contains  $\frac{1}{12}n(n+1)(3n-2)(n-1)$  nontrivial relations with  $j \neq l, i \neq k, i \leq j$ , and  $k \leq l$ .<sup>1</sup> In all, equation (142) implies  $\frac{1}{24}n^2(n+1)^2(n-1)(3n-2)$  nontrivial relations, as does equation (141). On the other hand, if we restrict ourselves to considering only the  $N$  boxes nondegenerate in  $(\alpha, \beta)$ ,  $(i, j)$ , and  $(k, l)$ , the number of constraints drops to  $\frac{1}{12}n(n-1)(n-2)(3n-5)$   $j \neq l, i \neq k, i < j$ ,  $k < l$  combinations for each of the  $N$   $\alpha < \beta$  pairings,<sup>2</sup> leading to a total number of nondegenerate constraints given by  $\frac{1}{24}n^2(n-1)^2(n-2)(3n-5)$ . Degenerate boxes participate in the majority of the relations implied by equations (141) and (142). For  $n = 3$ , the number of  $i, j, k, l$  combinations

<sup>1</sup> We arrive at this number by considering all  $\left(\frac{1}{2}n(n+1)\right)^2$  ( $i \leq j, k \leq l$ ) pairings, then subtracting the  $\frac{1}{2}n(n+1)$  ( $l = j, k = i, i \leq j$ ) possibilities, followed by the  $\binom{n}{3} = \frac{1}{3}n(n-1)(n-2)$  ( $l \neq j, k = i, i < \min(j, l)$ ) combinations and the same number of ( $j = l, k \neq i, j > \max(i, k)$ ) combinations. We must also subtract the  $2\binom{n}{2} = n(n-1)$  ( $l \neq j, k = i = \min(j, l)$ ) possibilities and the same number of ( $k \neq i, j = l = \max(i, k)$ ) possibilities. So the number of terms in the sum  $\sum_{j \neq l, i \neq k, i \leq j, k \leq l}$  is  $\left(\frac{1}{2}n(n+1)\right)^2 - \frac{1}{2}n(n+1) - 2\binom{n}{3} - 2n(n-1) = \frac{1}{12}n(n+1)(3n-2)(n-1)$ .

<sup>2</sup> To obtain this number, we remove the  $i = j$  and  $k = l$  possibilities. So we start with only  $\left(\frac{1}{2}n(n-1)\right)^2$  ( $i < j, k < l$ ) pairings and subtract  $\frac{1}{2}n(n-1)$  ( $l = j, k = i, i < j$ ) combinations followed by  $\frac{1}{3}n(n-1)(n-2)$  twice as above. The  $2n(n-1)$  pairings for ( $l \neq j, k = i = \min(j, l)$ ) and ( $k \neq i, j = l = \max(i, k)$ ) do not occur in our original sum since  $i \neq j$  and  $k \neq l$  in that sum. The number of terms in the sum  $\sum_{j \neq l, i \neq k, i < j, k < l}$  is therefore  $\left(\frac{1}{2}n(n-1)\right)^2 - \frac{1}{2}n(n-1) - 2\binom{n}{3} = \frac{1}{12}n(n-1)(n-2)(3n-5)$ .

in equation (142) including degenerate boxes is 14; without degenerate boxes this number decreases to 2. These numbers are doubled once the relationships implied by equation (141) are considered as well.

This index rearrangement of equations (141) and (142) may straightforwardly be extended to obtain higher-order relationships (trilinear, quadrilinear, *et cetera*) in the boxes. These higher-order relationships do not enter in our treatment of oscillation probabilities, so we will not examine them here.

We may find  $|V_{\alpha i}| = (\alpha^i \square_{\alpha i})^{\frac{1}{4}}$  in terms of three singly-degenerate boxes by setting  $\alpha = \beta$  in equation (139). Using equation (138) to substitute for the singly-degenerate boxes yields an expression for the doubly-degenerate box in terms of nine nondegenerate boxes:

$$|V_{\alpha i}|^4 = \alpha^i \square_{\alpha i} = \frac{\alpha^i \square_{\alpha x} \alpha^i \square_{\alpha y}}{\alpha x \square_{\alpha y}} = \frac{\alpha x \square_{\tau i} \alpha^i \square_{\sigma x} \alpha y \square_{\rho i} \alpha^i \square_{\zeta y} \omega x \square_{\mu y}}{\tau i \square_{\sigma x} \rho i \square_{\zeta y} \alpha y \square_{\omega x} \alpha x \square_{\mu y}}, \quad \left\{ \begin{array}{l} \tau \neq \sigma \neq \alpha \\ \zeta \neq \rho \neq \alpha \\ \mu \neq \omega \neq \alpha \\ x \neq y \neq i \end{array} \right. \quad (143)$$

As noted earlier, flavor-degenerate boxes give the probabilities for flavor-conserving oscillations, while nondegenerate boxes give the probabilities for flavor-changing oscillations. Thus individual  $|V_{\alpha i}|$  may be deduced from a set of measurements of either kind. One can obtain a relationship similar to equation (143) by setting  $i = j$  in equation (138) and then using equation (139) to substitute for the singly-degenerate boxes:

$$|V_{\alpha i}|^4 = \alpha^i \square_{\alpha i} = \frac{\alpha^i \square_{\lambda i} \alpha^i \square_{\eta i}}{\lambda i \square_{\eta i}} = \frac{\alpha^i \square_{\lambda n} \lambda i \square_{\alpha p} \alpha^i \square_{\eta r} \eta i \square_{\alpha s} \eta t \square_{\lambda u}}{\lambda n \square_{\alpha p} \eta r \square_{\alpha s} \lambda i \square_{\eta t} \eta i \square_{\lambda u}}, \quad \left\{ \begin{array}{l} n \neq p \neq i \\ r \neq s \neq i \\ t \neq u \neq i \\ \lambda \neq \eta \neq \alpha \end{array} \right. \quad (144)$$

In the three-generation case, these equations are unique and equivalent to each other, since all nine boxes are used in both equations. This equivalence may be seen by choosing  $s = n = u = x$ ,

$r = p = t = y$ ,  $\sigma = \rho = \omega = \lambda$ , and  $\tau = \zeta = \mu = \eta$ , which yields for either expression (143) or (144)

$$|V_{11}|^4 = \frac{^{11}\square_{22} \ ^{21}\square_{13} \ ^{11}\square_{33} \ ^{31}\square_{12} \ ^{33}\square_{22}}{^{22}\square_{13} \ ^{33}\square_{12} \ ^{21}\square_{33} \ ^{31}\square_{22}} = \frac{^{11}\square_{22} \ ^{11}\square_{23}^* \ ^{11}\square_{33} \ ^{11}\square_{32}^* \ ^{22}\square_{33}}{^{12}\square_{23}^* \ ^{12}\square_{33} \ ^{21}\square_{33} \ ^{21}\square_{32}^*} \quad (145)$$

for the case  $\alpha = i = 1$ . The second equality merely represents a substitution of ordered boxes for disordered boxes. Two other examples are

$$|V_{21}|^4 = \frac{^{21}\square_{32} \ ^{11}\square_{22} \ ^{21}\square_{33} \ ^{11}\square_{23} \ ^{12}\square_{33}}{^{11}\square_{32} \ ^{11}\square_{33} \ ^{22}\square_{33} \ ^{12}\square_{23}}, \text{ and} \quad (146)$$

$$|V_{31}|^4 = \frac{^{11}\square_{32} \ ^{21}\square_{32}^* \ ^{21}\square_{33} \ ^{11}\square_{33}^* \ ^{12}\square_{23}}{^{11}\square_{22} \ ^{11}\square_{23}^* \ ^{12}\square_{33} \ ^{22}\square_{33}^*}. \quad (147)$$

The equalities (145), (146), and (147) are illustrated in Figure 8.

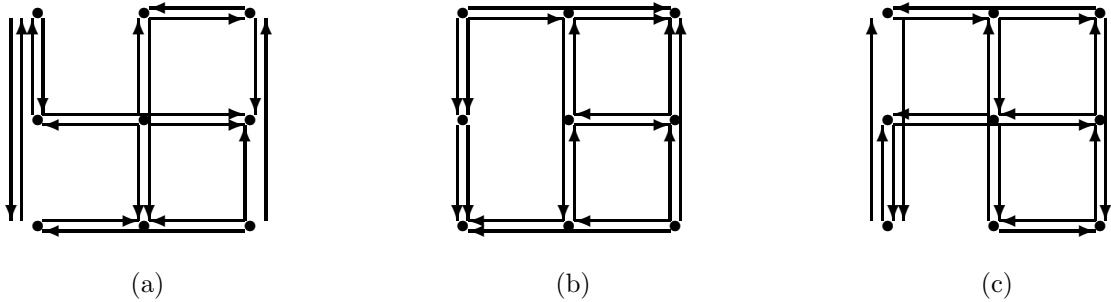


**Figure 8:** The graphical representation for (a)  $|V_{11}|^4$ , (b)  $|V_{21}|^4$ , and (c)  $|V_{31}|^4$ . Notice that each matrix point except the one being represented has an equal number of vertical arrows as horizontal arrows entering and leaving. The element being represented has two vertical arrows leaving (representing  $V_{\alpha i}^2$ ) and two entering (representing  $V_{\alpha i}^{*2}$ ) to produce  $|V_{\alpha i}|^2$ . Appendix E describes how these were produced, using  $|V_{21}|^4$  as an example.

Before continuing, we should note that all of the relationships in this Section follow from the definitions of the boxes in equation (125) and so are valid for any matrix, unitary or otherwise. The unitarity of  $V$  will impose further relations among the boxes which may not hold for models which only approximate unitarity of the mixing matrix. Equations (138) to (142), however, will always hold.

### 4.2.2 Using Unitarity to Reduce the Number of Independent Boxes

An  $n \times n$  arbitrary matrix has  $n^2$  elements, which may be complex, leading to  $2n^2$  parameters. Our mixing matrix, however, is unitary, and has  $n^2$  unitarity conditions as constraints. Of the  $n^2$  remaining parameters,  $\frac{1}{2}n(n-1)$  (the number of parameters in a real unitary, or orthogonal, matrix) are real, and the remaining  $\frac{1}{2}n(n+1)$  are imaginary phases. As discussed in Section 4.1, we may remove  $2n-1$  relative phases from the mixing matrix, leaving  $\frac{1}{2}n(n+1)-(2n-1)=\frac{1}{2}(n-1)(n-2)$  phases measurable in oscillations. If the phases are all zero, all of the boxes are real, so CP violation, as expressed in equation (134) disappears. Similarly, if any of the phases are not zero, CP is violated in the neutrino sector.

The total number of CKM mixing matrix parameters is  $n^2 - (2n - 1) = (n - 1)^2$ . The number of real and imaginary independent box parameters should be the same as the number of real and imaginary CKM parameters [39], but the reduction to a basis is complicated for boxes. The number of ordered boxes  $N^2$  grows much faster than the number of mixing matrix elements  $n^2$  and exceeds that number once  $n > 3$ , so we need more box constraints than mixing matrix constraints for the higher numbers of generations. The parameter counts for the mixing matrix and the boxes are summarized in Table 1.

**Table 1:** Parameter counting for the mixing matrix and boxes.  $N^2$  is the number of ordered, nondegenerate boxes, with  $N \equiv \frac{1}{2}n(n-1)$ .

Number of generations	$n$	2	3	4	6
Params. for arbitrary matrix	$2n^2$	8	18	32	72
Unitarity constraints	$n^2$	4	9	16	36
Relative phases	$2n - 1$	3	5	7	11
Real params for unitary $V$	$N$	1	3	6	15
Remaining phases in $V$	$\frac{1}{2}(n-1)(n-2)$	0	1	3	10
Initial boxes	$n^4$	16	81	256	1296
Doubly-degenerate boxes	$n^2$	4	9	16	36
Ordered singly-degenerate boxes	$2nN$	4	18	48	180
Ordered nondegenerate boxes	$N^2$	1	9	36	225
Independent $\text{Im}(\alpha^i \square_{\beta j})$ s	$\frac{1}{2}(n-1)(n-2)$	0	1	3	10
Independent $\text{Re}(\alpha^i \square_{\beta j})$ s	$N$	1	3	6	15

Unitarity requires that

$$\sum_{\eta=1}^n V_{\eta i} V_{\eta j}^* = \delta_{ij}, \quad \text{and} \quad (148)$$

$$\sum_{y=1}^n V_{\alpha y} V_{\beta y}^* = \delta_{\alpha\beta}. \quad (149)$$

These equations are not independent sets of constraints at this point.<sup>3</sup> Equation (148) states  $V^\dagger V \equiv \mathbb{1}$ , and equation (149) states  $V V^\dagger \equiv \mathbb{1}$ , which is implied by the previous expression and the associativity of matrix multiplication:

$$V V^\dagger \equiv \mathbb{1} \Rightarrow (V V^\dagger) V = V (V^\dagger V) = V \Rightarrow (V^\dagger V) \equiv \mathbb{1}. \quad (150)$$

We can, however, use these equivalent equations to obtain two separate sets of constraints on boxes by multiplying equation (148) by  $V_{\lambda i}^* V_{\lambda j}$  and equation (149) by  $V_{\alpha x}^* V_{\beta x}$ :

$$\sum_{\eta=1}^n V_{\lambda i}^* V_{\lambda j} V_{\eta i} V_{\eta j}^* = V_{\lambda i}^* V_{\lambda j} \delta_{ij}, \quad \text{so} \quad (151)$$

$$\sum_{\eta=1}^n {}^{\eta i} \square_{\lambda j} = \sqrt{{}^{\lambda i} \square_{\lambda i}} \delta_{ij}, \quad \text{and} \quad (152)$$

$$\sum_{y=1}^n V_{\alpha x}^* V_{\beta x} V_{\alpha y} V_{\beta y}^* = V_{\alpha x}^* V_{\beta x} \delta_{\alpha\beta}, \quad \text{or} \quad (153)$$

$$\sum_{y=1}^n {}^{\alpha y} \square_{\beta x} = \sqrt{{}^{\alpha x} \square_{\alpha x}} \delta_{\alpha\beta}. \quad (154)$$

Separating the manifestly degenerate boxes and the nondegenerate boxes, equation (152) becomes

$$\sum_{\eta \neq \lambda} {}^{\eta i} \square_{\lambda j} = \sqrt{{}^{\lambda i} \square_{\lambda i}} \delta_{ij} - {}^{\lambda i} \square_{\lambda j}, \quad (155)$$

and equation (154) becomes

$$\sum_{y \neq x} {}^{\alpha y} \square_{\beta x} = \sqrt{{}^{\alpha x} \square_{\alpha x}} \delta_{\alpha\beta} - {}^{\alpha x} \square_{\beta x}. \quad (156)$$

---

<sup>3</sup> The number of unitarity constraints  $n^2$  becomes clear from examination of either equation (148) or (149). Equation (148) gives a real constraint for each of the  $n$   $i = j$  choices,  $N$  constraints from the real parts of the sum when  $i \neq j$ , and  $N$  constraints from the imaginary parts of the  $i \neq j$  sum. Thus we have  $n + 2N = n^2$  unitarity constraints from either one of the equations (148) and (149). As argued next, the two equations are redundant, so the total number of constraints on the mixing matrix is just  $n^2$ .

Summing equation (152) over  $\lambda$  in the  $i \neq j$  case, we find

$$0 = \sum_{\lambda=1}^n \sum_{\eta=1}^n \eta^i \square_{\lambda j} = \sum_{\lambda=1}^n \left[ \lambda^i \square_{\lambda j} + \sum_{\eta \neq \lambda} \eta^i \square_{\lambda j} \right] = \sum_{\lambda=1}^n \lambda^i \square_{\lambda j} + 2 \sum_{\lambda=1}^n \sum_{\eta < \lambda} \eta^i \square_{\lambda j}. \quad (157)$$

Comparison with equations (136) and (138) shows that the sum of a column of  $\text{Re}(\mathcal{B})$  which has a fixed  $i$  and  $j$  should equal  $-\frac{1}{2} \sum_{\lambda=1}^n |V_{\lambda i}|^2 |V_{\lambda j}|^2$ . We may in a similar manner show that the sum of a row of  $\text{Re}(\mathcal{B})$  with fixed  $\alpha$  and  $\beta$  equals  $-\frac{1}{2} \sum_{x=1}^n |V_{\alpha x}|^2 |V_{\beta x}|^2$ .

An alternative way to obtain constraints from unitarity is to start with the definition of the boxes (125) and use the unitarity of the mixing matrix:

$${}^{\alpha i} \square_{\beta j} = (V_{\alpha i} V_{\alpha j}^*) (V_{\beta j} V_{\beta i}^*) = \left( \delta_{ij} - \sum_{\eta \neq \alpha} V_{\eta i} V_{\eta j}^* \right) \left( \delta_{ij} - \sum_{\lambda \neq \beta} V_{\lambda j} V_{\lambda i}^* \right). \quad (158)$$

After a bit of algebra, this becomes

$$\sum_{\eta \neq \alpha} \sum_{\lambda \neq \beta} \eta^i \square_{\lambda j} = {}^{\alpha i} \square_{\beta j} - \delta_{ij} (-1 + |V_{\alpha i}|^2 + |V_{\beta i}|^2). \quad (159)$$

This relation is equivalent to using our result (152), as shown below:

$$\begin{aligned} \sum_{\lambda \neq \beta} \sum_{\eta \neq \alpha} \eta^i \square_{\lambda j} &= \sum_{\lambda \neq \beta} \left( \sum_{\eta=1}^n \eta^i \square_{\lambda j} - {}^{\alpha i} \square_{\lambda j} \right) = \sum_{\lambda \neq \beta} (|V_{\lambda i}|^2 \delta_{ij} - {}^{\alpha i} \square_{\lambda j}) \\ &= \delta_{ij} \sum_{\lambda \neq \beta} |V_{\lambda i}|^2 - \left( \sum_{\lambda=1}^n {}^{\alpha i} \square_{\lambda j} - {}^{\alpha i} \square_{\beta j} \right) \\ &= \delta_{ij} (1 - |V_{\beta i}|^2) - |V_{\alpha i}|^2 \delta_{ij} + {}^{\alpha i} \square_{\beta j} \end{aligned} \quad (160)$$

Equations (152) and (154) each present  $\frac{1}{2} n^2 (n+1)$  relations among the  $N^2$  complex ordered nondegenerate boxes, the  $2nN$  real ordered singly-degenerate boxes, and the  $n^2$  doubly-degenerate boxes. Not all of these constraints are independent. We can identify one source of redundancy by summing equation (152) over  $\lambda$ :

$$\sum_{\lambda=1}^n \sum_{\eta=1}^n \eta^i \square_{\lambda j} = \sum_{\lambda=1}^n \sqrt{\lambda^i \square_{\lambda i}} \delta_{ij} = \sum_{\lambda=1}^n |V_{\lambda i}|^2 \delta_{ij} = \delta_{ij}, \quad (161)$$

which is pure real, so

$$\sum_{\lambda=1}^n \sum_{\eta=1}^n \mathfrak{J}_{\lambda j}^i = 0, \quad (162)$$

where we have introduced the notation  $\mathfrak{J}_{\beta j}^i \equiv \text{Im}(\alpha^i \square_{\beta j})$ . We will similarly define  $\mathfrak{R}_{\beta j} \equiv \text{Re}(\alpha^i \square_{\beta j})$ .

Since the imaginary sum in equation (162) vanishes, at most  $n - 1$  of the values for  $\lambda$  give independent imaginary constraints. The real constraints exhibit no such obvious dependency, so all  $n$  values of  $\lambda$  appear at this point to offer independent constraints. Equations (152) and (154) therefore each offer at most  $\frac{1}{2}n(n - 1)^2$  imaginary constraints and  $\frac{1}{2}n^2(n - 1)$  real constraints for  $i \neq j$  and  $\alpha \neq \beta$ , respectively.

The number of unitarity constraints from equations (152) and (154), both real and imaginary, grows as  $n^3$ , while the number of ordered boxes grows as  $n^4$ , so additional relationships between ordered boxes must be used to identify the  $(n - 1)^2$  independent  $J$ s and  $R$ s. These additional identities will come from the definitions of the boxes, and the resulting tautologies (141) and (142), each of which grows as  $n^6$ , implying a high degree of redundancy. Some of these relationships are explored below in equations (201) to (205).

The constraints (152) and (154) hold independently for the real and imaginary parts of each sum. Because the right-hand sides of the equations are manifestly real, as are terms on the left-hand side involving degenerate boxes, the sums of nondegenerate boxes in equations (154) and (152) must be real. This leads to imaginary constraints of the form<sup>4</sup>

$$\sum_{\eta \neq \lambda} \mathfrak{J}_{\lambda j}^i = 0, \quad \text{and} \quad (165)$$

$$\sum_{y \neq x} \alpha \mathfrak{J}_{\beta x} = 0. \quad (166)$$

---

<sup>4</sup> The constraints (165) and (166) may be written exclusively in terms of ordered boxes as

$$\sum_{\eta < \lambda} \mathfrak{J}_{\lambda j}^i - \sum_{\eta > \lambda} \mathfrak{J}_{\eta j}^i = 0, \quad \text{and} \quad (163)$$

$$\sum_{y < x} \alpha \mathfrak{J}_{\beta x} - \sum_{y > x} \alpha \mathfrak{J}_{\beta y} = 0. \quad (164)$$

While expressing everything in terms of ordered boxes is our goal, we will find it more convenient to use the complete sums of equations (165) and (166) in mathematical manipulations and switch to ordered boxes at the end rather than to deal with the two separate terms in equations (163) and (164).

In three generations, each sum in equation (165) or (166) contains only two terms, leading to the equality (up to a sign) of two  $J$ s. For example, choosing  $\lambda = 1$  in three generations yields

$${}^1\mathbb{J}_{2i} = - {}^1\mathbb{J}_{3i}. \quad (167)$$

Choosing  $\lambda = 2$  relates the imaginary parts of  ${}^{2j}\square_{3i}$  and  ${}^{1j}\square_{2i}^*$ . As discussed above, at least one value of  $\lambda$  leads to redundant constraints from equation (165); choosing  $\lambda = 3$ , which relates the imaginary parts of  ${}^{2j}\square_{3i}^*$  and  ${}^{1j}\square_{3i}^*$ , is not independent of the first two constraints. For each of the  $n - 1$  choices of  $\lambda$  not manifestly redundant, we may choose  $\frac{1}{2}n(n - 1)$  combinations for  $i < j$ . Equation (166) has  $\frac{1}{2}n(n - 1)^2$  possible index combinations as well, giving  $n(n - 1)^2$  total imaginary constraints. In three generations, this results in 12 constraints on 9 ordered  $J$ s; clearly more redundancies among relations (165) and (166) must exist!

The first set of imaginary constraints (165) relates boxes that are part of a column of  $\mathcal{B}$ , which was defined in equation (135); the second set (166) relates boxes that are part of a row of  $\mathcal{B}$ . Given this separation, it becomes clear that the constraints derived from equation (152) and those derived from equation (154) are both necessary. Once one combines the two sets of constraints, however, more redundancies appear.

For example, we may relate  ${}^1\mathbb{J}_{22}$  to  ${}^1\mathbb{J}_{33}$  by using equation (165) for  $i = 1, j = 2$  with  $\lambda = 2$  and then  $\lambda = 3$ , followed by equation (166) for  $\alpha = 1, \beta = 3$  with  $x = 2$  and then  $x = 3$ :

$${}^1\mathbb{J}_{22} = {}^2\mathbb{J}_{32} = - {}^1\mathbb{J}_{32} = - {}^1\mathbb{J}_{33} = {}^1\mathbb{J}_{33}. \quad (168)$$

This path is indicated in Figure 9 by the solid arrows. Note that the matrix points in this Figure represent boxes in the matrix  $\text{Im}(\mathcal{B})$ , not mixing matrix elements. We may alternatively use equation (166) for  $\alpha = 1, \beta = 2$  with  $x = 2$  and then  $x = 3$ , followed by equation (165) for  $i = 1, j = 3$  with  $\lambda = 2$  and then  $\lambda = 3$ :

$${}^1\mathbb{J}_{22} = {}^1\mathbb{J}_{23} = - {}^1\mathbb{J}_{23} = - {}^2\mathbb{J}_{33} = {}^1\mathbb{J}_{33}. \quad (169)$$

This path is represented by the dashed arrows in Figure 9.

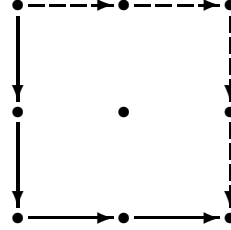


**Figure 9:** An illustration of two different paths relating  $\mathbb{H}_{22}$  with  $\mathbb{H}_{33}$ . An equality (up to a minus sign) between two  $J$ s is represented by an arrow connecting those two  $J$ s. The solid arrows represent the path of equation (168), and the dashed arrows represent the path of equation (169). The matrix represented here is  $\text{Im}(\mathcal{B})$ , not  $V$ ; this illustration is not an application of the graphical representation developed in Appendix E.

The number of independent constraints contained in equations (165) and (166) may be determined in three generations by counting the number of non-redundant connecting lines in a graph like Figure 9. Figure 10a contains all 18 connecting lines implied by equations (165) and (166) for  $n = 3$ . Figure 10b illustrates the minimum number (8) of independent lines required to connect all nine imaginary parts. Thus eight of our original eighteen constraints are independent, leaving us with only one imaginary part as expected, which we'll call  $\mathcal{J} \equiv \mathbb{H}_{22}$ . Using these remaining constraints, we find

$$\text{Im}(\mathcal{B}) = \begin{pmatrix} \mathcal{J} & \mathcal{J} & -\mathcal{J} \\ \mathcal{J} & \mathcal{J} & -\mathcal{J} \\ -\mathcal{J} & -\mathcal{J} & \mathcal{J} \end{pmatrix} \quad (170)$$

for three generations.

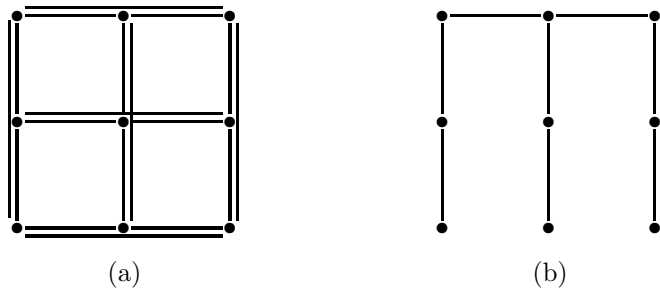


**Figure 10:** An illustration of a) all imaginary constraints, and b) eight independent imaginary constraints.

For  $n > 3$  generations, the sums in equations (165) and (166) contain more than two terms,

so individual  $J$ s become equal to sums of other  $J$ s rather than just equal to another individual  $J$ . Our illustrative method is therefore not applicable to the  $n > 3$  case. In addition, the reduction of imaginary parameters using equations (165) and (166) is no longer sufficient to eliminate all the extra degrees of freedom. In four generations, the total number of sums relating the 36  $J$ s is 48, but we can demonstrate the redundancy of 21 constraints, leaving 9 apparently independent imaginary parameters. But we know from consideration of the mixing matrix and from the work of [39] that only 3 imaginary parameters are truly independent. The additional 6 constraints must come from the expressions relating real and imaginary parameters discussed below. Such a reduction to a basis for the four-generation case, while possible, is fodder for another's dissertation and therefore will not be presented here.

The equality of imaginary boxes for  $n = 3$  has an interesting implication for CP invariance. The CP-violating contribution to oscillation probabilities (134) becomes

$$\pm 4\mathcal{J} (\sin 2\Phi_{12} + \sin 2\Phi_{23} - \sin 2\Phi_{13}), \quad (171)$$

where the plus sign applies for  $P_{\nu_e \rightarrow \nu_\mu}(x)$  and  $P_{\nu_\mu \rightarrow \nu_\tau}(x)$ , and the minus sign for  $P_{\nu_e \rightarrow \nu_\tau}(x)$ . CP is violated if two conditions are met [33]: i)  $\mathcal{J} \neq 0$ , and ii)  $m_i^2 \neq m_j^2$ , for all  $i, j$ . The first condition should be obvious, since a vanishing  $\mathcal{J}$  clearly makes the expression (171) vanish. The second condition follows rather simply also. If any two masses are degenerate,  $m_i^2 = m_j^2$ , the corresponding  $\Phi_{ij}$  vanishes, and the remaining two terms in equation (171) will be equal but opposite. For example, if  $m_1^2 = m_2^2$ , then  $\Phi_{12} = 0$ ,  $\Phi_{23} = \frac{x}{4p} (m_2^2 - m_3^2)$ ,  $\Phi_{13} = \frac{x}{4p} (m_1^2 - m_3^2) = \frac{x}{4p} (m_2^2 - m_3^2) = \Phi_{23}$ , and the CP-violating term disappears as predicted.

Even if the conditions i) and ii) are met, CP-violation may be difficult to directly observe in experiments. The CP-violating term contains the sum

$$\sin 2\Phi_{12} + \sin 2\Phi_{23} - \sin 2\Phi_{13} = \sin \frac{x\Delta m_{12}^2}{2p} + \sin \frac{x\Delta m_{23}^2}{2p} - \sin \frac{x(\Delta m_{12}^2 + \Delta m_{23}^2)}{2p}. \quad (172)$$

Using trigonometric identities, we may write

$$\sin \frac{x(\Delta m_{12}^2 + \Delta m_{23}^2)}{2p} = \sin \frac{x\Delta m_{12}^2}{2p} \cos \frac{x\Delta m_{23}^2}{2p} + \cos \frac{x\Delta m_{12}^2}{2p} \sin \frac{x\Delta m_{23}^2}{2p}, \quad (173)$$

so the CP-violating term is

$$\begin{aligned} \sin \frac{x\Delta m_{12}^2}{2p} + \sin \frac{x\Delta m_{23}^2}{2p} - \sin \frac{x\Delta m_{12}^2}{2p} \cos \frac{x\Delta m_{23}^2}{2p} - \cos \frac{x\Delta m_{12}^2}{2p} \sin \frac{x\Delta m_{23}^2}{2p} \\ = \sin \frac{x\Delta m_{12}^2}{2p} \left( 1 - \cos \frac{x\Delta m_{23}^2}{2p} \right) + \sin \frac{x\Delta m_{23}^2}{2p} \left( 1 - \cos \frac{x\Delta m_{12}^2}{2p} \right) \\ = 2 \sin 2\Phi_{12} \sin^2 \Phi_{23} + 2 \sin 2\Phi_{23} \sin^2 \Phi_{12}. \end{aligned} \quad (174)$$

If  $\Phi_{12}$  is small, CP violation is of the order

$$4\Phi_{12} \sin^2 \Phi_{23}. \quad (175)$$

If all phases are small,  $\sin 2\Phi_{ij} \sim 2\Phi_{ij} - \frac{4}{3}\Phi_{ij}^3$ , and the CP-violating term becomes

$$\begin{aligned} & \pm 4\mathcal{J} \left( \frac{x}{2p} [(m_1^2 - m_2^2) + (m_2^2 - m_3^2) - (m_1^2 - m_3^2)] \right. \\ & \left. - \frac{x^3}{48p^3} [(m_1^2 - m_2^2)^3 + (m_2^2 - m_3^2)^3 - (m_1^2 - m_3^2)^3] + \dots \right) \\ & = \pm \mathcal{J} \frac{3x^3}{4p^3} ((m_1^2 - m_2^2)(m_2^2 - m_3^2)(m_3^2 - m_1^2)) + \dots \end{aligned} \quad (176)$$

In particular, the first order term in  $\Phi_{ij}$  has vanished; even though the kinematic phases scale with the square of neutrino mass, the CP-violating linear combination of phases scales with the sixth power of neutrino mass.

This phenomenon holds even for higher numbers of generations: the CP-violating term (134) is

$$\begin{aligned} 4 \sum_i \sum_{j>i} \mathfrak{J}_{\beta j}^i \sin 2\Phi_{ij} &= 4 \sum_i \sum_{j>i} \mathfrak{J}_{\beta j}^i (2\Phi_{ij} + \mathcal{O}(m^6)) \\ &\approx 4 \frac{x}{p} \sum_i \sum_{j>i} \mathfrak{J}_{\beta j}^i (m_i^2 - m_j^2) \\ &= 4 \frac{x}{p} \left[ \sum_i m_i^2 \sum_{j>i} \mathfrak{J}_{\beta j}^i - \sum_i \sum_{j>i} m_j^2 \mathfrak{J}_{\beta j}^i \right]. \end{aligned} \quad (177)$$

The double sum in equation (177)  $\sum_i \sum_{j>i}$  contains all  $i < j$  combinations, as does the double sum  $\sum_j \sum_{i< j}$ , so we may substitute the latter for the former in the second term of equation (177). We may then exchange the dummy indices  $i, j$  in the second term to obtain an overall sum which is equivalent to the sum in equation (165):

$$\begin{aligned}
\sum_i m_i^2 \sum_{j>i} \alpha_{\beta j}^i - \sum_i \sum_{j>i} m_j^2 \alpha_{\beta j}^i &= \sum_i m_i^2 \sum_{j>i} \alpha_{\beta j}^i - \sum_j \sum_{i< j} m_j^2 \alpha_{\beta j}^i \\
&= \sum_i m_i^2 \sum_{j>i} \alpha_{\beta j}^i - \sum_i \sum_{j< i} m_i^2 \alpha_{\beta j}^i \\
&= \sum_i m_i^2 \sum_{j>i} \alpha_{\beta j}^i + \sum_i \sum_{j< i} m_i^2 \alpha_{\beta j}^i \\
&= \sum_i m_i^2 \sum_{j \neq i} \alpha_{\beta j}^i = 0.
\end{aligned} \tag{178}$$

Thus, for any number of generations, the CP-violating contribution to neutrino oscillations when the phases are small becomes on the order of  $(\Phi_{ij})^3$ , which is the order of  $(\Delta m_{ij})^6$  and therefore negligible for small  $m$ .<sup>5</sup>

In Chapter VI we show that reasonable values for the mass-squared differences yield phases too small to produce a CP-violating effect observable at current accelerator experiments. Longer baseline experiments would, of course, allow larger phases, so CP violation too small to be detected at accelerator sites could possibly be detected by long-baseline experiments unless matter effects conspire to reduce its effect [40]. We will discuss below the possibility of detecting the effects of CP violations, even when CP violation is not directly observable.

The real parts of the constraints (152) and (154) also lead to interesting conclusions. Consider first the homogeneous constraints for which the Kronecker delta is zero. These relationships give the singly-degenerate boxes as sums of ordered boxes:

$$|V_{\lambda i}|^2 |V_{\lambda j}|^2 = {}^{\lambda i} \square_{\lambda j} = - \sum_{\eta \neq \lambda} {}^{\eta i} \square_{\lambda j} = - \sum_{\eta \neq \lambda} \mathbb{R}_{\lambda j}, \quad i \neq j, \text{ and} \tag{180}$$

---

<sup>5</sup> The manipulation of the double sum performed here can also be used on the exact CP-violating term (134). The result is

$$4 \sum_{i=1}^n \sum_{j>i} \alpha_{\beta j}^i \sin 2\Phi_{ij} = 8 \sum_{i=1}^n \sin \frac{m_i^2 x}{2p} \sum_{j \neq i} \cos \frac{m_j^2 x}{2p} \alpha_{\beta j}^i. \tag{179}$$

$$|V_{\alpha x}|^2 |V_{\beta x}|^2 = {}^{\alpha x} \square_{\beta x} = - \sum_{y \neq x} {}^{\alpha y} \square_{\beta x} = - \sum_{y \neq x} {}^{\alpha y} \mathfrak{R}_{\beta x}, \quad \alpha \neq \beta. \quad (181)$$

For three generations, each of the sums contains two terms, so we now have expressions for our singly-degenerate boxes in terms of two nondegenerate boxes measurable in neutrino oscillations.

For fixed  $(i, j)$  in equation (180),  $\lambda$  can take  $n$  possible values, implying  $n$  constraint equations.  $N$  ordered nondegenerate boxes appear in these  $n$  equations. Thus, for  $N \leq n$ , which is true for  $n \leq 3$ , the unitarity constraint (180) and (181) may be inverted to find a nondegenerate box in terms of singly-degenerate boxes. Adding the sums in equation (181) for  $x = i$  and  $x = j$ , then subtracting the  $x = k$  sum yields the expression:

$$\mathfrak{R}_{\beta j} = -\frac{1}{2} (|V_{\alpha i}|^2 |V_{\beta i}|^2 + |V_{\alpha j}|^2 |V_{\beta j}|^2 - |V_{\alpha k}|^2 |V_{\beta k}|^2), \quad (182)$$

where we have used the property that  $R$ s are unchanged under mass (or flavor) index interchanges.

Many sources, such as reference [13], use these sums as the coefficients of the oscillatory terms in oscillation probabilities. In terms of the  $|V_{\alpha i}|^2 |V_{\beta i}|^2$  for three generations,

$$\begin{aligned} P_{\nu_\alpha \rightarrow \nu_\beta} (x) = & 2 (\sin^2 \Phi_{12} + \sin^2 \Phi_{13} - \sin^2 \Phi_{23}) |V_{\alpha 1}|^2 |V_{\beta 1}|^2 \\ & + 2 (\sin^2 \Phi_{12} - \sin^2 \Phi_{13} + \sin^2 \Phi_{23}) |V_{\alpha 2}|^2 |V_{\beta 2}|^2 \\ & + 2 (-\sin^2 \Phi_{12} + \sin^2 \Phi_{13} + \sin^2 \Phi_{23}) |V_{\alpha 3}|^2 |V_{\beta 3}|^2. \end{aligned} \quad (183)$$

Such an expression does not include the possibility of CP-violation. Our boxes are clearly preferable for their compactness and versatility.

Similar manipulation of equation (181) gives an alternate expression in term of the cyclic triad  $(\alpha, \beta, \gamma)$ :

$$\mathfrak{R}_{\beta j} = -\frac{1}{2} (|V_{\alpha i}|^2 |V_{\alpha j}|^2 + |V_{\beta i}|^2 |V_{\beta j}|^2 - |V_{\gamma i}|^2 |V_{\gamma j}|^2). \quad (184)$$

The unitarity constraints (180) and (181) greatly simplify our expressions for a doubly-degenerate

box:

$$\alpha^i \square_{\alpha i} = \frac{\alpha^i \square_{\alpha x} \alpha^i \square_{\alpha y}}{\alpha x \square_{\alpha y}} = \frac{\left( -\sum_{\eta \neq \alpha} \Re_{\eta x} \right) \left( -\sum_{\lambda \neq \alpha} \Re_{\lambda y} \right)}{\left( -\sum_{\tau \neq \alpha} \Re_{\tau y} \right)}, \quad x \neq y \neq i, \text{ and} \quad (185)$$

$$\alpha^i \square_{\alpha i} = \frac{\alpha^i \square_{\lambda i} \alpha^i \square_{\eta i}}{\lambda i \square_{\eta i}} = \frac{\left( -\sum_{x \neq i} \Re_{\lambda x} \right) \left( -\sum_{y \neq i} \Re_{\eta y} \right)}{\left( -\sum_{z \neq i} \Re_{\eta z} \right)}, \quad \lambda \neq \eta \neq \alpha. \quad (186)$$

For three generations, doubly-degenerate boxes are expressible in terms of the real parts of six ordered boxes, rather than the nine complex boxes used in equations (143) and (144). For example, in three generations

$$|V_{11}|^4 = {}^{11} \square_{11} = -\frac{(\Re_{22} + \Re_{32})(\Re_{23} + \Re_{33})}{\Re_{23} + \Re_{33}}. \quad (187)$$

Summing equation (180) over  $j \neq i$  yields another expression for  $|V_{\lambda i}|^2$  in terms of nondegenerate boxes:

$$|V_{\lambda i}|^2 \sum_{j \neq i} |V_{\lambda j}|^2 = |V_{\lambda i}|^2 (1 - |V_{\lambda i}|^2) = -\sum_{j \neq i} \sum_{\eta \neq \lambda} \Re_{\lambda j}. \quad (188)$$

The same result is obtained by summing equation (152) over all  $j$ . The explicit solution, valid for any number of generations, of the above equation has a two-fold ambiguity:

$$|V_{\lambda i}|^2 = \frac{1}{2} \left[ 1 \pm \sqrt{1 + 4 \sum_{j \neq i} \sum_{\eta \neq \lambda} \Re_{\lambda j}} \right]. \quad (189)$$

This solution gives the doubly-degenerate box in terms of the  $(n - 1)^2$  nondegenerate boxes of the double sum. When the double sum is small, an approximation to the exact equation (189) is

$$|V_{\lambda i}|^2 \approx \left( -\sum_{j \neq i} \sum_{\eta \neq \lambda} \Re_{\lambda j}, 1 + \sum_{j \neq i} \sum_{\eta \neq \lambda} \Re_{\lambda j} \right). \quad (190)$$

For three generations, this yields  $|V_{\lambda i}|^2$  as a linear equation of four nondegenerate boxes. For example,

$$\begin{aligned} |V_{12}|^2 &= \frac{1}{2} \left[ 1 \pm \sqrt{1 + 4(\Re_{22} + \Re_{32} + \Re_{23} + \Re_{33})} \right] \\ &\approx (-(\Re_{22} + \Re_{32} + \Re_{23} + \Re_{33}), 1 + (\Re_{22} + \Re_{32} + \Re_{23} + \Re_{33})). \end{aligned}$$

We may use the homogeneous unitarity conditions (180) and (181), along with the tautologies (138) and (139) to obtain constraints between ordered boxes, thereby reducing the number of real degrees of freedom. Recognizing that the tautologies (138) and (139) give

$$\begin{aligned} {}^{\alpha i} \square_{\alpha j} &= \operatorname{Re} \left( \frac{{}^{\alpha i} \square_{\eta j}^* {}^{\alpha i} \square_{\lambda j}}{{}^{\eta i} \square_{\lambda j}} \right) \\ &= \frac{{}^{\alpha i} \square_{\eta j} {}^{\alpha} \mathbf{R}_{\lambda j} + {}^{\alpha} \mathbf{J}_{\eta j} {}^{\alpha} \mathbf{J}_{\lambda j} {}^{\alpha} \mathbf{R}_{\lambda j} - {}^{\alpha} \mathbf{J}_{\eta j} {}^{\alpha} \mathbf{R}_{\lambda j} {}^{\alpha} \mathbf{J}_{\lambda j} + {}^{\alpha} \mathbf{R}_{\eta j} {}^{\alpha} \mathbf{J}_{\lambda j} {}^{\alpha} \mathbf{J}_{\lambda j}}{({}^{\alpha} \mathbf{R}_{\lambda j})^2 + ({}^{\alpha} \mathbf{J}_{\lambda j})^2}, \quad \text{and} \end{aligned} \quad (191)$$

$$\begin{aligned} {}^{\alpha i} \square_{\beta i} &= \operatorname{Re} \left( \frac{{}^{\alpha i} \square_{\beta x}^* {}^{\alpha i} \square_{\beta y}}{{}^{\alpha x} \square_{\beta y}} \right) \\ &= \frac{{}^{\alpha} \mathbf{R}_{\beta x} {}^{\alpha} \mathbf{R}_{\beta y} {}^{\alpha} \mathbf{R}_{\beta y} + {}^{\alpha} \mathbf{J}_{\beta x} {}^{\alpha} \mathbf{J}_{\beta y} {}^{\alpha} \mathbf{R}_{\beta y} - {}^{\alpha} \mathbf{J}_{\beta x} {}^{\alpha} \mathbf{R}_{\beta y} {}^{\alpha} \mathbf{J}_{\beta y} + {}^{\alpha} \mathbf{R}_{\beta x} {}^{\alpha} \mathbf{J}_{\beta y} {}^{\alpha} \mathbf{J}_{\beta y}}{({}^{\alpha} \mathbf{R}_{\beta y})^2 + ({}^{\alpha} \mathbf{J}_{\beta y})^2}, \end{aligned} \quad (192)$$

our unitarity constraints (180) and (181) become

$$\begin{aligned} {}^{\alpha} \mathbf{R}_{\eta j} {}^{\alpha} \mathbf{R}_{\lambda j} {}^{\alpha} \mathbf{R}_{\lambda j} + {}^{\alpha} \mathbf{J}_{\eta j} {}^{\alpha} \mathbf{J}_{\lambda j} {}^{\alpha} \mathbf{R}_{\lambda j} - {}^{\alpha} \mathbf{J}_{\eta j} {}^{\alpha} \mathbf{R}_{\lambda j} {}^{\alpha} \mathbf{J}_{\lambda j} + {}^{\alpha} \mathbf{R}_{\eta j} {}^{\alpha} \mathbf{J}_{\lambda j} {}^{\alpha} \mathbf{J}_{\lambda j} = \\ - \left( ({}^{\alpha} \mathbf{R}_{\lambda j})^2 + ({}^{\alpha} \mathbf{J}_{\lambda j})^2 \right) \sum_{\tau \neq \alpha} {}^{\alpha} \mathbf{R}_{\tau j}, \end{aligned} \quad (193)$$

and

$$\begin{aligned} {}^{\alpha} \mathbf{R}_{\beta x} {}^{\alpha} \mathbf{R}_{\beta y} {}^{\alpha} \mathbf{R}_{\beta y} + {}^{\alpha} \mathbf{J}_{\beta x} {}^{\alpha} \mathbf{J}_{\beta y} {}^{\alpha} \mathbf{R}_{\beta y} - {}^{\alpha} \mathbf{J}_{\beta x} {}^{\alpha} \mathbf{R}_{\beta y} {}^{\alpha} \mathbf{J}_{\beta y} + {}^{\alpha} \mathbf{R}_{\beta x} {}^{\alpha} \mathbf{J}_{\beta y} {}^{\alpha} \mathbf{J}_{\beta y} = \\ - \left( ({}^{\alpha} \mathbf{R}_{\beta y})^2 + ({}^{\alpha} \mathbf{J}_{\beta y})^2 \right) \sum_{z \neq i} {}^{\alpha} \mathbf{R}_{\beta z}, \end{aligned} \quad (194)$$

with the usual inequalities  $\eta \neq \lambda \neq \alpha$ ,  $i \neq j$ , in equations (191) and (193), and  $\alpha \neq \beta$ , and  $x \neq y \neq i$  in equations (192) and (191) satisfied.

We may rename some indices and solve both equations (193) and (194) for one  ${}^{\alpha} \mathbf{R}_{\beta j}$ :

$${}^{\alpha} \mathbf{R}_{\beta j} = - \frac{{}^{\alpha} \mathbf{J}_{\beta j} ({}^{\alpha} \mathbf{J}_{\lambda j} {}^{\alpha} \mathbf{R}_{\lambda j} - {}^{\alpha} \mathbf{R}_{\lambda j} {}^{\alpha} \mathbf{J}_{\lambda j}) + \left( ({}^{\alpha} \mathbf{R}_{\lambda j})^2 + ({}^{\alpha} \mathbf{J}_{\lambda j})^2 \right) \sum_{\tau \neq \alpha, \beta} {}^{\alpha} \mathbf{R}_{\tau j}}{{}^{\alpha} \mathbf{J}_{\lambda j} ({}^{\alpha} \mathbf{J}_{\lambda j} + {}^{\alpha} \mathbf{J}_{\lambda j}) + {}^{\alpha} \mathbf{R}_{\lambda j} ({}^{\alpha} \mathbf{R}_{\lambda j} + {}^{\alpha} \mathbf{R}_{\lambda j})} \quad (195)$$

$$= - \frac{{}^{\alpha} \mathbf{J}_{\beta j} ({}^{\alpha} \mathbf{J}_{\beta y} {}^{\alpha} \mathbf{R}_{\beta y} - {}^{\alpha} \mathbf{R}_{\beta y} {}^{\alpha} \mathbf{J}_{\beta y}) + \left( ({}^{\alpha} \mathbf{R}_{\beta y})^2 + ({}^{\alpha} \mathbf{J}_{\beta y})^2 \right) \sum_{z \neq i, j} {}^{\alpha} \mathbf{R}_{\beta z}}{{}^{\alpha} \mathbf{J}_{\beta y} ({}^{\alpha} \mathbf{J}_{\beta y} + {}^{\alpha} \mathbf{J}_{\beta y}) + {}^{\alpha} \mathbf{R}_{\beta y} ({}^{\alpha} \mathbf{R}_{\beta y} + {}^{\alpha} \mathbf{R}_{\beta y})}. \quad (196)$$

Similar expressions could be found for  ${}^{\alpha} \mathbf{J}_{\beta j}$  if so desired.

These constraints interrelate imaginary and real parts of boxes through unitarity for any number of generations. If CP is a good symmetry, all of the  ${}^{\alpha} \mathbf{J}_{\beta j}$  vanish, and the above expressions for

$\Re^i_{\beta j}$  will be different than if CP were not conserved. For three generations,  $\tau$  must equal  $\lambda$ , and  $\Re^i_{\beta j} = -\Re^i_{\lambda j} = \Re^i_{\lambda j}$  by equation (165). Similarly,  $z = y$ , and  $\Re^i_{\beta j} = -\Re^i_{\beta y} = \Re^i_{\beta y}$  by equation (166).

Equations (195) and (196) for  $n = 3$  become

$$\Re^i_{\beta j} = \frac{(\Re^i_{\beta j})^2 - \Re^i_{\lambda j} \Re^i_{\lambda j}}{\Re^i_{\lambda j} + \Re^i_{\lambda j}} \quad (197)$$

$$= \frac{(\Re^i_{\beta j})^2 - \Re^i_{\beta y} \Re^i_{\beta y}}{\Re^i_{\beta y} + \Re^i_{\beta y}} \quad (198)$$

Rearranging the equations gives a measure of CP-violation in three generations:

$$(\Re^i_{\beta j})^2 = \Re^i_{\beta j} \Re^i_{\lambda j} + \Re^i_{\beta j} \Re^i_{\lambda j} + \Re^i_{\lambda j} \Re^i_{\lambda j} \quad (199)$$

$$= \Re^i_{\beta j} \Re^i_{\beta y} + \Re^i_{\beta j} \Re^i_{\beta y} + \Re^i_{\beta y} \Re^i_{\beta y}. \quad (200)$$

These relationships between  $Rs$  and  $Js$  in three generations exhibit a simple parameter symmetry.  $(\Re^i_{\beta j})^2$  in equation (199) equals  $\Re^i_{\beta j} \Re^i_{\beta j} +$  terms cyclic in  $(\alpha, \beta, \lambda)$ ; in equation (200), it equals  $\Re^i_{\beta j} \Re^i_{\beta j} +$  terms cyclic in  $(i, j, y)$ .

If CP is violated,  $\Re^i_{\beta j} \neq 0$ , so the combination of real parts on the right-hand sides of equations (199) and (200), measurable with CP-conserving averaged neutrino oscillations (discussed in detail in Chapter VI), cannot be zero. Thus, even if CP violation is not directly observable in an experiment because of a short baseline or small mass differences, the effects of CP violation may be seen through the relationships among the real parts of different boxes!

We may infer similar constraints by setting the imaginary part of a singly-degenerate box to zero:

$$\begin{aligned} \text{Im} \left( \alpha^i \square_{\alpha j} \right) &= \text{Im} \left( \frac{\alpha^i \square_{\eta j}^* \alpha^i \square_{\lambda j}}{\eta^i \square_{\lambda j}} \right) = \\ &\frac{\Re_{\eta j} \Re^i_{\lambda j} \Re_{\lambda j} - \Re^i_{\eta j} \Re_{\lambda j} \Re^i_{\lambda j} - \Re_{\eta j} \Re_{\lambda j} \Re^i_{\lambda j} - \Re^i_{\eta j} \Re^i_{\lambda j} \Re^i_{\lambda j}}{\Re_{\lambda j}^2 + \Re_{\lambda j}^2} = 0, \end{aligned} \quad (201)$$

and

$$\text{Im} \left( \alpha^i \square_{\beta i} \right) = \text{Im} \left( \frac{\alpha^i \square_{\beta x}^* \alpha^i \square_{\beta y}}{\alpha x \square_{\beta y}} \right) = \quad (202)$$

$$\frac{\mathfrak{R}_{\beta x}^i \mathfrak{J}_{\beta y}^i \mathfrak{R}_{\beta y} - \mathfrak{J}_{\beta x}^i \mathfrak{R}_{\beta y}^i \mathfrak{R}_{\beta y} - \mathfrak{R}_{\beta x}^i \mathfrak{R}_{\beta y}^i \mathfrak{J}_{\beta y} - \mathfrak{J}_{\beta x}^i \mathfrak{J}_{\beta y}^i \mathfrak{J}_{\beta y}}{\alpha \mathfrak{R}_{\beta y}^2 + \alpha \mathfrak{J}_{\beta y}^2} = 0,$$

so

$$\mathfrak{R}_{\eta j}^i \mathfrak{J}_{\lambda j}^i \mathfrak{R}_{\lambda j} - \mathfrak{J}_{\eta j}^i \mathfrak{R}_{\lambda j}^i \mathfrak{R}_{\lambda j} - \mathfrak{R}_{\eta j}^i \mathfrak{R}_{\lambda j}^i \mathfrak{J}_{\lambda j} - \mathfrak{J}_{\eta j}^i \mathfrak{J}_{\lambda j}^i \mathfrak{J}_{\lambda j} = 0, \quad (203)$$

and

$$\mathfrak{R}_{\beta x}^i \mathfrak{J}_{\beta y}^i \mathfrak{R}_{\beta y} - \mathfrak{J}_{\beta x}^i \mathfrak{R}_{\beta y}^i \mathfrak{R}_{\beta y} - \mathfrak{R}_{\beta x}^i \mathfrak{R}_{\beta y}^i \mathfrak{J}_{\beta y} - \mathfrak{J}_{\beta x}^i \mathfrak{J}_{\beta y}^i \mathfrak{J}_{\beta y} = 0. \quad (204)$$

With a bit of index switching, these lead to constraints of the form

$$\mathfrak{R}_{\beta j} = \frac{\mathfrak{J}_{\beta j}^i \mathfrak{R}_{\lambda j}^i \mathfrak{R}_{\lambda j} - \mathfrak{J}_{\beta j}^i \mathfrak{J}_{\lambda j}^i \mathfrak{J}_{\lambda j}}{\mathfrak{J}_{\lambda j}^i \mathfrak{R}_{\lambda j} - \mathfrak{R}_{\lambda j}^i \mathfrak{J}_{\lambda j}} = \frac{\mathfrak{J}_{\beta j}^i \mathfrak{R}_{\beta y}^i \mathfrak{R}_{\beta y} - \mathfrak{J}_{\beta j}^i \mathfrak{J}_{\beta y}^i \mathfrak{J}_{\beta y}}{\mathfrak{J}_{\beta y}^i \mathfrak{R}_{\beta y} - \mathfrak{R}_{\beta y}^i \mathfrak{J}_{\beta y}}. \quad (205)$$

For three generations, unitarity enforces the simple relations (165) and (166) among the  $J$ s, and we find that equation (205) reproduces the same expressions (197) and (198) which were derived from the unitarity constraints (195) and (196) above. For  $n > 3$ , however, equation (205) is different from the prior equations, since the sums  $\sum_{\tau \neq \alpha, \beta}$  and  $\sum_{z \neq i, j}$  in equations (195) and (196) ensure that boxes with all  $n$  flavor or mass indices enter into equations (197) or (198), respectively. Equation (205) involves only three such indices, so it will be different from the unitarity constraints in higher generations, providing additional identities among the real parts of boxes.

We have not yet used the inhomogeneous unitarity constraints (152) and (154) that occur when the Kronecker delta is not zero. The homogeneous unitarity constraints cannot provide the absolute normalization of the  $V_{\alpha i}$  or the boxes, so we must need the inhomogeneous unitarity constraints. These inhomogeneous constraints are functions of degenerate boxes:<sup>6</sup>

$$\alpha^i \square_{\alpha i} + \sum_{\eta \neq \alpha} \alpha^i \square_{\eta i} = \sqrt{\alpha^i \square_{\alpha i}}, \quad \text{and} \quad (208)$$

---

<sup>6</sup> In terms of mixing-matrix elements, equations (208) and (209) are trivial. For example, equation (208) is

$$|V_{\alpha i}|^4 + \sum_{\eta \neq \alpha} |V_{\alpha i}|^2 |V_{\eta i}|^2 = |V_{\alpha i}|^2, \quad (206)$$

or

$$\sum_{\eta=1}^n |V_{\eta i}|^2 = 1. \quad (207)$$

$${}^{\alpha i} \square_{\alpha i} + \sum_{z \neq i} {}^{\alpha i} \square_{\alpha z} = \sqrt{{}^{\alpha i} \square_{\alpha i}}. \quad (209)$$

Parenthetically, we note by comparing equations (208) and (209) that a sum over mass-degenerate boxes equals a sum over flavor-degenerate boxes:

$$\sum_{\eta \neq \alpha} {}^{\alpha i} \square_{\eta i} = \sum_{z \neq i} {}^{\alpha i} \square_{\alpha z}. \quad (210)$$

Equations (208) and (209) can be rewritten strictly in terms of nondegenerate boxes by using the homogeneous unitarity constraints (180) and (181). (If these expressions were not available, we would need to use the tautologies (143) and (144) for the doubly-degenerate boxes, and equations (138) and (139) for the singly-degenerate boxes, resulting in an incredibly ugly mess (as compared to the merely unincriddibly ugly mess derived below)). We find

$$\frac{\left( -\sum_{\lambda \neq \alpha} {}^{\alpha i} \mathbb{R}_{\lambda x} \right) \left( -\sum_{\sigma \neq \alpha} {}^{\alpha i} \mathbb{R}_{\sigma y} \right)}{\left( -\sum_{\tau \neq \alpha} {}^{\alpha i} \mathbb{R}_{\tau y} \right)} - \sqrt{\frac{\left( -\sum_{\lambda \neq \alpha} {}^{\alpha i} \mathbb{R}_{\lambda x} \right) \left( -\sum_{\sigma \neq \alpha} {}^{\alpha i} \mathbb{R}_{\sigma y} \right)}{\left( -\sum_{\tau \neq \alpha} {}^{\alpha i} \mathbb{R}_{\tau y} \right)}} + \sum_{\eta \neq \alpha} \left( -\sum_{z \neq i} {}^{\alpha i} \mathbb{R}_{\eta z} \right) = 0, \quad (211)$$

with  $x \neq y \neq i$ , and

$$\frac{\left( -\sum_{x \neq i} {}^{\alpha i} \mathbb{R}_{\lambda i} \right) \left( -\sum_{y \neq i} {}^{\alpha i} \mathbb{R}_{\eta y} \right)}{\left( -\sum_{t \neq i} {}^{\alpha i} \mathbb{R}_{\eta i} \right)} - \sqrt{\frac{\left( -\sum_{x \neq i} {}^{\alpha i} \mathbb{R}_{\lambda i} \right) \left( -\sum_{y \neq i} {}^{\alpha i} \mathbb{R}_{\eta y} \right)}{\left( -\sum_{t \neq i} {}^{\alpha i} \mathbb{R}_{\eta i} \right)}} + \sum_{z \neq i} \left( -\sum_{\eta \neq \alpha} {}^{\alpha i} \mathbb{R}_{\eta z} \right) = 0, \quad (212)$$

with  $\lambda \neq \eta \neq \alpha$ .

In three generations, each of the sums has only two terms. Eliminating the square root, and multiplying through by the denominator, we find constraints of the form

$$\begin{aligned} & \left( \mathbb{R}_{\lambda x} + \mathbb{R}_{\eta x} \right) \left( \mathbb{R}_{\lambda y} + \mathbb{R}_{\eta y} \right) \left( {}^{\alpha} \mathbb{R}_{\lambda y} + {}^{\alpha} \mathbb{R}_{\eta y} \right) \left[ 1 + 2 \left( \mathbb{R}_{\lambda x} + \mathbb{R}_{\eta x} + \mathbb{R}_{\lambda y} + \mathbb{R}_{\eta y} \right) \right] + \\ & \left( \mathbb{R}_{\lambda x} + \mathbb{R}_{\eta x} \right)^2 \left( \mathbb{R}_{\lambda y} + \mathbb{R}_{\eta y} \right)^2 + \left( \mathbb{R}_{\lambda x} + \mathbb{R}_{\eta x} + \mathbb{R}_{\lambda y} + \mathbb{R}_{\eta y} \right)^2 \left( {}^{\alpha} \mathbb{R}_{\lambda y} + {}^{\alpha} \mathbb{R}_{\eta y} \right)^2 = 0, \end{aligned} \quad (213)$$

and

$$\begin{aligned} & (\Re_{\lambda x} + \Re_{\lambda y}) (\Re_{\eta x} + \Re_{\eta y}) (\Re_{\eta x} + \Re_{\eta y}) [1 + 2(\Re_{\lambda x} + \Re_{\lambda y} + \Re_{\eta x} + \Re_{\eta y})] + \\ & (\Re_{\lambda x} + \Re_{\lambda y})^2 (\Re_{\eta x} + \Re_{\eta y})^2 + (\Re_{\lambda x} + \Re_{\lambda y} + \Re_{\eta x} + \Re_{\eta y})^2 (\Re_{\eta x} + \Re_{\eta y})^2 = 0, \end{aligned} \quad (214)$$

where  $x \neq y \neq i$ , and  $\lambda \neq \eta \neq \alpha$ . So, for  $\alpha = 2$  and  $i = 1$ , we find

$$\begin{aligned} & (\Re_{22} + \Re_{32}) (\Re_{23} + \Re_{33}) (\Re_{23} + \Re_{33}) [1 + 2(\Re_{22} + \Re_{32} + \Re_{23} + \Re_{33})] + \\ & (\Re_{22} + \Re_{32})^2 (\Re_{23} + \Re_{33})^2 + (\Re_{22} + \Re_{32} + \Re_{23} + \Re_{33})^2 (\Re_{23} + \Re_{33})^2 = 0, \end{aligned} \quad (215)$$

and

$$\begin{aligned} & (\Re_{22} + \Re_{23}) (\Re_{32} + \Re_{33}) (\Re_{32} + \Re_{33}) [1 + 2(\Re_{22} + \Re_{23} + \Re_{32} + \Re_{33})] + \\ & (\Re_{22} + \Re_{23})^2 (\Re_{32} + \Re_{33})^2 + (\Re_{22} + \Re_{23} + \Re_{32} + \Re_{33})^2 (\Re_{32} + \Re_{33})^2 = 0. \end{aligned} \quad (216)$$

As with the constraints on the imaginary parts of boxes, many of the constraints (195) to (214) are redundant, but an independent set may be used to reduce the number of parameters significantly. The homogeneous constraints are much simpler than the inhomogeneous constraints, so we want to use as many of those as are possible. For the three-generation case, we may eliminate  $\Re_{23}$  by either equation (197) or equation (198)

$$\Re_{23} = \frac{\Re_{33} \Re_{33} - \mathcal{J}^2}{-\Re_{33} - \Re_{33}} = \frac{\Re_{22} \Re_{23} - \mathcal{J}^2}{-\Re_{23} - \Re_{22}}. \quad (217)$$

We may similarly eliminate  $\Re_{32}$  and  $\Re_{33}$

$$\Re_{32} = \frac{\Re_{22} \Re_{32} - \mathcal{J}^2}{-\Re_{32} - \Re_{22}} = \frac{\Re_{33} \Re_{33} - \mathcal{J}^2}{-\Re_{33} - \Re_{33}}, \quad (218)$$

and

$$\Re_{33} = \frac{\Re_{23} \Re_{33} - \mathcal{J}^2}{-\Re_{33} - \Re_{23}} = \frac{\Re_{32} \Re_{33} - \mathcal{J}^2}{-\Re_{33} - \Re_{32}}. \quad (219)$$

$\Re_{33}$  may be eliminated from equation (217), and  $\Re_{33}$  may be eliminated from equation (219):

$$\Re_{33} = \frac{\Re_{33} \Re_{22} \Re_{23} + \mathcal{J}^2 (\Re_{23} + \Re_{22} - \Re_{33})}{\Re_{33} \Re_{23} + \Re_{33} \Re_{22} - \Re_{22} \Re_{23} + \mathcal{J}^2}, \quad \text{and} \quad (220)$$

$$\mathbb{H}_{33} = \frac{\mathbb{H}_{33} \mathbb{H}_{23} \mathbb{H}_{32} + \mathcal{J}^2 (\mathbb{H}_{32} + \mathbb{H}_{33} - \mathbb{H}_{23})}{\mathbb{H}_{23} \mathbb{H}_{32} + \mathbb{H}_{33} \mathbb{H}_{23} - \mathbb{H}_{32} \mathbb{H}_{33} + \mathcal{J}^2}. \quad (221)$$

Equation (218) will not provide an additional constraint; it is redundant to the other two. We must turn to equations (213) and (214) to eliminate the last degree of freedom. This necessity is expected, since without this set of inhomogeneous constraints, the rows/columns of  $V$  will not be normalized and our set of boxes will not yield a unitary  $V$ . We will here choose the constraint (215), with  $\alpha = 1$  and  $i = 1$  since its expression in terms of our four remaining boxes is the least complicated. We may substitute the second equality from equation (219) for  $\mathbb{H}_{33}$  and the second equality of equation (217) for  $\mathbb{H}_{23}$ , leaving a constraint which contains the four parameters  $\mathbb{H}_{22}$ ,  $\mathbb{H}_{23}$ ,  $\mathbb{H}_{32}$ , and  $\mathbb{H}_{33}$ :

$$\begin{aligned} & (\mathbb{H}_{22} + \mathbb{H}_{32}) \left( \mathbb{H}_{23} + \frac{\mathbb{H}_{32} \mathbb{H}_{33} - \mathcal{J}^2}{-\mathbb{H}_{33} - \mathbb{H}_{32}} \right) \left( \frac{\mathbb{H}_{22} \mathbb{H}_{23} - \mathcal{J}^2}{-\mathbb{H}_{23} - \mathbb{H}_{22}} + \mathbb{H}_{33} \right) [1 + 2(\mathbb{H}_{22} \\ & + \mathbb{H}_{32} + \mathbb{H}_{23} + \frac{\mathbb{H}_{32} \mathbb{H}_{33} - \mathcal{J}^2}{-\mathbb{H}_{33} - \mathbb{H}_{32}})] + (\mathbb{H}_{22} + \mathbb{H}_{32})^2 \left( \mathbb{H}_{23} + \frac{\mathbb{H}_{32} \mathbb{H}_{33} - \mathcal{J}^2}{-\mathbb{H}_{33} - \mathbb{H}_{32}} \right)^2 \\ & + \left( \mathbb{H}_{22} + \mathbb{H}_{32} + \mathbb{H}_{23} + \frac{\mathbb{H}_{32} \mathbb{H}_{33} - \mathcal{J}^2}{-\mathbb{H}_{33} - \mathbb{H}_{32}} \right)^2 \left( \frac{\mathbb{H}_{22} \mathbb{H}_{23} - \mathcal{J}^2}{-\mathbb{H}_{23} - \mathbb{H}_{22}} + \mathbb{H}_{33} \right)^2 = 0. \end{aligned} \quad (222)$$

Multiplying through to place all of the terms in the numerator, we are left with

$$\begin{aligned} 0 = & (\mathbb{H}_{22} + \mathbb{H}_{23})^2 (\mathbb{H}_{22} + \mathbb{H}_{32})^2 (-\mathbb{H}_{32} \mathbb{H}_{33} + \mathbb{H}_{23} (\mathbb{H}_{32} + \mathbb{H}_{33}) + \mathcal{J}^2)^2 \\ & \left( (\mathbb{H}_{32})^2 + (\mathbb{H}_{23} + \mathbb{H}_{22}) (\mathbb{H}_{32} + \mathbb{H}_{33}) + \mathcal{J}^2 \right)^2 \\ & \times (\mathbb{H}_{23} \mathbb{H}_{33} + \mathbb{H}_{22} (-\mathbb{H}_{23} + \mathbb{H}_{33}) \mathcal{J}^2)^2 \\ & - (\mathbb{H}_{22} + \mathbb{H}_{32}) (\mathbb{H}_{22} + \mathbb{H}_{23}) (\mathbb{H}_{22} (\mathbb{H}_{23} - \mathbb{H}_{33}) - \mathbb{H}_{23} \mathbb{H}_{33} - \mathcal{J}^2) \\ & \times \left( \mathbb{H}_{32} + 2 \mathbb{H}_{22} \mathbb{H}_{32} + 2 (\mathbb{H}_{32})^2 + 2 \mathbb{H}_{32} \mathbb{H}_{23} \right. \\ & \left. + \mathbb{H}_{33} + 2 \mathbb{H}_{22} \mathbb{H}_{33} + 2 \mathbb{H}_{23} \mathbb{H}_{33} + 2 \mathcal{J}^2 \right). \end{aligned} \quad (223)$$

This equation is quartic in  $\mathbb{H}_{33}$ ; we may eliminate this box by solving the equation

$$A + B (\mathbb{H}_{33}) + C (\mathbb{H}_{33})^2 + D (\mathbb{H}_{33})^3 + E (\mathbb{H}_{33})^4 = 0, \quad (224)$$

with

$$\begin{aligned}
A = & \left( \mathbb{H}_{22} \right)^6 \left( \mathbb{H}_{32} \right)^2 - 2 \left( \mathbb{H}_{22} \right)^5 \mathbb{H}_{32} \left( 2 \mathbb{H}_{32} \mathbb{H}_{23} + \mathcal{J}^2 \right) \\
& - \left( \mathbb{H}_{22} \right)^4 \left[ 9 \left( \mathbb{H}_{32} \right)^2 \left( \mathbb{H}_{23} \right)^2 + 10 \mathbb{H}_{32} \mathbb{H}_{23} \mathcal{J}^2 + \mathcal{J}^4 \right] \\
& - \left( \mathbb{H}_{22} \right)^3 \left[ 6 \left( \mathbb{H}_{32} \right)^3 \left( \mathbb{H}_{23} \right)^2 + \left( \mathbb{H}_{32} \right)^2 \left( \mathbb{H}_{23} \right)^2 \left( 1 + 10 \mathbb{H}_{23} \right) \right. \\
& \quad \left. + \mathbb{H}_{32} \left( \mathbb{H}_{23} + 20 \left( \mathbb{H}_{23} \right)^2 - 2 \mathcal{J}^2 \right) \mathcal{J}^2 + 6 \mathbb{H}_{23} \mathcal{J}^4 \right] \\
& + \mathbb{H}_{22} \left\{ \left( \mathbb{H}_{32} \right)^2 \left( 1 + 10 \mathbb{H}_{23} \right) \mathcal{J}^4 + 4 \mathbb{H}_{23} \mathcal{J}^4 \left( - \left( \mathbb{H}_{23} \right)^2 + \mathcal{J}^2 \right) \right. \\
& \quad \left. - 2 \left( \mathbb{H}_{32} \right)^4 \left[ \left( \mathbb{H}_{23} \right)^3 - 2 \mathbb{H}_{23} \mathcal{J}^2 \right. \right. \\
& \quad \left. \left. + \mathbb{H}_{32} \mathbb{H}_{23} \mathcal{J}^2 \left( -2 \left( \mathbb{H}_{23} \right)^3 + \mathcal{J}^2 + 6 \mathbb{H}_{23} \mathcal{J}^2 \right) \right. \right. \\
& \quad \left. \left. + \left( \mathbb{H}_{32} \right)^3 \mathbb{H}_{23} \left( - \left( \mathbb{H}_{23} \right)^2 - 2 \left( \mathbb{H}_{23} \right)^3 + \mathcal{J}^2 + 8 \mathbb{H}_{23} \mathcal{J}^2 \right) \right. \right. \\
& \quad \left. \left. - \left( \mathbb{H}_{22} \right)^2 \left[ 3 \left( \mathbb{H}_{32} \right)^4 \left( \mathbb{H}_{23} \right)^2 + \left( \mathbb{H}_{32} \right)^3 \mathbb{H}_{23} \left( \mathbb{H}_{23} + 8 \left( \mathbb{H}_{23} \right)^2 - 6 \mathcal{J}^2 \right) \right] \right. \right. \\
& \quad \left. \left. + \left( 9 \left( \mathbb{H}_{23} \right)^2 - 2 \mathcal{J}^2 \right) \mathcal{J}^4 + \mathbb{H}_{32} \mathcal{J}^2 \left[ \left( \mathbb{H}_{23} \right)^2 + 14 \left( \mathbb{H}_{23} \right)^3 - \mathcal{J}^2 - 8 \mathbb{H}_{23} \mathcal{J}^2 \right] \right. \right. \\
& \quad \left. \left. + \left( \mathbb{H}_{32} \right)^2 \left[ \left( \mathbb{H}_{23} \right)^3 + 4 \left( \mathbb{H}_{23} \right)^4 + 2 \left( \mathbb{H}_{23} \right)^2 \mathcal{J}^2 - 3 \mathcal{J}^4 \right] \right\} \right. \\
& \quad \left. + \mathcal{J}^2 \left[ \left( \mathbb{H}_{32} \right)^3 \left( \mathbb{H}_{23} \right)^2 \left( 1 + 2 \mathbb{H}_{23} \right) + \left( \mathbb{H}_{32} \right)^4 \left( 2 \left( \mathbb{H}_{23} \right)^2 - \mathcal{J}^2 \right) \right. \right. \\
& \quad \left. \left. + \left( \mathbb{H}_{32} \right)^2 \left( \mathbb{H}_{23} + 3 \left( \mathbb{H}_{23} \right)^2 - 2 \mathcal{J}^2 \right) \mathcal{J}^2 - \mathcal{J}^2 \left( \left( \mathbb{H}_{23} \right)^4 + \mathcal{J}^4 \right) \right], \right. \tag{225}
\end{aligned}$$

$$\begin{aligned}
B = & - \left( \mathbb{H}_{22} + \mathbb{H}_{23} \right) \left\{ 2 \left( \mathbb{H}_{22} \right)^5 \mathbb{H}_{32} - \left( \mathbb{H}_{32} \right)^4 \left( \left( \mathbb{H}_{23} \right)^2 - 2 \mathcal{J}^2 \right) \right. \\
& - \left( \mathbb{H}_{32} \right)^3 \left( 1 + 2 \mathbb{H}_{23} \right) \left( \left( \mathbb{H}_{23} \right)^2 - \mathcal{J}^2 \right) + 4 \mathcal{J}^6 \\
& - \mathbb{H}_{32} \mathcal{J}^2 \left( 2 \left( \mathbb{H}_{23} \right)^3 + \mathcal{J}^2 \right) + \left( \mathbb{H}_{22} \right)^4 \left( -2 \left( \mathbb{H}_{32} \right)^2 + 6 \mathbb{H}_{32} \mathbb{H}_{23} + 2 \mathcal{J}^2 \right) \\
& + \left( \mathbb{H}_{32} \right)^2 \mathcal{J}^2 \left( -3 \mathbb{H}_{23} - 6 \left( \mathbb{H}_{23} \right)^2 + 8 \mathcal{J}^2 \right) \\
& - 4 \left( \mathbb{H}_{22} \right)^3 \left[ \left( \mathbb{H}_{32} \right)^2 \mathbb{H}_{23} - 2 \mathbb{H}_{23} \mathcal{J}^2 + \mathbb{H}_{32} \left( -3 \mathbb{H}_{23} + \mathcal{J}^2 \right) \right] \\
& - \mathbb{H}_{22} \left[ 6 \left( \mathbb{H}_{32} \right)^4 \mathbb{H}_{23} + 2 \left( \mathbb{H}_{32} \right)^3 \left( \mathbb{H}_{23} + 5 \left( \mathbb{H}_{23} \right)^2 - 3 \mathcal{J}^2 \right) \right. \tag{226} \\
& + 2 \mathbb{H}_{32} \left( \mathbb{H}_{23} + 9 \left( \mathbb{H}_{23} \right)^2 - 2 \mathcal{J}^2 \right) \mathcal{J}^2 + \mathcal{J}^2 \left( -2 \left( \mathbb{H}_{23} \right)^3 + \mathcal{J}^2 + 12 \mathbb{H}_{23} \mathcal{J}^2 \right) \\
& + \left( \mathbb{H}_{32} \right)^2 \mathbb{H}_{23} \left( - \mathbb{H}_{23} + 2 \left( \mathbb{H}_{23} \right)^2 + 18 \mathcal{J}^2 \right) \\
& - \left( \mathbb{H}_{22} \right)^2 \left[ 12 \left( \mathbb{H}_{32} \right)^3 \mathbb{H}_{23} + 2 \left( \mathbb{H}_{32} \right)^2 \mathbb{H}_{23} \left( 1 + 4 \mathbb{H}_{23} \right) \right] \\
& + \mathcal{J}^2 \left[ - \mathbb{H}_{23} - 12 \left( \mathbb{H}_{23} \right)^2 + 4 \mathcal{J}^2 \right]
\end{aligned}$$

$$+ \Re_{32} \left( -2 (\Re_{23})^2 - 8 (\Re_{23})^3 + \mathcal{J}^2 + 24 \Re_{23} \mathcal{J}^2 \right) \Big] \Big\} ,$$

$$\begin{aligned}
C = & - (\Re_{22} + \Re_{23}) \left\{ (\Re_{22})^5 + 3 (\Re_{32})^4 \Re_{23} + (\Re_{32})^3 \Re_{23} (1 + 2 \Re_{23}) \right. \\
& + (\Re_{22})^4 (-2 \Re_{32} + \Re_{23}) - 2 \Re_{32} \Re_{23} \mathcal{J}^2 + 6 \Re_{23} \mathcal{J}^4 \\
& + (\Re_{22})^3 \left[ 4 (\Re_{32})^2 - 16 \Re_{32} \Re_{23} + 6 (\Re_{32})^2 - 2 \mathcal{J}^2 \right] \\
& + (\Re_{32})^2 \left[ -2 (\Re_{23})^2 - 2 (\Re_{23})^3 + \mathcal{J}^2 + 10 \Re_{23} \mathcal{J}^2 \right] \\
& + \Re_{22} \left[ 3 (\Re_{32})^4 + (\Re_{32})^3 (1 + 8 \Re_{23}) \right. \\
& - \Re_{32} \Re_{23} \left( \Re_{23} + 8 (\Re_{23})^2 - 8 \mathcal{J}^2 \right) \\
& - 2 (\Re_{32})^2 \left( \Re_{23} + 4 (\Re_{32})^2 - 5 \mathcal{J}^2 \right) - 2 \left( \Re_{23} + 6 (\Re_{23})^2 - 3 \mathcal{J}^2 \right) \mathcal{J}^2 \\
& + (\Re_{22})^2 \left[ 6 (\Re_{32})^3 + (\Re_{22})^2 (1 - 2 \Re_{23}) + (\Re_{23})^2 + 4 (\Re_{23})^3 - \mathcal{J}^2 \right. \\
& \left. \left. - 14 \Re_{23} \mathcal{J}^2 + \Re_{32} \left( -3 \Re_{23} - 22 (\Re_{23})^2 + 8 \mathcal{J}^2 \right) \right] \right\} , \tag{227}
\end{aligned}$$

$$\begin{aligned}
D = & - (\Re_{22} + \Re_{23})^2 \left\{ 4 (\Re_{22})^2 (\Re_{32} - \Re_{23}) \right. \\
& - \Re_{32} \Re_{23} + (\Re_{32})^2 (1 + 4 \Re_{23}) + 4 \Re_{23} \mathcal{J}^2 \\
& \left. + \Re_{22} \left[ \Re_{32} + 4 (\Re_{32})^2 - \Re_{23} + 4 \Re_{32} \Re_{23} - 4 (\Re_{23})^2 + 4 \mathcal{J}^2 \right] \right\} , \text{ and} \tag{228}
\end{aligned}$$

$$E = - (\Re_{22} + \Re_{23})^4 . \tag{229}$$

Eliminating  $\Re_{33}$  with this constraint leaves us with three real parameters  $\Re_{22}$ ,  $\Re_{23}$ , and  $\Re_{32}$ , and the one imaginary component  $\mathcal{J}$  as our basis. This final constraint relating the four boxes, while not as ugly as it would be without the use of equations (180) and (181), is quite complicated. The algebraic solutions (which are obtainable) are too messy to be particularly illuminating, so we will choose to eliminate our final spurious parameter by solving equation (215) numerically rather than algebraically when we compare to experiment in Chapter VI.

### 4.3 More Unmeasurables

The previous Sections have developed relationships between the lepton mixing matrix and the boxes. Now we turn our attention to relationships between the neutrino mass matrix and the boxes.

We showed in Section 2.7 that we cannot distinguish experimentally between theories containing a diagonal  $M_l$  with  $U_{\nu_L} = V$  and theories containing mixing in both the neutrino sector and the charged lepton sector. We thus lose no physical information by restricting the mixing to the neutrino sector. Most models for fundamental lepton mass matrices, however, do not make this *ansatz* of a diagonal mass matrix for the charged leptons. On the contrary, many models postulate as a symmetry principle the same initial form for the charged lepton mass matrix as for the neutrino mass matrix. Such models will yield predictions equivalent to those of many other models, including a model that contains all of the lepton mixing in the neutrino sector.

Consider a model for lepton mass matrices that contains a neutrino mass matrix  $M_\nu$  and a lepton mass matrix  $M_l$ . We will first assume a Dirac mass term for the neutrinos for simplicity, then extend our treatment to the general case. The Lagrangian in the mass basis (64) which we derived in Section 2.7 contains the terms

$$\overline{\nu_L}^m D_\nu N_R^m + \overline{l_L^m} D_l l_R^m + c_2 W_\mu^+ \overline{\nu_L}^m V^{-1} \gamma^\mu l_L^m + h.c.. \quad (230)$$

We illustrated in that Section how the Lagrangian is invariant under a rotation of the mixing matrices  $U_{\nu_L, l_L} \rightarrow RU_{\nu_L, l_L}$  by any unitary matrix  $R$ . Such a transformation is equivalent to rotating the mass matrices  $M_\nu$  and  $M_l$  by the same arbitrary unitary matrix. In particular, we may choose this arbitrary rotation such that one of the mass matrices is diagonal from the beginning. This implies the mixing matrices  $U_{\nu_L} = V$  and  $U_{l_L} \neq \mathbb{1}$ , which we assumed when we derived our box relationships. The charged lepton mass matrix is diagonal in this basis, which we will call the *standard basis*. The neutrino mass matrix  $\hat{M}_\nu$  in this basis is related to the original mass matrix  $M_\nu$  by  $\hat{M}_\nu = U_{l_L}^{-1} M_\nu$ , which can be seen by equating the diagonal mass matrices in the two bases:

$$D_\nu = U_{\nu_L}^{-1} M_\nu U_{N_R} = V^{-1} \hat{M}_\nu U_{N_R} = U_{\nu_L}^{-1} U_{l_L} \hat{M} U_{N_R}, \text{ so} \quad (231)$$

$$\hat{M}_\nu = VU_{\nu_L}^{-1}M_\nu = U_{l_L}^{-1}U_{\nu_L}U_{\nu_L}^{-1}M_\nu = U_{l_L}^{-1}M_\nu. \quad (232)$$

When more generations of neutrinos are introduced, the left-handed neutrino mixing matrix  $U_{\nu_L}$  no longer has the same dimensions as the left-handed charged-lepton mixing matrix. We will use the general block form of the neutrino mass matrix from Section 2.5,

$$M_\nu = \begin{pmatrix} M_T & M_D & M_{\nu\chi} \\ M_D^T & M_S & M_{N\chi} \\ M_{\nu\chi}^T & M_{N\chi}^T & M_\chi \end{pmatrix}. \quad (53)$$

The mass term (52) containing this matrix is of the Majorana form, so the matrix  $M_\nu$  must be symmetric and may be diagonalized by  $U_\nu^{-1}M_\nu(U_\nu^T)^{-1}$ , as described in Section 2.1. We may combine the spinors of all three types of neutrinos into one  $n$ -dimensional vector  $\psi_\nu$ :

$$\psi_\nu = \begin{pmatrix} \nu \\ N \\ \chi \end{pmatrix}. \quad (233)$$

In addition, we will sometimes break the neutrino rotation matrix  $U_\nu$  into three submatrices,  $U_1$ ,  $U_2$ , and  $U_3$  such that

$$U_\nu = \begin{pmatrix} U_1 \\ U_2 \\ U_3 \end{pmatrix}. \quad (234)$$

$U_1$  is  $n_L \times n$ ,  $U_2$  is  $n_R \times n$ , and  $U_3$  is  $n_\chi \times n$ , with  $n = n_L + n_R + n_\chi$ . Such a decomposition is necessary because the charged current term contains only  $\nu_L$ , which is related to the  $n$  mass states contained in  $\psi_\nu^m$  by  $\nu_L = U_1^{-1}\psi_\nu^m$ . These  $U_i$  are not square and so are not unitarity, but  $U_i U_i^\dagger = \mathbb{1}$  (here has dimensions  $n_L \times n_L$ ), so  $U_i^\dagger$  is the right inverse of  $U_i$ .

Using these definitions, the mass-basis Lagrangian (230) is

$$\begin{aligned} & \overline{\psi_{\nu_L}} U_\nu U_\nu^{-1} M_\nu U_\nu^T U_\nu^{-1} U_\nu^T \psi_{\nu_R} + \overline{l_L} U_{l_L} U_{l_L}^{-1} M_l U_{l_R} U_{l_R}^{-1} l_R + \overline{\nu_L} U_1 U_1^{-1} \gamma^\mu U_{l_L} U_{l_L}^{-1} l_L + h.c. \\ &= \overline{\psi_{\nu_L}^m} D_\nu \psi_{\nu_R}^m + \overline{l_L^m} D_l l_R^m + \overline{\nu_L^m} V^{-1} \gamma^\mu l_L^m + h.c. \end{aligned} \quad (235)$$

The matrix in the charged current term  $V = U_{l_L}^{-1}U_1$  is not square, but has dimension  $n_L \times n$ .

We still have the freedom to incorporate all of the lepton mixing in the neutrino sector, effectively replacing  $U_1$  with  $V$ , so the neutrino mixing matrix in this standard basis is

$$\hat{U}_\nu = \begin{pmatrix} V \\ U_2 \\ U_3 \end{pmatrix} = \begin{pmatrix} U_{l_L}^{-1} & 0 & 0 \\ 0 & 1 & 0 \\ 0 & 0 & 1 \end{pmatrix} U_\nu. \quad (236)$$

This replacement implies a different non-diagonalized neutrino mass matrix  $\hat{M}_\nu$ :

$$\begin{aligned} \hat{M}_\nu &= \hat{U}_\nu D \hat{U}_\nu^T = \begin{pmatrix} U_{l_L}^{-1} & 0 & 0 \\ 0 & 1 & 0 \\ 0 & 0 & 1 \end{pmatrix} U_\nu D U_\nu^T \begin{pmatrix} U_{l_L}^{T-1} & 0 & 0 \\ 0 & 1 & 0 \\ 0 & 0 & 1 \end{pmatrix} \\ &= \begin{pmatrix} U_{l_L}^{-1} & 0 & 0 \\ 0 & 1 & 0 \\ 0 & 0 & 1 \end{pmatrix} M_\nu \begin{pmatrix} U_{l_L}^{T-1} & 0 & 0 \\ 0 & 1 & 0 \\ 0 & 0 & 1 \end{pmatrix}. \end{aligned} \quad (237)$$

This transformation includes both a right and left rotation because it involves Majorana neutrinos. The transformation for  $n_L$  generations developed in equations (231) and (232) assumes the right-handed fields  $N_R$  are independent of the left-handed fields  $\nu_L$ , so the right-handed rotation matrix  $U_{N_R}$  appearing in equation (231) is unaffected by our new choice of  $U_{\nu_L}$ . For the Majorana mass term indicated in equation (53), this is no longer true. The right-handed fields are related to the left-handed fields, and the right-handed rotation matrix must equal  $(U_\nu^T)^{-1}$ . So changing to the standard basis rotates the mass matrix on the right as well on the left. Such an additional rotation could be performed in the three-generation Dirac case for consistency's sake (since we cannot measure  $U_{N_R}$  in the absence of a right-handed current), but it is not necessary on mathematical grounds. We note that under the transformation in equation (237) the Dirac subblocks  $M_D$  and  $M_D^T$  in the matrix (53) do transform to  $U_{l_L} M_D$  and  $M_D^T U_{l_L}^T$ , in agreement with equations (231) and (232). The issue here will become moot in the next Section when we restrict ourselves to the hermitian mass-squared matrix  $MM^\dagger$ . The extra rotation cancels in this product.

Even the diagonal mass matrix  $D$  is not completely measurable. The mass matrix  $M$  does not have to be hermitian, so the  $m_i$  in  $D$  are not necessarily real. We have the freedom to perform a chiral rotation  $e^{i\theta\gamma_5}$  on the fermion field definitions; under  $\psi \rightarrow e^{i\theta\gamma_5}\psi$ , mass terms become

$$\overline{\psi_L} M \psi_R + h.c. \rightarrow \overline{\psi_L} M e^{2i\theta\gamma_5} \psi_R + h.c. = \quad (238)$$

$$\overline{\psi_L} M (\cos 2\theta + i\gamma_5 \sin 2\theta) \psi_R + \overline{\psi_R} M^\dagger (\cos 2\theta + i\gamma_5 \sin 2\theta) \psi_L, \quad (239)$$

where we have used the properties  $\gamma_5^{2k} = \mathbb{1}$  and  $\gamma_5^{2k+1} = \gamma_5$  for integer  $k$  in the Taylor expansions of  $e^{2i\theta\gamma_5}$ ,  $\sin \theta$ , and  $\cos \theta$ . Since  $\gamma_5 P_L = -P_L$ , and  $\gamma_5 P_R = P_R$ , we have

$$\overline{\psi_L} M i\gamma_5 \psi_R + \overline{\psi_R} M^\dagger i\gamma_5 \psi_L = \overline{\psi_L} M i\psi_R - \overline{\psi_R} M^\dagger i\psi_L, \quad (240)$$

so our whole mass term has become

$$\overline{\psi_L} M e^{2i\theta} \psi_R + \overline{\psi_R} M^\dagger e^{-2i\theta} \psi_L = \overline{\psi_L} e^{2i\theta} M \psi_R + h.c. \quad (241)$$

A chiral rotation by  $\theta = \frac{\pi}{2}$  has the same effect as the transformation  $M \rightarrow -M$ ; a rotation by  $\theta = \frac{\pi}{4}$  effects  $M \rightarrow iM$ . We can separately perform chiral rotations on particular flavor fields, so the phases of individual mass eigenvalues are arbitrary. These rotations lead to corresponding effects on the diagonal  $D$ ; the phase of the mass matrix, and the phases of the fermion masses contained in the diagonal mass matrix  $D$ , cannot be measurable since we may absorb these phases into the fermion field definitions.

In the next Section, we will derive equations expressing the elements of the matrix  $\hat{M}_\nu \hat{M}^\dagger$  in terms of the observable boxes. To use these relationships to place constraints on the elements of the mass matrices given by particular models, the transformation (232) must be invoked. Once extra neutrinos are included, the CKM matrix  $V = \hat{U}_1$  appearing in the charged-current term is no longer equivalent to the full neutrino mixing matrix  $U_\nu$ . The matrix  $V$  knows about all  $n$  of the neutrino *mass* states, since it connects  $\nu_L$  with  $\psi^m$ , but it knows nothing of the sterile *flavor* neutrinos and therefore cannot be used to describe mixing between active and sterile flavors. The entire matrix

$U_\nu$  is necessary to completely describe neutrino mixing. In what follows, however, we will use the symbol  $V$  to denote the left-handed neutrino mixing matrix, as we did in the previous Sections of this Chapter. For three generations, this assignment presents no ambiguity; for  $n > 3$ , the neutrino mixing matrix  $V$  will have different dimensions than the CKM matrix  $V$ , so again there should be no confusion.

#### 4.4 More Measurables

We showed in Section 4.1 that  $2n - 1$  relative phases can not be observed. For Dirac neutrinos, we also have the freedom to rotate  $U_{N_R}$  *ad nauseum* since it is not observable in the absence of right-handed currents. The effects of this last degree of freedom may be ignored if we consider only the hermitian product  $MM^\dagger$  rather than the generally non-hermitian mass matrix  $M$ . Should right-handed currents be found, one may explore  $U_{N_R}$  via the hermitian matrix  $M^\dagger M$ . Note that in the absence of the symmetry imposed by Majorana neutrinos,  $M^\dagger M = \hat{M}^\dagger \hat{M}$ , since the rotation by  $U_{\nu_L}$  in  $\hat{M} = U_{\nu_L}^{-1} M U_{N_R}$  is canceled; this matrix is diagonalized by  $U_{N_R}$  alone into  $D^2$ :

$$U_{N_R}^\dagger M^\dagger M U_{N_R} = D^2. \quad (242)$$

The phase ambiguity of the mixing matrix requires that any observables which are functions of the left-handed neutrino mixing matrix  $V$  and/or the product  $MM^\dagger$  must be invariant under the simultaneous transformations

$$V \rightarrow Y V X, \quad \text{and} \quad \hat{M} \hat{M}^\dagger \rightarrow X^{-1} \hat{M} \hat{M}^\dagger X, \quad (243)$$

where  $X$  and  $Y$  are diagonal matrices of phases. These invariances are identical to those possessed by traces of products of  $MM^\dagger$  and diagonal basis matrices, or of traces of products of  $V$  and diagonal basis matrices. Such traces offer an elegant method of obtaining the measurable functions of the mixing matrix and the mass matrix.

We introduce the notation

$$H \equiv \hat{M} \hat{M}^\dagger, \quad (244)$$

and the diagonal basis matrices

$$(E_i)_{mn} \equiv \delta_{mi}\delta_{mn}, \quad (245)$$

We may express mass-matrix invariants in terms of these newly-defined quantities as

$$\text{Tr} \left[ \prod_{\alpha} (HE_{\alpha}) \right]. \quad (246)$$

Thus,

$$\text{Tr} [HE_{\alpha}] = H_{\alpha\alpha} \quad (247)$$

is an invariant, as is

$$\text{Tr} [HE_{\alpha}HE_{\beta}] = |H_{\alpha\beta}|^2. \quad (248)$$

Higher-order traces such as  $\text{Tr} [HE_{\alpha}HE_{\beta}HE_{\gamma}]$  are also invariants.

Turning to the mixing matrix, we see that equal numbers of  $V$ s and  $V^{\dagger}$ s provide invariants.  $V$  placed into a trace by itself is not invariant, since the phase matrices  $X$  and  $Y$  occurring on either side of the rotated mixing matrix do not cancel in the trace:

$$\text{Tr} [VE_i] \neq \text{Tr} [YVE_iX]. \quad (249)$$

Here we have used the commutativity of the diagonal matrices  $X$  and  $E_i$ . The product  $V^{\dagger}V$ , however, is rotated by the single transformation  $X$ , which will cancel in the trace, so

$$\text{Tr} [V^{\dagger}E_{\alpha}VE_i] = \text{Tr} [X^{-1}V^{\dagger}E_{\alpha}Y^{-1}YVE_iX] = |V_{\alpha i}|^2 \quad (250)$$

is invariant [35], as is the fourth-order trace

$$\text{Tr} [VE_{\alpha}V^{\dagger}E_iVE_{\beta}V^{\dagger}E_j] = V_{\alpha i}V_{i\beta}^{\dagger}V_{\beta j}V_{j\alpha}^{\dagger}, \quad (251)$$

which is a box. Again, traces of products higher-order in even powers of  $V$  are also measurable.

The mass-matrix invariant traces are related to the mixing-matrix invariant traces by

$$H = V D^2 V^\dagger = V \left[ \sum_{j=1}^n E_j m_j^2 \right] V^\dagger = \sum_{j=1}^n m_j^2 V E_j V^\dagger. \quad (252)$$

So we find

$$H_{\alpha\alpha} = \text{Tr} [HE_\alpha] = \sum_{j=1}^n m_j^2 \text{Tr} [VE_j V^\dagger E_\alpha] = \sum_{j=1}^n m_j^2 |V_{\alpha j}|^2 = \sum_{j=1}^n m_j^2 \sqrt{\alpha_j \square_{\alpha j}}, \quad (253)$$

and

$$|H_{\alpha\beta}|^2 = \text{Tr} [HE_\alpha HE_\beta] = \sum_{i=1}^n \sum_{j=1}^n m_i^2 m_j^2 \text{Tr} [VE_\alpha V^\dagger E_i V E_\beta V^\dagger E_j] = \sum_{i=1}^n \sum_{j=1}^n m_i^2 m_j^2 \alpha_i \square_{\beta j}. \quad (254)$$

The next-order expression becomes

$$H_{\alpha\beta} H_{\beta\gamma} H_{\gamma\alpha} = \text{Tr} [HE_\beta HE_\gamma HE_\alpha] = \sum_{i=1}^n \sum_{j=1}^n \sum_{k=1}^n m_i^2 m_j^2 m_k^2 V_{\alpha i} V_{i\beta}^\dagger V_{\beta j} V_{j\gamma}^\dagger V_{\gamma k} V_{k\alpha}^\dagger. \quad (255)$$

These products of six mixing matrix elements and even the product of eight mixing matrix elements could be measured in processes such as the decay  $\mu^\pm \rightarrow e^\pm e^+ e^-$  which proceeds through penguin and box graphs with internal neutrino lines.

The right-hand side of equation (254) may be written as

$$\sum_{i=1}^n m_i^4 \alpha_i \square_{\beta j} + \sum_{i=1}^n \sum_{j \neq i} m_i^2 m_j^2 \alpha_i \square_{\beta j} = \sum_{i=1}^n m_i^4 |V_{\alpha i}|^2 |V_{\beta i}|^2 + 2 \sum_{i=1}^n \sum_{j > i} m_i^2 m_j^2 \alpha_i \square_{\beta j}. \quad (256)$$

From this we see that not only is information about relative phases lost, but that the measurable  $J$ s do not enter either. The missing information is carried in the higher-order observables, such as those found in equation (255). An alternative approach is suggested by the unitarity constraints (195) and (196) which may be rearranged to express  $\alpha_i$  in terms of  $R$ s. Unitarity therefore provides a mechanism for implicitly obtaining the  $J$ s from real trace relations.

Equations (253) and (254) involve the neutrino mass matrix in the standard basis, with all of the mixing in the neutrino sector. If we want to compare the predictions of mass models specified

in a non-standard basis to the measurable quantities in the right-hand side of equations (253) and (254), we need to rotate  $\hat{M}$  back to the  $M_\nu$  of the specific model as described in equation (232). Performing this rotation on  $H_{\alpha\beta}$ , we find

$$|H_{\alpha\beta}|^2 = \left| \left( \hat{M} \hat{M}^\dagger \right)_{\alpha\beta} \right|^2 = \sum_{i,j=1}^n |(U_{lL})_{\alpha i}^{-1} (M_\nu M_\nu^\dagger)_{ij} (U_{lL})_{j\beta}|^2. \quad (257)$$

$U_{lL}$  and  $M_\nu$  are given by the model, while the right-hand side of equation (254) (which equals (257)) contains measurable quantities. Finding individual elements of  $M_\nu M_\nu^\dagger$  in terms of the observables might be messy, but it is possible using the above equations.

Consider next the converse issue of constructing the boxes from a given  $M$  (and therefore a given  $H$ ). Equations (253) and (254) present equations for each of the  $n^2$  possible  $\alpha, \beta$ . These equations involve  $N^2 \sim n^4$  ordered boxes. Equations (253) and (254) therefore cannot be simply inverted to obtain the boxes from the mass matrix in the general case. [41]. The unitarity constraints presented in the earlier Sections of this Chapter reduce the number of independent boxes so the inversion could in principle be done. But the relations would be highly non-linear and intractable. To obtain the boxes from a given mass matrix, we will diagonalize the specified matrix and solve for the eigenvectors. These eigenvectors may then be used to construct the mixing matrix  $V$ , which gives the boxes. This procedure is illustrated in Chapter V for a few selected mass matrix textures.

## CHAPTER V

### APPLICATIONS OF THE BOXES TO SPECIFIC PHENOMENOLOGICAL MODELS

Having developed a parameterization for neutrino oscillation which is independent of neutrino mass and mixing models, we will now examine how different models may be expressed in terms of the boxes.

#### 5.1 Models of the Mixing Matrix

##### 5.1.1 The Standard KM Parameterization

For Dirac neutrinos, the mixing matrix  $V$  becomes the familiar CKM matrix from quark mixing (although the mixing angles need not have the same values as for the quark case), and  $V$  may be characterized by three mixing angles  $\theta_a$  and a phase  $\delta$ . A popular choice of  $V$  is the Kobayashi-Maskawa matrix of equation (98):

$$\begin{pmatrix} c_1 & s_1 c_3 & s_1 s_3 \\ -s_1 c_2 & c_1 c_2 c_3 - s_2 s_3 e^{i\delta} & c_1 c_2 s_3 + s_2 c_3 e^{i\delta} \\ -s_1 s_2 & c_1 s_2 c_3 + c_2 s_3 e^{i\delta} & c_1 s_2 s_3 - c_2 c_3 e^{i\delta} \end{pmatrix}. \quad (98)$$

In terms of these angles, we find that  $\mathcal{J}$ , the imaginary part of the boxes is

$$\begin{aligned} \mathcal{J} &= c_1 s_1^2 c_2 s_2 c_3 s_3 \sin \delta \\ &= \frac{1}{8} \sin \theta_1 \sin 2\theta_1 \sin 2\theta_2 \sin 2\theta_3 \sin \delta \equiv J \sin \delta, \end{aligned} \quad (258)$$

as predicted in Chapter III's equation (99). Using this definition of  $J$ , we may express our boxes as

$$\begin{aligned} {}^{11}\square_{22} &= -c_1^2 s_1^2 c_2^2 c_3^2 + J e^{i\delta} \\ {}^{12}\square_{23} &= s_1^2 c_3^2 s_3^2 (c_1^2 c_2^2 - s_2^2) + J \cos \delta (c_3^2 - s_3^2) + i J \sin \delta \\ {}^{11}\square_{23} &= -c_1^2 s_1^2 c_2^2 s_3^2 - J e^{i\delta} \end{aligned}$$

$$\begin{aligned}
{}^{21}\square_{32} &= s_1^2 c_2^2 s_2^2 (c_1^2 c_3^2 - s_3^2) + J \cos \delta (c_2^2 - s_2^2) + i J \sin \delta \\
{}^{22}\square_{33} &= c_3^2 s_3^2 [s_2^2 c_2^2 (s_1^4 + 6c_1^2 + 2c_1^2 \cos 2\delta) - c_1^2] \\
&\quad + \frac{J}{s_1^2} (1 + c_1^2) (c_2^2 - s_2^2) (s_3^2 - c_3^2) \cos \delta + i J \sin \delta \\
{}^{21}\square_{33} &= s_1^2 c_2^2 s_2^2 (c_1^2 s_3^2 - c_3^2) + J \cos \delta (s_2^2 - c_2^2) - i J \sin \delta \\
{}^{11}\square_{32} &= -c_1^2 s_1^2 s_2^2 c_3^2 - J e^{i\delta} \\
{}^{12}\square_{33} &= s_1^2 c_3^2 s_3^2 (c_1^2 s_2^2 - c_2^2) + J \cos \delta (s_3^2 - c_3^2) - i J \sin \delta \\
{}^{11}\square_{33} &= -c_1^2 s_1^2 s_2^2 s_3^2 + J e^{i\delta}
\end{aligned} \tag{259}$$

In terms of the standard parameterization the observable probabilities, presented here as boxes, are big ugly messes. It is no wonder that approximations have been commonly used when comparing experimental results to the standard mixing angles and phase!

In principle, one can solve equations (259) with  $\delta = 0$  for  $\theta_1$ ,  $\theta_2$ , and  $\theta_3$  in terms of a basis of the real parts of any three independent nondegenerate boxes. Then substitutions into equations (259) give the remaining six nondegenerate real boxes in terms of these chosen three.  $\delta$  is then given in terms of these three boxes and the imaginary part  $\pm \mathcal{J}$  of any box from

$$\delta = \sin^{-1} \left( \frac{\mathcal{J}}{J(\theta_1, \theta_2, \theta_3)} \right). \tag{260}$$

In practice, we have been unable to analytically invert equation (259) with only three basis boxes.<sup>1</sup> Thus we have another reason to eschew the arbitrary unitary parameterization of  $V$  and work directly with the box algebra.

---

<sup>1</sup> Allowing four nondegenerate boxes as a dependent basis does provide an analytic inversion of equation (259). We find

$$\sin^2 2\theta_1 = -4 \left( {}^{11}\square_{22} + {}^{11}\square_{23} + {}^{11}\square_{32} + {}^{11}\square_{33} \right), \tag{261}$$

$$\tan^2 \theta_2 = \frac{{}^{11}\square_{32} + {}^{11}\square_{33}}{{}^{11}\square_{22} + {}^{11}\square_{23}}, \text{ and} \tag{262}$$

$$\tan^2 \theta_3 = \frac{{}^{11}\square_{23} + {}^{11}\square_{33}}{{}^{11}\square_{22} + {}^{11}\square_{32}}. \tag{263}$$

We see, however, no way to reduce this basis to three independent boxes. We choose the four basis boxes by examination of the relationships (259); the boxes which are most simply expressed in terms of the mixing angles are the boxes we choose for our basis. Thus the choice of which four boxes to isolate as the basis depends on the unitary parameterization used for  $V$ .  $V$  is constructed by three successive rotations and a phase matrix; one may choose the rotation axes  $(\hat{i}, \hat{j}, \hat{k})$  in  $V(\delta = 0) = R_{\hat{i}}(\theta_1)R_{\hat{j}}(\theta_2)R_{\hat{k}}(\theta_3)$  such that each of the desired four basis boxes has only two terms, being composed from three of the simplest  $V$ s and one binomial  $V$ .

### 5.1.2 The Wolfenstein Parameterization

Wolfenstein suggested [42] a now-popular parameterization of the CKM matrix based on data from the quark sector. The parameter  $\lambda$  is defined by  $\lambda = V_{12}$ , and the rest of the matrix is determined by comparing matrix elements with powers of this small angle [42]. (For example, the element  $V_{23}$  is on the order of  $V_{12}^2$  in the quark sector, so it is expressed in terms of  $\lambda^2$ . Keeping the matrix unitary to the desired order of  $\lambda$  yields the higher-order terms in  $V_{11}$  and  $V_{22}$ . The Wolfenstein mixing matrix to  $\mathcal{O}(\lambda^3)$  is

$$V = \begin{pmatrix} 1 - \frac{1}{2}\lambda^2 & \lambda & \lambda^3 A(\rho - i\eta) \\ -\lambda & 1 - \frac{1}{2}\lambda^2 & \lambda^2 A \\ \lambda^3 A(1 - \rho - i\eta) & -\lambda^2 A & 1 \end{pmatrix}. \quad (264)$$

This matrix is only unitary to order  $\lambda^3$ , so any relationships between our boxes based on the unitarity of the mixing matrix, such as the relationships proving the equality of the imaginary parts of boxes, will hold only to order  $\lambda^3$ . Wolfenstein describes the mixing matrix in terms of 4 parameters:  $\lambda$ ,  $A$ ,  $\rho$ , and  $\eta$ . We choose the three boxes  ${}^{11}\square_{22}$ ,  ${}^{21}\square_{32}$ , and  ${}^{11}\square_{23}$  as our basis. Combining the definitions of our boxes (125) with Wolfenstein's mixing matrix (264), we find

$${}^{11}\square_{22} = -\lambda^2(1 - \frac{1}{2}\lambda^2)^2 \simeq -\lambda^2, \quad (265)$$

$${}^{21}\square_{32} = A^2\lambda^6(1 - \frac{1}{2}\lambda^2)(1 - \rho - i\eta) \simeq A^2\lambda^6(1 - \rho - i\eta), \text{ and} \quad (266)$$

$${}^{11}\square_{23} = -A^2\lambda^6(1 - \frac{1}{2}\lambda^2)(1 - \rho - i\eta) \simeq -A^2\lambda^6(\rho - i\eta). \quad (267)$$

${}^{11}\square_{22}$  is real, and the imaginary component of  ${}^{21}\square_{32}$  has equal magnitude but opposite sign as the imaginary component of  ${}^{11}\square_{23}$ , so the three boxes act as four independent parameters. (Again, the boxes do not appear to have the same imaginary parts because Wolfenstein has thrown out terms higher order in  $\lambda$ . If we were to keep the leading-order imaginary term for all of the boxes, all  $\mathfrak{g}_{\beta j}^i$  would be  $\pm A^2\lambda^6\eta$ .) We can now find the rest of the boxes and express them in terms of our chosen

three boxes.

$${}^{11}\square_{33} \simeq A^2 \lambda^6 (\rho - i\eta)(1 - \rho - i\eta) \simeq \frac{{}^{11}\square_{23} \quad {}^{21}\square_{32}}{{}^{11}\square_{23}^* - {}^{21}\square_{32}} \quad (268)$$

$${}^{12}\square_{23} \simeq - {}^{12}\square_{33} \simeq A^2 \lambda^6 (\rho - i\eta) \simeq - {}^{11}\square_{23} \quad (269)$$

$${}^{11}\square_{32} \simeq + {}^{21}\square_{33} \simeq - A^2 \lambda^6 (1 - \rho - i\eta) \simeq - {}^{21}\square_{32} \quad (270)$$

$\mathcal{B}$ , our matrix of boxes in (135) becomes the following for the Wolfenstein parameterization:

$$\mathcal{B} = \begin{pmatrix} {}^{11}\square_{22} & - {}^{11}\square_{23} & {}^{11}\square_{23} \\ {}^{21}\square_{32} & \frac{{}^{21}\square_{32} - {}^{11}\square_{23}^*}{{}^{11}\square_{22}} & - {}^{21}\square_{32} \\ - {}^{21}\square_{32} & {}^{11}\square_{23} & \frac{{}^{11}\square_{23} \quad {}^{21}\square_{32}}{{}^{11}\square_{23}^* - {}^{21}\square_{32}} \end{pmatrix}. \quad (271)$$

The dominant box in this approximation is  ${}^{11}\square_{22}$ . Thus the  $\nu_e \leftrightarrow \nu_\mu$  transition would be most probable, with its primary contribution coming from the  $\Delta m_{12}^2$  term. The transition  $\nu_\mu \leftrightarrow \nu_\tau$  is next-probable, down by the order of  $\lambda^2$  from the  $\nu_e \leftrightarrow \nu_\mu$  transition, and it receives its dominant contribution from the  $\Delta m_{23}^2$  term. The least likely transition according to the Wolfenstein model, down the order of  $\lambda^4$  from the  $\nu_e \leftrightarrow \nu_\mu$  transition, is the  $\nu_e \leftrightarrow \nu_\tau$  transition, and it receives equal contributions from all three mass differences.

### 5.1.3 The One-Angle Approximation

A related near-unitary parameterization fitting the quark data uses only one real parameter,  $\theta$ , and a phase  $\delta$ . Experimental determinations of the quark mixing matrix elements are consistent with the following form for  $V$  [34]:

$$V = \begin{pmatrix} 1 & \theta & \theta^3 e^{-i\delta} \\ -\theta & 1 & \theta^2 \\ -\theta^3 e^{i\delta} & -\theta^2 & 1 \end{pmatrix}. \quad (272)$$

This approximation is a special case of the Wolfenstein parameterization, setting  $A = |\rho - i\eta| = 1$  and results in the following matrix of boxes:

$$\mathcal{B} = \begin{pmatrix} {}^{11}\square_{22} & -{}^{21}\square_{32}^* & {}^{21}\square_{32}^* \\ {}^{21}\square_{32} & -({}^{11}\square_{22})^2 & -{}^{21}\square_{32} \\ -{}^{21}\square_{32} & {}^{21}\square_{32}^* & ({}^{11}\square_{22})^3 \end{pmatrix}, \quad (273)$$

with

$${}^{11}\square_{22} = -\theta^2, \text{ and } {}^{21}\square_{32} = -\theta^6 e^{i\delta}. \quad (274)$$

The mixing matrix in (272) contains only two independent parameters, but our matrix  $\mathcal{B}$  seems to contain three:  ${}^{11}\square_{22}$ , which is real,  $(\mathbb{R}_{32})$ , and  $(\mathbb{I}_{32})$ . But the three are related by

$$|{}^{21}\square_{32}|^2 = (\mathbb{R}_{32})^2 + (\mathbb{I}_{32})^2 = ({}^{11}\square_{22})^6 \quad (275)$$

So we are indeed left with two independent parameters.

Because this one-angle approximation is a special case of the Wolfenstein parameterization, it produces the same predictions for the relative significance of transition probabilities:  $\nu_e \leftrightarrow \nu_\mu$  is the most probable, and  $\nu_e \leftrightarrow \nu_\tau$  is the least probable. Discerning between the general Wolfenstein parameterization and this extension would require measurements of probabilities at different lengths so boxes within a row may be measured individually.

#### 5.1.4 The Dominant Mass Scale Approximation

A popular approximation for neutrino masses and mixing assumes  $m_3 \gg m_1, m_2$  [43], [44], so  $\Phi_{23} \approx \Phi_{13} \approx \frac{m_3^2}{4p}$ . Under this approximation,

$$\text{Re}(\mathcal{B}) S^2(\Phi) = \begin{pmatrix} \mathbb{R}_{22} & \mathbb{R}_{23} + \mathbb{R}_{23} \\ \mathbb{R}_{32} & \mathbb{R}_{33} + \mathbb{R}_{33} \\ \mathbb{R}_{32} & \mathbb{R}_{33} + \mathbb{R}_{33} \end{pmatrix} \begin{pmatrix} \sin^2 \Phi_{12} \\ \sin^2 \Phi_{13} \end{pmatrix}, \quad (276)$$

and

$$\begin{aligned}
\text{Im}(\mathcal{B}) S(2\Phi) &= \begin{pmatrix} {}^1\mathbb{J}_{22} & {}^1\mathbb{J}_{23} + {}^1\mathbb{J}_{32} \\ {}^2\mathbb{J}_{32} & {}^2\mathbb{J}_{33} + {}^2\mathbb{J}_{33} \\ {}^1\mathbb{J}_{32} & {}^1\mathbb{J}_{33} + {}^1\mathbb{J}_{33} \end{pmatrix} \begin{pmatrix} \sin(2\Phi_{12}) \\ \sin(2\Phi_{13}) \end{pmatrix} \\
&= \begin{pmatrix} {}^1\mathbb{J}_{22} \\ {}^2\mathbb{J}_{32} \\ {}^1\mathbb{J}_{32} \end{pmatrix} \sin(2\Phi_{12}) = \mathcal{J} \sin(2\Phi_{12}) \begin{pmatrix} 1 \\ 1 \\ -1 \end{pmatrix}. \tag{277}
\end{aligned}$$

The second column of  $\text{Im}(\mathcal{B})$  vanishes because the sums of boxes are real by equations (165) and (166).

For small  $x$ ,

$$\sin^2 \Phi_{12} \ll \sin^2 \Phi_{13} \tag{278}$$

due to the mass hierarchy. Thus experiments with a small  $x$  will measure the factors multiplying the bigger phase  $\Phi_{13}$ , such as the sum

$${}^1\mathbb{R}_{23} + {}^1\mathbb{R}_{32}. \tag{279}$$

In Chapter VI, we apply a dominant-mass-scale approach to the oscillation data currently available; in that treatment, the LSND experiment measures the sum (279). This sum is equal to the degenerate box  ${}^1\mathbb{R}_{23}$  by equation (181).

Sources producing neutrinos with uncertainties in  $p$  or  $x$  large enough that all the oscillatory terms average will provide measurements of a sum of all three boxes in a row of  $\mathcal{B}$ :

$$\text{Re}\mathcal{B}(S^2(\Phi)) = \frac{1}{2} \begin{pmatrix} {}^1\mathbb{R}_{22} + {}^1\mathbb{R}_{23} + {}^1\mathbb{R}_{32} \\ {}^2\mathbb{R}_{32} + {}^2\mathbb{R}_{33} + {}^2\mathbb{R}_{33} \\ {}^1\mathbb{R}_{32} + {}^1\mathbb{R}_{33} + {}^1\mathbb{R}_{33} \end{pmatrix} = -\frac{1}{4} \begin{pmatrix} \sum_{x=1}^n |V_{1x}|^2 |V_{2x}|^2 \\ \sum_{x=1}^n |V_{2x}|^2 |V_{3x}|^2 \\ \sum_{x=1}^n |V_{1x}|^2 |V_{3x}|^2 \end{pmatrix}, \tag{280}$$

where the last equality comes from equation (157). This type of asymptotic measurement could not detect CP violation directly since the average of the  $\sin 2\Phi_{ij}$  function is zero. Our analysis in Chapter VI applies this averaging to both solar neutrinos and atmospheric neutrinos.

CP violation is a very small effect in this dominant mass-scale approximation, even when the oscillatory terms do not vanish. As seen in equation (277), the CP-violating term depends on  $\sin(2\Phi_{12})$ , so the CP-violating effects for local neutrino sources are of order  $\frac{m_1^2 - m_2^2}{2p} x$ . Oscillatory behavior would eventually develop over longer baselines.

## 5.2 Models of the Mass Matrix

### 5.2.1 Using a Fritzsch Mass Matrix

In the late 1970s, Fritzsch [45] proposed a form of the quark mass matrices which has proven to be consistent with experiment. Extending this model to the lepton sector means the mass matrices  $M_\nu$  and  $M_l$  for neutrinos and charged leptons will both be Dirac matrices and have the Fritzsch form [45]:

$$M_\nu = \begin{pmatrix} 0 & ae^{i\xi_1} & 0 \\ ae^{i\xi_2} & 0 & be^{i\xi_3} \\ 0 & be^{i\xi_4} & ce^{i\xi_5} \end{pmatrix}, \text{ and} \quad (281)$$

$$M_l = \begin{pmatrix} 0 & Ae^{i\Xi_1} & 0 \\ Ae^{i\Xi_2} & 0 & Be^{i\Xi_3} \\ 0 & Be^{i\Xi_4} & Ce^{i\Xi_5} \end{pmatrix}. \quad (282)$$

The parameters  $a, b, c, A, B$ , and  $C$  may be taken to be real positive and will be determined by the lepton masses. The postulated zero entries are today known as “texture zeros.” They can be motivated by invoking symmetries in the Higgs sector; such symmetries may be natural in grand unified theories. Each of the mass matrices originally has five independent phases, but we may rotate the mass matrix and absorb the phases in the lepton fields:

$$\begin{aligned} \overline{\nu_L} M_\nu N_R + \overline{l_L} M_l l_R + h.c. &= \overline{\nu_L} X_{\nu_L} X_{\nu_L}^{-1} M_\nu X_{N_R} X_{N_R}^{-1} N_R + \overline{l_L} X_{l_L} X_{l_L}^{-1} M_l X_{l_R} X_{l_R}^{-1} l_R + h.c \\ &= \overline{\tilde{\nu}_L} \tilde{M}_\nu \tilde{N}_R + \overline{\tilde{l}_L} \tilde{M}_l \tilde{l}_R + h.c., \text{ with} \end{aligned} \quad (283)$$

$$\tilde{\nu}_L = X_{\nu_L}^{-1} \nu_L, \quad \tilde{N}_R = X_{N_R}^{-1} N_R, \quad \tilde{l}_L = X_{l_L}^{-1} l_L, \quad \text{and} \quad \tilde{l}_R = X_{l_R}^{-1} l_R. \quad (284)$$

As before,  $\nu_L, l_L, N_R$ , and  $l_R$  are the  $1 \times 3$  vectors containing all three generations of spinors.

Following Fritzsch's treatment in [45], we choose

$$X_{\nu_L} = \begin{pmatrix} 1 & 0 & 0 \\ 0 & e^{-i(\xi_1 - \xi_3 - \xi_4 + \xi_5)} & 0 \\ 0 & 0 & e^{-i(\xi_1 - \xi_4)} \end{pmatrix}, \quad \text{and} \quad (285)$$

$$X_{N_R} = \begin{pmatrix} e^{-i(\xi_1 + \xi_2 - \xi_3 - \xi_4 + \xi_5)} & 0 & 0 \\ 0 & e^{-i\xi_1} & 0 \\ 0 & 0 & e^{-i(\xi_1 - \xi_4 + \xi_5)} \end{pmatrix}, \quad (286)$$

with  $X_{l_L}$  and  $X_{l_R}$  found by substituting  $\Xi$  for  $\xi$ . Under this transformation,

$$M_\nu \rightarrow \tilde{M}_\nu = X_{\nu_L}^{-1} M_\nu X_{N_R} = \begin{pmatrix} 0 & a & 0 \\ a & 0 & b \\ 0 & b & c \end{pmatrix}, \quad \text{and} \quad (287)$$

$$M_l \rightarrow \tilde{M}_l = X_{l_L}^{-1} M_l X_{l_R} = \begin{pmatrix} 0 & A & 0 \\ A & 0 & B \\ 0 & B & C \end{pmatrix}. \quad (288)$$

These real symmetric matrices may be diagonalized by the orthogonal matrices  $R_\nu$  and  $R_l$ :

$$R_\nu^{-1} \tilde{M}_\nu R_\nu = \begin{pmatrix} m_1 & 0 & 0 \\ 0 & -m_2 & 0 \\ 0 & 0 & m_3 \end{pmatrix}, \quad \text{and} \quad R_l^{-1} \tilde{M}_l R_l = \begin{pmatrix} m_e & 0 & 0 \\ 0 & -m_\mu & 0 \\ 0 & 0 & m_\tau \end{pmatrix}. \quad (289)$$

The  $m_i$  are positive, and the minus signs in front of the second mass eigenstates occur because the determinants of the  $\tilde{M}$  are negative. Such a sign factor may be absorbed by a chiral redefinition of the appropriate lepton fields. Under  $\psi \rightarrow e^{i\frac{\pi}{2}\gamma_5} \psi = i\gamma_5 \psi$ ,  $m\bar{\psi}\psi \rightarrow -m\bar{\psi}\psi$ , as discussed in Section 4.3. This chiral rotation, however, would put the mass matrix into a non-Fritzsch form. The

issue of the sign of the fermion mass is obviated if we work with  $MM^\dagger$  as in the previous Chapter, but we have here chosen instead to parallel Fritzsch's development.

These transformations  $R$  and  $X$  take us to the mass basis:  $\nu_L^m = R_\nu^{-1} X_{\nu_L}^{-1} \nu_L$ ,  $N_R^m = R_\nu^{-1} X_{N_R}^{-1} N_R$ , *et cetera*. As discussed in Section 2.7, the mixing matrix arises in the charged-current interaction:

$$\mathcal{J}_{CC} = \overline{\nu_L} \gamma^\mu l_L = \overline{\nu_L} X_{\nu_L} R_\nu (R_\nu^{-1} X_{\nu_L}^{-1} X_{l_L} R_l) R_l^{-1} X_{l_L}^{-1} \gamma^\mu l_L = \overline{\nu_L} V \gamma^\mu l_L^m, \quad (290)$$

Once  $R_\nu$  and  $R_l$  are found from (289), the mixing matrix may be calculated from

$$V = R_\nu^{-1} X_{\nu_L}^{-1} X_{l_L} R_l = R_\nu^{-1} \begin{pmatrix} 1 & 0 & 0 \\ 0 & e^{i\sigma} & 0 \\ 0 & 0 & e^{i\eta} \end{pmatrix} R_l. \quad (291)$$

The two phases  $\sigma$  and  $\eta$  contain all of the phases in  $X_{\nu_L}$  and  $X_{l_L}$ :  $\sigma = (\xi_1 - \Xi_1) - (\xi_3 - \Xi_3) - (\xi_4 - \Xi_4) + (\xi_5 - \Xi_5)$ , and  $\eta = (\xi_1 - \Xi_1) - (\xi_4 - \Xi_4)$ . One of these phases may be determined by measurement of the standard CKM phase  $\delta$  in (98). The other only appears in real terms (see below) and therefore may be absorbed in the definition of the mixing angles in the standard parameterization, as shown in [45].

This extra phase occurs because Fritzsch postulates a set form for the mass matrices, thereby depriving us of some extra degrees of freedom. As discussed above, any measurable quantities may be described by the masses and the mixing matrix,  $V$ . This matrix is unitary and therefore may have at most six phases. Five relative phases may be absorbed in the definitions of the left-handed leptons and right-handed neutrinos, leaving one phase in this observable matrix. Fritzsch, however, assumes a form for the mass matrices which yields ten phases. Only eight relative phases may be absorbed in the lepton fields (the left-handed neutrinos and charged leptons must be rotated together, so nine rotations may be performed on the left-handed leptons, the right-handed neutrinos, and the right-handed charged leptons), leaving two phases in the mass matrix. Under this method, the rotation

matrices have the form

$$X'_{\nu_L} = X'_{l_L} = \begin{pmatrix} e^{i(\xi_1 + \xi_2 - \xi_3 + \xi_4 - \xi_5)} & 0 & 0 \\ 0 & e^{i(\xi_2 + \sigma)} & 0 \\ 0 & 0 & e^{i(\xi_2 - \xi_3 + 2\xi_4 - \xi_5 + \eta)} \end{pmatrix}, \quad (292)$$

$$X'_{N_R} = \begin{pmatrix} 1 & 0 & 0 \\ 0 & e^{i(\xi_2 - \xi_3 + \xi_4 - \xi_5)} & 0 \\ 0 & 0 & e^{i(\xi_2 - \xi_3)} \end{pmatrix}, \text{ and} \quad (293)$$

$$X'_{l_R} = \begin{pmatrix} e^{i(\xi_2 - \Xi_2)} & 0 & 0 \\ 0 & e^{i(\xi_1 - X i_1 + \xi_2 - \xi_3 + \xi_4 - \xi_5)} & 0 \\ 0 & 0 & e^{i(\xi_2 - \Xi_3)} \end{pmatrix}. \quad (294)$$

These rotations yield the matrices  $\tilde{M}_l$  and  $X^{-1}\tilde{M}_\nu$ , with  $X$  equal to the net phase matrix above:

$$X = \begin{pmatrix} 1 & 0 & 0 \\ 0 & e^{i\sigma} & 0 \\ 0 & 0 & e^{i\eta} \end{pmatrix}. \quad (295)$$

Once we have simplified the mass matrices to  $\tilde{M}_\nu$  and  $\tilde{M}_l$  which have the same form, we need only solve for  $R_\nu$  by diagonalizing  $\tilde{M}_\nu$  in (289) and then obtain  $R_l$  by substitution. The first step in diagonalizing a matrix is to solve the eigenvalue equation, a task which is simplified because we know the eigenvalues,  $m_1$ ,  $-m_2$ , and  $m_3$ , and want only the unknown  $a$ ,  $b$ , and  $c$  in terms of the masses:

$$\text{Det}(\tilde{M}_\nu - mI) = -m^3 + cm^2 + (a^2 + b^2)m - a^2c = (m_1 - m)(-m_2 - m)(m_3 - m). \quad (296)$$

Solving for the unknown  $a$ ,  $b$ , and  $c$  by matching coefficients of  $m$ , we find

$$\begin{aligned} c &= m_1 - m_2 + m_3 \\ b^2 + a^2 &= m_1 m_2 + m_2 m_3 - m_3 m_1 \end{aligned} \quad (297)$$

$$a^2 c = m_1 m_2 m_3.$$

The first of these relations gives  $c$  explicitly, and we can solve for  $a$  and  $b$ :

$$\begin{aligned} a^2 &= \frac{m_1 m_2 m_3}{m_1 - m_2 + m_3} \\ b^2 &= m_1 m_2 + m_2 m_3 - m_3 m_1 - a^2. \end{aligned} \tag{298}$$

Because  $a$  and  $b$  were defined to be positive real numbers, we must always take the positive square root of the right sides of (298).

We may construct the diagonalizing matrix  $R_\nu$  out of the eigenvectors  $\psi$  of  $\tilde{M}_\nu$ . These eigenvectors satisfy the relationship

$$\tilde{M}_\nu \psi = m \psi, \tag{299}$$

which provides three constraints on the elements  $\psi_1$ ,  $\psi_2$ , and  $\psi_3$  of  $\psi$ :

$$\begin{aligned} a\psi_2 &= m\psi_1, \\ a\psi_1 + b\psi_3 &= m\psi_2, \text{ and} \\ b\psi_2 + c\psi_3 &= m\psi_3. \end{aligned} \tag{300}$$

The first and the second of the equations in (300) describe the form of  $\psi$ . The third, combined with the conclusions of the first two, reiterates the eigenvalue equation (296). We thus find that  $\psi$  has the form

$$\psi = n \begin{pmatrix} ab \\ mb \\ m^2 - a^2 \end{pmatrix}, \tag{301}$$

where  $n$  is a normalization constant, chosen to make the length of  $\psi$  equal to 1:

$$\frac{1}{n^2} = a^2 b^2 + m^2 b^2 + (m^2 - a^2)^2. \tag{302}$$

These relations hold for  $m$  equal to each of the eigenvalues  $m_1$ ,  $-m_2$ , or  $m_3$ , giving the apparently

simple form for  $R_\nu$

$$R_\nu = \begin{pmatrix} n_1 ab & n_2 ab & n_3 ab \\ n_1 m_1 b & -n_2 m_2 b & n_3 m_3 b \\ n_1(m_1^2 - a^2) & n_2(m_2^2 - a^2) & n_3(m_3^2 - a^2) \end{pmatrix}. \quad (303)$$

By analogy,  $R_l$  is given by

$$R_l = \begin{pmatrix} N_e AB & N_\mu AB & N_\tau AB \\ N_e m_e B & -N_\mu m_\mu B & N_\tau m_\tau B \\ N_e(m_e^2 - A^2) & N_\mu(m_\mu^2 - A^2) & N_\tau(m_\tau^2 - A^2) \end{pmatrix}, \text{ with} \quad (304)$$

$$C = m_e - m_\mu + m_\tau,$$

$$A^2 = \frac{m_e m_\mu m_\tau}{m_e - m_\mu + m_\tau}, \quad (305)$$

$$B^2 = m_e m_\mu + m_\mu m_\tau - m_\tau m_e - A^2, \text{ and}$$

$$\frac{1}{N_l^2} = A^2 B^2 + m_l^2 B^2 + (m_l^2 - A^2)^2, \quad (l = e, \mu, \tau). \quad (306)$$

Using  $R_\nu$  and  $R_l$  from (304) and (303) in (291), we find the following form for the elements of the mixing matrix:

$$V_{\alpha l} = n_\alpha N_l \left( ab AB + (-1)^{(\delta_{\alpha 2} + \delta_{l \mu})} m_\alpha m_l b B e^{i\sigma} + (m_\alpha^2 - a^2)(m_l^2 - A^2) e^{i\eta} \right), \quad (307)$$

for  $\alpha = 1, 2, 3$  and  $l = e, \mu, \tau$ .<sup>2</sup>

Obviously the boxes from the Fritzsch mixing matrix will be rather complicated functions of the masses. In a parameterization based on the mixing matrix elements, we would have to invert equations quartic in the  $V$ s given by equation (307) to find the Fritzsch parameters  $a, b$ , *et cetera* from the observable probabilities. The boxes, however, are the probabilities (more or less), and the

<sup>2</sup> Our assignment of numbers to the neutrino index and lepton flavors to the charged lepton index is slightly different from our normal convention of  $\alpha = e, \mu, \tau$  and  $l = 1, 2, 3$ . Because the charged lepton flavor states are not equivalent to mass states in the Fritzsch model, we have chosen to use flavor indices to represent the charged lepton flavor. To avoid complicated indexing of the neutrino states, we have labeled them by numbers. In retrospect, this appears a bit inconsistent, but it seemed like a good idea at the time.

Fritzsch parameters may be found by using equation (254). Unfortunately, we must first rotate the Fritzsch  $M_\nu$  to  $\hat{M}$  using the charged lepton rotation matrix (304) and equation (257). This again gives daunting equations, so we will content ourselves with considering only two limiting cases.

We know that the charged lepton masses obey a strong hierarchy:  $m_\tau \gg m_\mu \gg m_e$ . With these constraints,  $R_l$  becomes

$$R_l = \begin{pmatrix} 1 & \Lambda_1 & \Lambda_1 \Lambda_2^3 \\ \Lambda_1 & -1 & \Lambda_2 \\ -\Lambda_1 \Lambda_2 & \Lambda_2 & 1 \end{pmatrix}, \quad \text{where} \quad (308)$$

$$\Lambda_1 = \sqrt{\frac{m_e}{m_\mu}}, \quad \text{and} \quad \Lambda_2 = \sqrt{\frac{m_\mu}{m_\tau}}. \quad (309)$$

If neutrinos also obey a strong mass hierarchy,  $m_3 \gg m_2 \gg m_1$ ,  $R_\nu$  will have the same form (308), with  $\lambda$  substituted for  $\Lambda$  and

$$\lambda_1 = \sqrt{\frac{m_1}{m_2}}, \quad \text{and} \quad \lambda_2 = \sqrt{\frac{m_2}{m_3}}. \quad (310)$$

The diligent reader may notice that the matrix in equation (308) does not exactly diagonalize  $\hat{M}_l$ . But the mass eigenvalues do appear on the diagonal, and the off-diagonal elements are negligible under the mass hierarchy approximation. The mixing matrix for a Fritzsch model with dual mass hierarchies takes the form

$$V = \begin{pmatrix} 1 + \lambda_1 \Lambda_1 e^{i\sigma} & \Lambda_1 - \lambda_1 e^{i\sigma} & \lambda_1 \Lambda_2 e^{i\sigma} - \lambda_1 \lambda_2 e^{i\eta} \\ \lambda_1 - \Lambda_1 e^{i\sigma} & \lambda_1 \Lambda_1 + e^{i\sigma} + \lambda_2 \Lambda_2 e^{i\eta} & -\Lambda_2 e^{i\sigma} + \lambda_2 e^{i\eta} \\ \lambda_2 \Lambda_1 e^{i\sigma} - \Lambda_1 \Lambda_2 e^{i\eta} & -\lambda_2 e^{i\sigma} + \Lambda_2 e^{i\eta} & \lambda_2 \Lambda_2 e^{i\sigma} + e^{i\eta} \end{pmatrix} \quad (311)$$

This result disagrees with the CKM matrix given in [45] and [29] by the sign of  $V_{12}$ ,  $V_{21}$ ,  $V_{23}$ , and  $V_{32}$ . One possible explanation of this discrepancy is that the authors of [45] and [29] have absorbed an extra phase  $e^{i\pi}$  into the fields of the muon and muon-neutrino. Such an absorption will not affect the measurable boxes. Indeed, every box has an even number of the terms with the disputed sign, so the extra minus signs cancel.

The boxes formed from the CKM matrix in (311) are rather complicated functions of mass ratios.

For example,

$${}^{11}\square_{22} = e^{i\sigma} (\Lambda_1 \lambda_1 - \Lambda_1^2 e^{i\sigma} - \lambda_1^2 e^{i\sigma} + \lambda_1 \Lambda_1 e^{2i\sigma}), \text{ and} \quad (312)$$

$${}^{12}\square_{33} = e^{i\eta} \left( -\lambda_1 \lambda_2 \Lambda_1 \Lambda_2 e^{2i\sigma} - (\lambda_1 \lambda_2^2 \Lambda_1 + \lambda_1 \Lambda_1 \Lambda_2^2) e^{i(\sigma+\eta)} - (\lambda_2^2 \Lambda_1^2 + \Lambda_1^2 \Lambda_2^2) e^{i(2\sigma+\eta)} \right) \quad (313)$$

$$+ \lambda_2 \Lambda_1^2 \Lambda_2 e^{i(\sigma+2\eta)} - \lambda_1 \lambda_2 \Lambda_1 \Lambda_2 e^{2i\eta} - \lambda_2 \Lambda_1^2 \Lambda_2 e^{3i\sigma} \right). \quad (314)$$

Under this double-mass hierarchy, the dominant boxes are  ${}^{11}\square_{22}$   ${}^{22}\square_{33}$ , which are on the order of a mass ratio (two powers of  $\Lambda$  or  $\lambda$ ). The other boxes are on the order of a mass ratio squared.  ${}^{11}\square_{22}$  appears in the expression (135) for the probability of a  $\nu_e \leftrightarrow \nu_\mu$  transition, multiplied by  $\sin^2 \Phi_{12}$ , where  $\Phi_{12}$  is given by (94) to be

$$\Phi_{12} = \frac{m_1^2 - m_2^2}{4p} x, \quad (315)$$

which is on the order of  $m_2^2 \frac{x}{p}$  for small  $x$ , so its contribution is lessened by  $\lambda_2^4$  compared to boxes multiplied by  $\Phi_{23}$  or  $\Phi_{13}$ . This reduction more than cancels out the effect from the box's dominance.  ${}^{22}\square_{33}$ , on the other hand, appears in the probability of a  $\nu_\mu \leftrightarrow \nu_\tau$  transition, multiplied by  $\sin^2 \Phi_{23}$ , making the  $\nu_\mu \leftrightarrow \nu_\tau$  transition the most probable transition in the double-hierarchy Fritzsch model.

Another popular scenario for neutrino mass is the reverse hierarchy:  $m_1 \gg m_2 \gg m_3$ . Using this approximation in the Fritzsch model yields a rotation matrix given by

$$R_\nu = \begin{pmatrix} \lambda'_2 \lambda'_1{}^3 & \lambda'_2 & 1 \\ \lambda'_1 & -1 & \lambda'_2 \\ 1 & \lambda'_1 & -\lambda'_2 \lambda'_1 \end{pmatrix}, \text{ with} \quad (316)$$

$$\lambda'_1 = \sqrt{\frac{m_2}{m_1}}, \text{ and } \lambda'_2 = \sqrt{\frac{m_3}{m_1}}. \quad (317)$$

Using a straight hierarchy for the charged leptons and this reverse hierarchy for neutrinos, we arrive

at the following form for the mixing matrix:

$$V = \begin{pmatrix} \lambda'_1 \Lambda_1 e^{i\sigma} - \Lambda_1 \Lambda_2 e^{i\eta} & -\lambda'_1 e^{i\sigma} + \Lambda_2 e^{i\eta} & \lambda'_1 \Lambda_2 e^{i\sigma} + e^{i\eta} \\ \lambda'_2 - \Lambda_1 e^{i\sigma} & \lambda'_2 \Lambda_1 + e^{i\sigma} + \lambda'_1 \Lambda_2 e^{i\eta} & -\Lambda_2 e^{i\sigma} + \lambda'_1 e^{i\eta} \\ 1 + \lambda'_2 \Lambda_1 e^{i\sigma} & \Lambda_1 - \lambda'_2 e^{i\sigma} & \lambda'_2 \Lambda_2 e^{i\sigma} - \lambda'_1 \lambda'_2 e^{i\eta} \end{pmatrix}. \quad (318)$$

Under this approximation, the dominant boxes are  ${}^{21}\square_{32}$  and  ${}^{12}\square_{23}$ , which contribute to  $\nu_\mu \leftrightarrow \nu_\tau$  mixing scaled by  $\sin^2 \Phi_{12}$  and to  $\nu_e \leftrightarrow \nu_\mu$  mixing scaled by  $\sin^2 \Phi_{23}$ , respectively. In this case,  $\sin^2 \Phi_{12}$  is large at small distances, so once again the  $\nu_\mu \leftrightarrow \nu_\tau$  mixing predominates for neutrinos from local sources. These predictions of the Fritzsch model will be compared against experimental data in Chapter VI.

If neutrinos are not pure Dirac particles, then the matrix in (291) does not necessarily apply. But if a light-neutrino  $3 \times 3$  matrix  $M_\nu$  is obtained by the see-saw mechanism  $M_\nu = M_D^T M_S^{-1} M_D$ , as in Section 2.6, then the mixing matrix may have the form in (291), as long as  $M_S$ , the mass matrix for the right-handed neutrino singlet term, is proportional to the unit matrix in the basis where  $M_D$  is diagonal [29].

### 5.2.2 Using a Democratic Mass Matrix

Another texture of mass matrix popularized by the disparities in quark masses is the “democratic” mass matrix [46]:

$$M = \begin{pmatrix} 1 & 1 & 1 \\ 1 & 1 & 1 \\ 1 & 1 & 1 \end{pmatrix}. \quad (319)$$

This matrix has eigenvalues 0, 0, and 3. The mass matrix must be normalized to set the non-zero eigenvalue equal to the heaviest mass. We know from experiments the mass of the top quark is much heavier than those of the up and charm quarks, and the bottom quark mass is much heavier than the other down-type quark masses, so the democratic mass matrix is a reasonable approximation for the quark sector. The charged leptons also have one dominant mass scale, and it is not unreasonable

to assume the neutrino masses might follow the same pattern. So we have

$$M_\nu = \frac{m_3}{3} \begin{pmatrix} 1 & 1 & 1 \\ 1 & 1 & 1 \\ 1 & 1 & 1 \end{pmatrix}, \quad \text{and} \quad M_l = \frac{m_\tau}{3} \begin{pmatrix} 1 & 1 & 1 \\ 1 & 1 & 1 \\ 1 & 1 & 1 \end{pmatrix}. \quad (320)$$

Because of the degeneracy of two of the masses in each matrix, the eigenvectors depend on an undetermined parameter which we call  $a$ . They have the forms

$$\psi^1 = n_1 \begin{pmatrix} a \\ 1 \\ -(a+1) \end{pmatrix}, \quad \psi^2 = n_2 \begin{pmatrix} a+2 \\ -(2a+1) \\ a-1 \end{pmatrix}, \quad \text{and} \quad \psi^3 = 3^{-\frac{1}{2}} \begin{pmatrix} 1 \\ 1 \\ 1 \end{pmatrix}. \quad (321)$$

$n_1$  and  $n_2$  are fixed by normalizing the eigenvectors:

$$n_1 = 2(a^2 + a + 1); \quad (322)$$

$$n_2 = 2(3a^2 + 4a + 3). \quad (323)$$

As above, we will choose lowercase  $a$  and  $n_i$  for the neutrino matrices, and uppercase  $A$  and  $N_l$  for the charged lepton matrices. These eigenvectors may be used to form the  $R_\nu$  and  $R_l$  that diagonalize  $M_\nu$  and  $M_l$ . Constructing the CKM matrix from the  $R$  matrices, we find a rather simple result:

$$V = \begin{pmatrix} n_1 N_e (2 + 2aA + a + A) & n_1 N_\mu (3a - 3A - 2) & 0 \\ n_2 N_e (3A - 3a - 2) & 3n_2 N_\mu (2 + 2aA + a + A) & 0 \\ 0 & 0 & 1 \end{pmatrix}. \quad (324)$$

$a$  and  $A$  are completely arbitrary; the eigenvectors corresponding to the lighter particles are degenerate, so one can rotate freely between the two states with no observable effect. We can represent this freedom by parameterizing the mixing matrix with rotation angles  $\theta$  for the neutrino sector and

$\Theta$  for the charged-lepton sector. Orthonormality of the eigenvectors is met by setting

$$n_1 a = \frac{\cos \theta}{\sqrt{2}} + \frac{\sin \theta}{\sqrt{6}}, \text{ and} \quad (325)$$

$$N_1 A = \frac{\cos \Theta}{\sqrt{2}} + \frac{\sin \Theta}{\sqrt{6}}. \quad (326)$$

The mixing matrix has a quite obvious form with this choice of parameterization:

$$V = \begin{pmatrix} \cos(\theta - \Theta) & \sin(\theta - \Theta) & 0 \\ -\sin(\theta - \Theta) & \cos(\theta - \Theta) & 0 \\ 0 & 0 & 1 \end{pmatrix}. \quad (327)$$

The lighter states are rotated by a combination  $\theta - \Theta$ . If the charged lepton sector is described by the same angle as the neutrino sector, no mixing occurs at all. Also, if the lighter-mass degeneracy is exact, there is complete freedom to choose  $\theta - \Theta = 0$ . One expects, however, that “accidental” symmetries will be broken by higher-order effects. Parameterizing this symmetry breaking of the  $2 \times 2$  light mass matrix as

$$\begin{pmatrix} \sigma_1 & \epsilon \\ \epsilon^* & \sigma_2 \end{pmatrix}, \quad (328)$$

one finds

$$\tan 2\theta = \frac{2|\epsilon|}{\sigma_1 - \sigma_2}, \quad (329)$$

and

$$\Delta m_{12}^2 = (\sigma_1 + \sigma_2) \sqrt{(\sigma_1 - \sigma_2)^2 + 4|\epsilon|^2}. \quad (330)$$

Whether one chooses  $a$  and  $A$  or  $\theta$  and  $\Theta$ , the mixing matrix as given has only one non-zero box:

$${}^{11}\square_{22} = n_1^2 n_2^2 N_1^2 N_2^2 3(2 + 2aA + a + A)^2 (3a - 3A - 2)(3A - 3a - 2) = -\frac{1}{4} \sin^2(2(\theta - \Theta)). \quad (331)$$

This box appears in the expression (135) for the probability of a  $\nu_e \rightarrow \nu_\mu$  transition, multiplied by

$\sin^2 \Phi_{12}$ , where  $\Phi_{12}$  is given by (94) to be

$$\Phi_{12} = \frac{m_1^2 - m_2^2}{4p} x, \quad (332)$$

which is very small for a nearly exact democratic mass matrix except in the case of extremely large  $x$ . Symmetry breaking may also induce small nonzero boxes mixing the third mass with the first two. Here  $\Phi_{13}$  and  $\Phi_{23}$  would be large, but the amplitude of oscillation would be small. Oscillations may therefore not be measurable in this scenario for terrestrial experiments. Experiments looking for oscillations from cosmologically distant objects might, however, be sensitive to the  $\nu_1 \leftrightarrow \nu_2$  transition [47].

The democratic mass matrix is only an approximation. The masses of the electron and muon are not exactly zero, and we reasonably expect non-zero masses for the two lighter neutrinos too. The masses of the muon and electron are, however, much smaller than the tau mass, so the democratic mass matrix may be a good first approximation, with the smaller masses arising from corrections to it.

### 5.2.3 Using a Zee Mass Matrix

As discussed in Section 2.3.2, the Zee mechanism with diagonal coupling between a Higgs doublet and charged leptons gives rise to a neutrino mass matrix of the form (49). Such a matrix may be parameterized in terms of three parameters  $\alpha, \sigma$ , and  $m_0$  [25], [26], [12]:

$$M_\nu = m_0 \begin{pmatrix} 0 & \sigma & \cos \alpha \\ \sigma & 0 & \sin \alpha \\ \cos \alpha & \sin \alpha & 0 \end{pmatrix}. \quad (333)$$

These new parameters are related to the charged lepton masses and the coupling constants of (49) by

$$\cos \alpha = \frac{f_{e\tau}}{m_0} (m_\tau^2 - m_e^2) \approx \frac{f_{e\tau}}{\sqrt{f_{e\tau}^2 + f_{\mu\tau}^2}},$$

$$\begin{aligned}
\sin \alpha &= \frac{f_{\mu\tau}}{m_0} (m_\tau^2 - m_\mu^2) \approx \frac{f_{\mu\tau}}{\sqrt{f_{e\tau}^2 + f_{\mu\tau}^2}}, \\
\sigma &\approx \frac{f_{e\mu} m_\mu^2}{f_{e\tau} m_\tau^2} \cos \alpha, \quad \text{and} \\
m_0 &\approx m_\tau^2 \sqrt{f_{e\tau}^2 + f_{\mu\tau}^2}.
\end{aligned} \tag{334}$$

These relationships ignore  $m_e^2$  and  $m_\mu^2$  with respect to  $m_\tau^2$ , which is a fairly good approximation given the mass hierarchy of the charged leptons. We will also assume  $\sigma \ll 1$ , which holds unless  $f_{e\mu} \gtrsim 10^4 f_{e\tau}$  [12].

Upon diagonalizing the matrix in equation (333), we find the neutrino masses [12]

$$\begin{aligned}
m_1 &= -m_0 \sigma \sin 2\alpha \\
m_2 &= m_0 \left( 1 - \frac{1}{2} \sigma \sin 2\alpha \right) \\
m_3 &= m_0 \left( 1 + \frac{1}{2} \sigma \sin 2\alpha \right),
\end{aligned} \tag{335}$$

where an overall minus sign on  $m_3$  has been absorbed into the definition of the neutrino field through the chiral rotation  $\psi \rightarrow i\gamma_5 \psi$ . The mass differences for this Zee model are

$$\begin{aligned}
m_1^2 - m_2^2 &\approx -m_0^2 (1 - 2\sigma \cos \alpha \sin \alpha), \\
m_1^2 - m_3^2 &\approx -m_0^2 (1 + 2\sigma \cos \alpha \sin \alpha), \quad \text{and} \\
m_2^2 - m_3^2 &\approx -4m_0^2 \sigma \cos \alpha \sin \alpha.
\end{aligned} \tag{336}$$

$m_3$  and  $m_2$  are nearly degenerate and much larger than  $m_1$ .

Because the lepton mass matrix has been assumed diagonal for this model, the weak-interaction mixing matrix  $V$  is equivalent to the neutrino mixing matrix  $U_{\nu_L}$ , and is found by diagonalizing the mass matrix in equation (333) [26]:

$$V = \frac{1}{\sqrt{2}} \begin{pmatrix} \sqrt{2} \cos \alpha & \sin \alpha + \sigma \cos \alpha & \sin \alpha + \sigma \cos \alpha \\ -\sqrt{2} \sin \alpha & \cos \alpha & \cos \alpha \\ -\sqrt{2} \sigma & 1 & -1 \end{pmatrix}. \tag{337}$$

The boxes from this mixing matrix have the forms

$$\begin{aligned}
{}^{11}\square_{22} &= -\frac{1}{2} \sin \alpha \cos^2 \alpha (\sin \alpha + \sigma \cos \alpha) \\
{}^{11}\square_{23} &= -\frac{1}{2} \sin \alpha \cos^2 \alpha (\sin \alpha - \sigma \cos \alpha) \\
{}^{11}\square_{32} &= -\frac{1}{2} \sigma \cos \alpha (\sin \alpha + \sigma \cos \alpha) \\
{}^{11}\square_{33} &= -\frac{1}{2} \sigma \cos \alpha (\sin \alpha - \sigma \cos \alpha) \\
{}^{12}\square_{23} &= \frac{1}{4} \cos^2 \alpha (\sin^2 \alpha - \sigma^2 \cos^2 \alpha) \\
{}^{12}\square_{33} &= -\frac{1}{4} (\sin^2 \alpha - \sigma^2 \cos^2 \alpha) \\
{}^{21}\square_{32} &= \frac{1}{2} \sigma \cos \alpha \sin \alpha \\
{}^{21}\square_{33} &= -\frac{1}{2} \sigma \cos \alpha \sin \alpha \\
{}^{22}\square_{33} &= -\frac{1}{4} \cos^2 \alpha
\end{aligned} \tag{338}$$

If  $f_{e\tau} \sim f_{\mu\tau}$ , then  $\sin \alpha \gg \sigma \cos \alpha$  and the boxes have the following relative magnitudes:

$$\begin{aligned}
{}^{11}\square_{22} &\sim {}^{11}\square_{23} \sim -{}^{12}\square_{23} \sim -\sin^2 \alpha \cos^2 \alpha, \\
{}^{11}\square_{32} &\sim {}^{11}\square_{33} \sim -{}^{21}\square_{32} \sim {}^{21}\square_{33} \sim -\sigma \sin \alpha \cos \alpha,
\end{aligned} \tag{339}$$

$$\begin{aligned}
{}^{12}\square_{33} &\sim -\sin^2 \alpha, \text{ and} \\
{}^{22}\square_{33} &\sim -\cos^2 \alpha.
\end{aligned} \tag{340}$$

If, on the other hand,  $f_{e\tau} \gg f_{\mu\tau}$  we may neglect the first terms of the sums in the box relationships (338). In this scenario we find

$$\begin{aligned}
{}^{11}\square_{22} &\sim -{}^{11}\square_{23} \sim -\sigma \sin \alpha \cos^3 \alpha, \\
{}^{11}\square_{32} &\sim -{}^{11}\square_{33} \sim {}^{12}\square_{33} \sim -\sigma^2 \cos^2 \alpha,
\end{aligned} \tag{341}$$

$${}^{12}\square_{23} \sim -\sigma^2 \cos^4 \alpha \tag{342}$$

$$\begin{aligned}
{}^{21}\square_{32} &\sim -{}^{21}\square_{33} \sim \sigma \sin \alpha \cos \alpha, \text{ and} \\
{}^{22}\square_{33} &\sim -\cos^2 \alpha.
\end{aligned} \tag{343}$$

The predictions of both of these scenarios are compared with experimental results in Chapter VI.

## CHAPTER VI

### THE CONNECTION TO EXPERIMENT

The advantages of the box notation become clear when drawing conclusions from experimental results. To that purpose, we will examine the currently existing data. No direct evidence of neutrino oscillation has yet been confirmed. The LSND experiment at Los Alamos has preliminary data which may be explained by oscillations of muon antineutrinos into electron antineutrinos [48]. This oscillation interpretation has not yet been confirmed by another experiment, but we will consider LSND's result as a possible measurement of an oscillation probability. Other accelerator experiments put bounds on different oscillation probabilities, and we will use these bounds as constraints in what follows. Indirect evidence for neutrino oscillations comes from the solar neutrino deficit [6],[7] and the atmospheric neutrino anomaly [8], and we will use the oscillation interpretation for these phenomena also. The probabilities derived from such indefinite results are not meant to be definitive, but they will allow us to demonstrate the usefulness of the box notation. Once more conclusive data becomes available, the numbers used below may be adjusted, but the procedure will remain the same.

#### 6.1 The Data

Solar neutrino experiments measure the flux of neutrinos from the sun and compare it to the flux predicted by solar models such as Pinsonneault and Bahcall's [49]. With the exception of Kamiokande, the older solar neutrino detectors are sensitive only to electron type neutrinos, so the ratio of observed flux to predicted flux gives the survival probability for electron neutrinos,  $P_{\nu_e \rightarrow \nu_e}$ . The Kamiokande experiment measures neutral current events too, so it may detect muon and tau neutrinos. The neutral-current cross section in water is 0.17 (about one-sixth) times the charged-current cross section for the neutrino energies measured by Kamiokande [50]. Thus the probability measured by Kamiokande (and now by Super K) is

$$P_{\nu_e \rightarrow \nu_e} + 0.17(P_{\nu_e \rightarrow \nu_\mu} + P_{\nu_e \rightarrow \nu_\tau} + P_{\nu_e \rightarrow \nu_e}), \quad (344)$$

where  $P_{\nu_e \rightarrow \nu_e}$  is the probability as measured by charged-current-only detectors. The analysis of solar neutrinos used below [51] takes into account this additional contribution to the Kamiokande data. The quoted solar deficits contain hidden uncertainties, because the expected neutrino spectrum given by solar models is itself somewhat uncertain.

Atmospheric neutrino experiments measure the flux of muon and electron neutrinos produced in the atmosphere. The chain of events producing these neutrinos should create roughly two muon-type ( $\nu_\mu$  or  $\bar{\nu}_\mu$ ) neutrinos for every electron-type ( $\nu_e$  or  $\bar{\nu}_e$ ) neutrino. Experiments, however, have measured nearly equal amounts of electron-type and muon-type neutrinos. These results are expressed as a ratio of ratios,  $R_{atm} = r_{expected}/r_{measured}$ , where the ratios  $r$  are of electron-type to muon-type. For three generations, this anomaly could be due to  $\nu_\mu \leftrightarrow \nu_e$  mixing,  $\nu_\mu \leftrightarrow \nu_\tau$  mixing, or three-way mixing  $\nu_\mu \leftrightarrow \nu_e \leftrightarrow \nu_\tau$ , and these three possibilities are described in detail in the paper which first suggested oscillations as a solution to the atmospheric neutrino anomaly, [52]. We will abbreviate  $r_{expected}$  as simply  $r$ , and take its value to be 0.48 [53], the result of sophisticated Monte Carlo simulations assuming no oscillations. This number is somewhat dependent on detector efficiencies, but the differences between detectors will not affect our conclusions significantly.

If the atmospheric anomaly is caused solely by  $\nu_\mu \leftrightarrow \nu_e$  mixing, the ratio depends only on  $P_{\nu_e \rightarrow \nu_\mu}$  and its time-reversal conjugate  $P_{\nu_\mu \rightarrow \nu_e}$ :

$$R_{atm} = \frac{1 - P_{\nu_\mu \rightarrow \nu_e} + rP_{\nu_e \rightarrow \nu_\mu}}{1 - P_{\nu_e \rightarrow \nu_\mu} + r^{-1}P_{\nu_\mu \rightarrow \nu_e}}. \quad (345)$$

When CP is effectively conserved, such as when  $\sin 2\Phi_{ij}$  averages to zero, the two probabilities are equal, and the measured ratio is simply

$$R_{atm} = \frac{1 - P_{\nu_e \rightarrow \nu_\mu} (1 - r)}{1 - P_{\nu_e \rightarrow \nu_\mu} (1 - r^{-1})}. \quad (346)$$

The transition probability may be found from data by inverting this expression:

$$P_{\nu_e \rightarrow \nu_\mu} = \frac{y}{x}, \quad (347)$$

where  $x$  and  $y$  are defined for our use as

$$\begin{aligned} x &= 1 - r - R_{atm} + r^{-1}R_{atm}, \quad \text{and} \\ y &= 1 - R_{atm}. \end{aligned} \quad (348)$$

For the value of  $r = 0.48$  used here,

$$x = 0.52 + 1.1R_{atm}. \quad (349)$$

If the atmospheric anomaly is caused by  $\nu_\mu \leftrightarrow \nu_\tau$  mixing, the ratio is simply expressed:

$$R_{atm} = 1 - P_{\nu_\mu \rightarrow \nu_\tau}. \quad (350)$$

This possibility is similar to one with  $\nu_\mu \leftrightarrow \nu_\chi$  mixing, or oscillations to both  $\nu_\tau$  and  $\nu_\chi$ , since  $\nu_\tau$  is not measured by atmospheric neutrino experiments and therefore acts like a sterile neutrino. The transition probabilities in these scenarios are related to the measured ratio by

$$R_{atm} = 1 - P_{\nu_\mu \rightarrow \nu_\chi}, \quad \text{and} \quad (351)$$

$$R_{atm} = 1 - P_{\nu_\mu \rightarrow \nu_\tau} - P_{\nu_\mu \rightarrow \nu_\chi}, \quad (352)$$

respectively. Probabilities may be found from

$$P_{\nu_\mu \rightarrow \nu_\tau} + P_{\nu_\mu \rightarrow \nu_\chi} = 1 - R_{atm} = y, \quad (353)$$

using the definition of  $y$  given in equation (348)

The final possibility for the atmospheric anomaly involves all neutrino flavors. The measured ratio in this case, including a possible sterile neutrino, is

$$R_{atm} = \frac{1 - P_{\nu_\mu \rightarrow \nu_e} - P_{\nu_\mu \rightarrow \nu_\tau} - P_{\nu_\mu \rightarrow \nu_\chi} + rP_{\nu_e \rightarrow \nu_\mu}}{1 - P_{\nu_e \rightarrow \nu_\mu} - P_{\nu_e \rightarrow \nu_\tau} - P_{\nu_e \rightarrow \nu_\chi} + r^{-1}P_{\nu_\mu \rightarrow \nu_e}}. \quad (354)$$

Once some of the probabilities in equation (354) are measured directly by experiment, this four-way possibility could become a preferred solution. In what follows, we will confine our consideration of this possibility to cases for which  $P_{\nu_e \rightarrow \nu_\chi}$  and  $P_{\nu_\mu \rightarrow \nu_\chi}$  are negligible, and for which CP is conserved by atmospheric neutrinos. The expression for the measured ratio in this three-way mixing scheme is

$$R_{atm} = \frac{1 - P_{\nu_e \rightarrow \nu_\mu} - P_{\nu_\mu \rightarrow \nu_\tau} + rP_{\nu_e \rightarrow \nu_\mu}}{1 - P_{\nu_e \rightarrow \nu_\mu} + r^{-1}P_{\nu_e \rightarrow \nu_\mu} - P_{\nu_e \rightarrow \nu_\tau}}, \quad (355)$$

which may be rearranged to give

$$P_{\nu_\mu \rightarrow \nu_\tau} + xP_{\nu_e \rightarrow \nu_\mu} - R_{atm}P_{\nu_e \rightarrow \nu_\tau} = y. \quad (356)$$

The accelerator experiments considered here, LSND, CHORUS, KARMEN, and CHARM II, are, with the exception of KARMEN's  $\nu_e \rightarrow \nu_x$  "disappearance" (of an  $\nu_e$  to any other flavor  $x = \mu, \tau, \chi$ ) measurement, "appearance" experiments, so they measure (or constrain) individual transition probabilities. Analysis of these experiments' results is thus simpler than the analysis of the "disappearance" solar neutrino and atmospheric neutrino experiments. Many other experiments (Bugey in France, Gosgen in Switzerland, NOMAD and BEBC at Cern, CCFR and E531 at Fermilab, E776 at Brookhaven, and Krasnoyarsk in Russia) have searched (and/or are searching) for neutrino oscillations as well, but none of these have yet found any evidence of oscillations.

The data from the experiments which we will use is summarized in Table 2. Only the data from Kamiokande, SuperK, and IMB have been listed under atmospheric neutrinos; other experiments (Fréjus, Soudan2, Baksan, and Nusex) have also measured the fluxes of atmospheric neutrinos, but their uncertainties are considerably larger than those of the listed experiments, which makes them less useful.

If the uncertainty in a phase  $\Phi_{ij}$  of a neutrino is  $\gtrsim$  one-fourth an oscillation length, the oscillatory terms in the probability equation average, with  $\sin^2 \Phi_{ij}$  averaging to one-half, and  $\sin 2\Phi_{ij}$  averaging to zero. This assumption that the oscillations average thus becomes an assumption about the

**Table 2:** Experimental data pertaining to neutrino oscillations. Sources for the data are listed under reference [54]. When both systematic and statistical uncertainties were given for an experiment, they were added in quadrature to obtain the total uncertainty listed below. The measured ratio for solar experiments is the measured flux divided by the flux predicted by Bahcall's solar model [49]. Kamiokande and SuperK do not measure  $P_{\nu_e \rightarrow \nu_e}$  but the combination given in equation (344). The addition to their measured ratios is noted by “+NC” in the Table. For atmospheric experiments, the measured ratio is the ratio of ratios,  $R_{atm}$ . The probabilities for the atmospheric experiments are found from  $R_{atm}$  by assuming CP invariance. CP invariance is also assumed for the combined probability from the CHARM II experiment. The limits on measured probabilities from the accelerator experiments are reported for the 90 % confidence level. Energies marked with a  $\sim$  represent peak energies in the energy spectrum for the reaction specified. Accelerator neutrino energies with no such demarcation correspond to monoenergetic neutrinos. LSND-1 refers to the decay-at-rest results; LSND-2 refers to the newly-presented decay-in-flight results, for which values of  $L$  and  $E$  are not presently available.

Type	Experiment	Length (m)	Energy (MeV)	Measured Ratio	$\nu_\alpha$	$\nu_\beta$	$P_{\nu_\alpha \rightarrow \nu_\beta}(x)$
Solar	Homestake	$1.5 \times 10^{11}$	$> 0.814$	$0.28 \pm 0.04$	$\nu_e$	$\nu_e$	0.3
	Kamiok.	$1.5 \times 10^{11}$	$> 7.5$	$0.50 \pm 0.06$	$\nu_e$	$\nu_e + NC$	0.4
	SAGE	$1.5 \times 10^{11}$	$> 0.233$	$0.53 \pm 0.10$	$\nu_e$	$\nu_e$	0.5
	Gallex	$1.5 \times 10^{11}$	$> 0.233$	$0.51 \pm 0.06$	$\nu_e$	$\nu_e$	0.5
	SuperK	$1.5 \times 10^{11}$	$> 7.5$	$0.44 \pm 0.04$	$\nu_e$	$\nu_e + NC$	0.4
Atmos.	IMB	$10^4$ to $10^7$	$\gtrsim 10^3$	$0.54 \pm 0.09$	$\nu_\mu$	$\nu_\tau, \nu_\chi$	0.46
					$\nu_\mu$	$\nu_e$	0.37
					3-way		$x = 1.1, y = 0.46$
	Kamiok.	$10^4$ to $10^7$	$\gtrsim 10^3$	$0.60 \pm 0.06$	$\nu_\mu$	$\nu_\tau, \nu_\chi$	0.40
					$\nu_\mu$	$\nu_e$	0.30
					3-way		$x = 1.2, y = 0.40$
	SuperK	$10^4$ to $10^7$	$\gtrsim 10^3$	$0.67 \pm 0.08$	$\nu_\mu$	$\nu_\tau, \nu_\chi$	0.33
					$\nu_\mu$	$\nu_e$	0.27
					3-way		$x = 1.2, y = 0.33$
Accel.	LSND-1	30	$\sim 50$		$\bar{\nu}_\mu$	$\bar{\nu}_e$	$3.1 \pm 1.3 \times 10^{-3}$
	LSND-2				$\bar{\nu}_\mu$	$\bar{\nu}_e$	$2.7 \pm 1.4 \times 10^{-3}$
	KARMEN	17.6	30		$\nu_\mu$	$\nu_e$	$< 0.026$
			$\sim 35$		$\nu_e$	$\nu_\tau, \nu_\mu, \nu_\chi$	$< 0.197$
			$\sim 50$		$\bar{\nu}_\mu$	$\bar{\nu}_e$	$< 0.0038$
	CHORUS	590	$\sim 27000$		$\nu_\mu$	$\nu_\tau$	$< 0.004$
	CHARM II	650	$\sim 20000$		$\nu_\mu$	$\nu_e$	$< 0.0047$
					$\bar{\nu}_\mu$	$\bar{\nu}_e$	$< 0.0026$
					both combined		$< 0.0028$

magnitude of the mass-squared differences:

$$\Delta\Phi_{ij} \gtrsim \frac{\pi}{2} \Rightarrow m_i^2 - m_j^2 \gtrsim \frac{2\pi}{\Delta(\frac{x}{E})}, \quad (357)$$

where the symbol  $\Delta$  represents the uncertainty of a quantity. In our data analysis below, we will

consider only mass-squared differences for which this type of averaging occurs for both solar neutrinos and atmospheric neutrinos.

According to stellar evolution theory, solar neutrinos are produced in the inner part of the sun below  $0.2R_\odot$  [50], so the distance traveled varies between  $1 \text{ a.u.} - (0.2)R_\odot$  and  $1 \text{ a.u.} + (0.2)R_\odot$ . ( $1 \text{ a.u.} = 1 \text{ astronomical unit} = 1.5 \times 10^8 \text{ km, and } R_\odot = \text{solar radius} = 7.0 \times 10^5 \text{ km.}$ ) This leads to an uncertainty in distance of less than one percent. The energy of solar neutrinos, however, ranges from 0.2 MeV to 25 MeV [50]. Thus  $\frac{x}{E}$  varies from  $3.7 \times 10^{12} \text{ eV}^{-2}$  to  $3 \times 10^{10} \text{ eV}^{-2}$ , and we find

$$m_i^2 - m_j^2 \gtrsim 2\pi (2.7 \times 10^{-13}) \text{ eV}^2 \approx 1.7 \times 10^{-12} \text{ eV}^2 \quad (358)$$

as a rough criterion for the solar neutrino oscillations to average. A more refined calculation would include an energy integration over the neutrino spectrum and the detection cross section starting from the detector energy threshold, but the above estimate is sufficient for our purposes.

Making this same assumption for atmospheric neutrinos results in a stronger constraint on mass-squared differences. The detected neutrinos separate by energy into three distinct groups: contained, stopped, and through-going. Neutrinos in contained events produce charged leptons in the detector that are absorbed by, and thereby contained in, the detector. These events are caused by lower-energy neutrinos, with energies ranging from 0.2 GeV to 1.2 GeV [53], [56], [52]. Because the lepton is formed in the detector, down-going background events from cosmic rays are easily identified. Down-going signal events dominate the contained data, due to the closeness to the Earth's surface.

Stopped events are caused by upward-going muon neutrinos which create a muon outside the detector which travels into the detector and is stopped. Electron neutrinos do not contribute to this type of event since electrons will not travel far through the material surrounding the detector, and down-going events are vetoed because the down-going background is significantly larger than the signal. The muon neutrinos producing the stopped muons are more energetic than those causing contained events (since the muons from stopped events may travel further than the width of the detector), having energies between 1 and 100 GeV [56]. Still higher-energy up-going muon neutrinos may produce muons outside the detector which travel through the detector and out the other side. These through-going events result from neutrinos with energies between 1.1 GeV and  $10^4$  GeV [56].

In our data analysis, we follow the lead of reference [51] and consider only the contained events, which are identified roughly ten times as often as events of the other two types [56]. These events have an energy uncertainty of about a GeV. Because down-going events dominate, the majority of contained events' neutrinos originate in a cone of about  $90^\circ$  about the vertical [51]. Thus the distance traveled by a contained-event neutrino varies from 30 km, the depth of the atmosphere, to  $6.5 \times 10^3$  km, the radius of the Earth. Contained events therefore have an uncertainty in  $\frac{x}{E}$  of  $\frac{6.5 \times 10^3 \text{ km}}{0.2 \text{ GeV}} - \frac{30 \text{ km}}{1.2 \text{ GeV}} \approx 1.7 \times 10^6 \text{ eV}^{-2}$ . This uncertainty causes the oscillations to smear out if

$$m_i^2 - m_j^2 > 2\pi (5.9 \times 10^{-7}) \text{ eV}^2 \approx 3.7 \times 10^{-6} \text{ eV}^2. \quad (359)$$

When this average is made, the probabilities become simple sums of boxes:

$$\langle P_{\nu_\alpha \rightarrow \nu_\beta} \rangle = -2 (\Re_{\beta 2}^1 + \Re_{\beta 3}^2 + \Re_{\beta 3}^1). \quad (360)$$

As discussed following equation (157) in Chapter IV, this row sum equals the sum  $\sum_{x=1}^3 |V_{\alpha x}|^2 |V_{\beta x}|^2$ .

We cannot average oscillations for accelerator experiments. Upon observation of Table 2, we see that the oscillatory behavior must occur if the LSND results are to be consistent with the limit placed by CHARM II.

## 6.2 Interpreting the Data

The atmospheric and solar data may be analyzed independent of neutrino masses, provided the mass-squared differences are large enough to yield the averaging described above. The probabilities measured at accelerators, however, are functions of these mass-squared differences. We will follow the authors of reference [51] and choose the mass-squared difference  $\Delta m_{23}^2$  which puts the LSND experiment at an oscillation maximum, and the difference  $\Delta m_{12}^2$  to be much smaller:

$$m_3^2 - m_2^2 \sim m_3^2 - m_1^2 \sim 2 \text{ eV}^2, \quad \text{and} \quad m_2^2 - m_1^2 \sim 10^{-2} \text{ eV}^2. \quad (361)$$

The smaller difference  $\Delta m_{12}^2$  is small enough to be negligible in accelerator experiments but large enough to be above the limits set in equations (358) and (359). With this choice, oscillations average and CP is effectively conserved for both solar and atmospheric neutrinos.

The oscillatory factors for accelerator experiments are listed in Table 3 for our choice of mass-squared differences. We have used the typical  $E$  quoted in Table 2 to obtain the first column of numbers. For each of the  $\frac{x}{4E}$  given in the Table,  $\sin^2 \Phi_{12}$  and  $\sin 2\Phi_{12}$  are much smaller than the sin functions involving the other mass-squared differences, which are roughly equal. Under these conditions, the sum of sin functions in equation (171) is nearly zero. (The biggest value for this sum comes from the LSND experiment and is  $\pm 0.015\mathcal{J}$ .) CP is therefore roughly conserved, and  $P_{\nu_\alpha \rightarrow \nu_\beta}$  measured by an accelerator experiment will be approximately

$$\begin{aligned} P_{\nu_\alpha \rightarrow \nu_\beta}^{accel} &= -2 \left( {}^aR_{\beta 2}^1 \sin^2 \Phi_{12} + {}^aR_{\beta 3}^2 \sin^2 \Phi_{23} + {}^aR_{\beta 3}^1 \sin^2 \Phi_{13} \right) \\ &\approx -2 \left( \sim 10^{-4} {}^aR_{\beta 2}^1 + {}^aR_{\beta 3}^2 + {}^aR_{\beta 3}^1 \right) \sin^2 \Phi_{23}. \end{aligned} \quad (362)$$

Unless the real part of  ${}^a\Box_{\beta 2}$  is much larger than the other real boxes, its term will not contribute significantly to the transition probability.

**Table 3:** Values of oscillatory terms for accelerator experiments. The numbers were calculated using the mass-squared differences given in equation (361). The typical values of energy indicated in Table 2 were used to calculate the second column. A more complete treatment would integrate over the entire energy range, but the approximation we have chosen is sufficient for our purposes.

Experiment	$\frac{x}{4E}$ (eV $^2$ )	$\sin^2 \Phi_{12}$	$\sin^2 \Phi_{23}$	$\sin^2 \Phi_{13}$	$\sin 2\Phi_{12}$	$\sin 2\Phi_{23}$	$\sin 2\Phi_{13}$
LSND	0.76	$5.8 \times 10^{-5}$	1.0	1.0	0.015	0.10	0.10
KARMEN	0.64	$4.1 \times 10^{-5}$	0.92	0.92	0.013	0.55	0.55
CHORUS	0.028	$7.8 \times 10^{-8}$	$3.1 \times 10^{-3}$	$3.1 \times 10^{-3}$	$5.6 \times 10^{-4}$	0.11	0.11
CHARM II	0.041	$3.7 \times 10^{-2}$	$6.7 \times 10^{-3}$	$6.7 \times 10^{-3}$	$8.2 \times 10^{-4}$	0.16	0.16

Acker and Pakvasa [51] have analyzed the solar neutrino data, including the possible contributions from muon and tau neutrino neutral current interactions to the Kamiokande data. They find that all the solar neutrino data is consistent with  $\langle P_{\nu_e \rightarrow \nu_e} \rangle$  between 0.4 and 0.55 for reasonable values of the initial  ${}^8B$  neutrino flux from the sun. These values were attained by assuming the oscillatory part of the probability  $\sin^2(\Phi_{ij})$  averages to one-half for all three mass-squared differences, so  $\langle P_{\nu_e \rightarrow \nu_e} \rangle =$

$1 - \langle P_{\nu_e \rightarrow \nu_\mu} \rangle - \langle P_{\nu_e \rightarrow \nu_\tau} \rangle$ . The range of probabilities allowed by the solar neutrino deficit is therefore

$$0.45 \lesssim \langle P_{\nu_e \rightarrow \nu_\mu} \rangle + \langle P_{\nu_e \rightarrow \nu_\tau} \rangle \lesssim 0.60. \quad (363)$$

Using Kamiokande's results (which are comparable to IMB's and SuperK's numbers but with smaller error bars) with a range of  $1.5\sigma$ , the atmospheric neutrinos in this CP-conserving scenario should obey

$$0.51 \lesssim \frac{1 - \langle P_{\nu_e \rightarrow \nu_\mu} \rangle - \langle P_{\nu_\mu \rightarrow \nu_\tau} \rangle + r \langle P_{\nu_e \rightarrow \nu_\mu} \rangle}{1 - \langle P_{\nu_e \rightarrow \nu_\mu} \rangle + r^{-1} \langle P_{\nu_e \rightarrow \nu_\mu} \rangle - \langle P_{\nu_e \rightarrow \nu_\tau} \rangle} \lesssim 0.69. \quad (364)$$

Up to this point we have not used our choices for neutrino masses, except to argue that oscillations average for atmospheric and solar neutrinos.

The LSND experiment measures  $P_{\nu_\mu \rightarrow \nu_e}$ , which equals  $P_{\nu_e \rightarrow \nu_\mu}$  by CPT conservation. Since only the decay-at-rest (LSND-1) result was available when this analysis was carried out, we restrict ourselves to consideration of that data. Using that measured probability and our choices of mass-squared differences, we find the constraint (again using 1.5 standard deviations as our limit)

$$1.2 \times 10^{-3} \lesssim -2 (10^{-4} \mathbb{H}_{22} + \mathbb{H}_{23}^2 + \mathbb{H}_{23}) \sin^2 \Phi_{23} \lesssim 5.1 \times 10^{-3} \quad (365)$$

from equation (362). Since  $10^{-4} \mathbb{H}_{22} \ll 10^{-3}$  for reasonable values of  $\mathbb{H}_{22}$  and  $\sin^2 \Phi_{23} = 1$  from Table 3, this constraint requires

$$2.5 \times 10^{-4} < -(\mathbb{H}_{23}^2 + \mathbb{H}_{23}) < 2.8 \times 10^{-3}. \quad (366)$$

KARMEN's 90% confidence level places a tighter upper bound than the  $1.5\sigma$  bound from LSND:

$$- (\mathbb{H}_{23}^2 + \mathbb{H}_{23}) < 1.0 \times 10^{-3} \quad (367)$$

By a similar argument, the constraints from CHORUS and KARMEN may each be turned into a constraint on the sum of two boxes for the other oscillation possibilities. From CHORUS, we find

a limit on  $\nu_\mu$ - $\nu_\tau$  mixing:

$$- \left( \frac{2}{3} \mathbb{R}_{33} + \frac{1}{3} \mathbb{R}_{33} \right) < 0.32. \quad (368)$$

KARMEN provides a limit on  $\nu_e$ - $\nu_\tau$  mixing:

$$- \left( \frac{1}{2} \mathbb{R}_{33} + \frac{1}{2} \mathbb{R}_{33} \right) < 5.4 \times 10^{-2}. \quad (369)$$

We may combine the constraints on  $\nu_e$ - $\nu_\mu$  mixing with equation (217) to eliminate  $\mathbb{R}_{23}$ , and solve for  $\mathbb{R}_{23}$ . If we call the sum  $- \left( \frac{1}{2} \mathbb{R}_{23} + \frac{1}{2} \mathbb{R}_{23} \right)$  as measured by LSND or other accelerator experiments  $s$ ,

$$\mathbb{R}_{23} = \frac{\frac{1}{2} \mathbb{R}_{22} \mathbb{R}_{23} - \mathcal{J}^2}{-\mathbb{R}_{23} - \frac{1}{2} \mathbb{R}_{22}} = -s - \frac{1}{2} \mathbb{R}_{23}, \quad (370)$$

so

$$\mathbb{R}_{23} = \frac{-s \pm \sqrt{s^2 - 4 \mathbb{R}_{22} s - 4 \mathcal{J}^2}}{2}. \quad (371)$$

If  $\mathbb{R}_{23}$  is to be real, which it is by definition,

$$4 \mathcal{J}^2 < s^2 - 4 \mathbb{R}_{22} s. \quad (372)$$

Assuming  $-\mathbb{R}_{22}$  has its maximum value of half  $\langle P_{\nu_e \rightarrow \nu_\mu} (x) \rangle_{max}$ , or 0.3, and  $s$  equals  $10^{-3}$ , the maximum value allowed by KARMEN, we find the following minimal constraint on  $\mathcal{J}^2$ :

$$\mathcal{J}^2 < 3 \times 10^{-4}. \quad (373)$$

Even though CP is essentially undetectable due to our choice of masses, the imaginary part of the boxes,  $\mathcal{J}$ , may still play a role in determining the oscillation probabilities. Using the above maximum values of  $-\mathbb{R}_{22}$  and  $s$  along with this maximum value of  $\mathcal{J}^2$  in equations (370) and (371) yields

$$\mathbb{R}_{23} = \mathbb{R}_{23} = -\frac{s}{2} = -5 \times 10^{-4}. \quad (374)$$

If, on the other hand,  $\mathcal{J}^2 = 0$ ,

$$(\mathbb{H}_{23}, \mathbb{R}_{23}) = (1.7 \times 10^{-2}, 1.8 \times 10^{-2}) \quad \text{or} \quad (1.8 \times 10^{-2}, 1.7 \times 10^{-2}) \quad (375)$$

A set of measurements of probabilities at different distances which pinpointed the values of individual boxes would thus probe the value of  $\mathcal{J}^2$ , even if CP were hidden from observation in the oscillations being observed! The above ambiguity between the values of  $\mathbb{H}_{23}$  and  $\mathbb{R}_{23}$  arises because  $\sin^2 \Phi_{23} \approx \sin^2 \Phi_{13}$ . We have chosen one mass scale to dominate the other, a situation examined in Section 5.1.4. Consideration of equation (276) shows that only the sums  $\mathbb{R}_{\beta 3} + \mathbb{H}_{\beta 3}$  are measurable. Unitarity constraints of the form (217) for a known  $\mathcal{J}^2$  and  $\mathbb{R}_{\beta 2}$  allow us to determine the choices for  $\mathbb{R}_{\beta 3}$  and  $\mathbb{H}_{\beta 3}$  but not to say which has which value.

### 6.3 Finding Solutions

As promised in Section 4.2.2, we numerically find boxes which match the data. Different values of the five parameters  $\mathbb{H}_{22}$ ,  $\mathbb{H}_{23}$ ,  $\mathbb{H}_{32}$ ,  $\mathbb{R}_{33}$ , and  $\mathcal{J}^2$  are stepped through, the other five  $R$ s found by equations (217) to (221), and the resulting oscillation probabilities compared to the solar neutrino, atmospheric neutrino, and LSND results discussed above. The boxes must also produce a mixing matrix which is unitary.

We find many solution sets which meet all of these conditions. For  $\mathcal{J}^2 = 0$ , the two best fits are found with

$$\mathcal{B}_1 = \begin{pmatrix} -18 & -1.0 & 0.95 \\ -1.0 & -0.67 & -2.0 \\ 0.95 & -2.0 & -1.8 \end{pmatrix} \times 10^{-2}, \quad (376)$$

which is symmetric, and

$$\mathcal{B}_2 = \begin{pmatrix} -10 & 0.91 & -1.0 \\ -13 & -1.0 & -0.93 \\ 5.6 & -10 & -13 \end{pmatrix} \times 10^{-2}. \quad (377)$$

The first solution gives a solar ratio  $\langle P_{\nu_e \rightarrow \nu_e} \rangle$  of 0.42, an atmospheric ratio  $R_{atm}$  of 0.55, and an LSND probability of  $2.1 \times 10^{-3}$ . The second gives a solar ratio of 0.55, an atmospheric ratio of 0.69,

and an LSND probability of  $3.6 \times 10^{-3}$ .

We may obtain the magnitudes  $|V_{\alpha i}|$  from the boxes from equation (143). Using the notation  $|V|$  for the matrix of these magnitudes, the two solutions yield

$$|V|_1 = \begin{pmatrix} 0.88 & 0.47 & 0.20 \\ 0.50 & 0.88 & 0.12 \\ 0.12 & 0.20 & 0.99 \end{pmatrix}, \quad (378)$$

and

$$|V|_2 = \begin{pmatrix} 0.50 & 0.41 & 0.74 \\ 0.65 & 0.73 & 0.04 \\ 0.53 & 0.51 & 0.65 \end{pmatrix}. \quad (379)$$

Inspection reveals appropriate places to insert minus signs to make these matrices unitary to within the tolerance required by our numerical technique. Such an assignment, however, is not unique due to the phase ambiguities discussed in Section 4.1.

Comparing the solutions (376) and (377), we see that by the first solution,  $\nu_e$ - $\nu_\mu$  mixing comprises most of the solar neutrino deficit, while the second solution uses  $\nu_e$ - $\nu_\tau$  mixing to account for most of the solar deficit.

Acker and Pakvasa in [51] expressed their solution in terms of the mixing matrix:

$$V_{AP} = \begin{pmatrix} 0.70 & 0.70 & 0.14 \\ -0.71 & 0.69 & 0.12 \\ -0.010 & -0.19 & 0.98 \end{pmatrix}. \quad (380)$$

We find the corresponding box matrix to be

$$\mathcal{B}_{AP} = \begin{pmatrix} -24 & 0.84 & -0.87 \\ -0.92 & -1.6 & 0.87 \\ -0.92 & -1.8 & -0.96 \end{pmatrix} \times 10^{-2}. \quad (381)$$

This solution was not selected by our technique because the resulting atmospheric ratio,  $R_{atm} = 0.50$ ,

is not within the  $1.5\sigma$  range of Kamiokande's data. Acker and Pakvasa's solution yields  $\langle P_{\nu_e \rightarrow \nu_e'} \rangle = 0.48$  for the solar neutrino deficit, and an LSND probability of  $1.2 \times 10^{-3}$ .

The above solutions all contain no CP violation. We found solution sets for CP-violating cases too, with  $\mathcal{J}^2$  going as high as  $2.7 \times 10^{-4}$ . The only solution for that maximum  $\mathcal{J}^2$  is

$$\mathcal{B}_3 = \begin{pmatrix} -22 & -0.12 & 5 \times 10^{-4} \\ -1.0 & -1.0 & 0.85 \\ 0.84 & -2.3 & -3.2 \end{pmatrix} \times 10^{-2}, \quad (382)$$

yielding

$$|V|_3 = \begin{pmatrix} 0.73 & 0.63 & 0.25 \\ 0.65 & 0.74 & 0.14 \\ 0.21 & 0.19 & 0.95 \end{pmatrix}. \quad (383)$$

This CP-non-conserving solution gives a solar ratio of 0.53, an atmospheric ratio of 0.51, and an LSND probability of  $4.9 \times 10^{-3}$ . None of the solutions which conserved CP found this combination of high solar ratio and low atmospheric ratio. The CP-conserving solution set which most closely reproduces these CP-violating probabilities is

$$\mathcal{B}_4 = \begin{pmatrix} -10 & -1.1 & 1.0 \\ 5.0 & -16 & 7.3 \\ -10 & 1.0 & -1.1 \end{pmatrix} \times 10^{-2}, \quad (384)$$

which produces a solar ratio of 0.40, an atmospheric ratio of 0.52, and an LSND probability of  $4.5 \times 10^{-3}$ . One can see that CP violation may have a measurable effect, even if the mass-squared differences conspire to hide direct evidence of it.

## 6.4 How Do Specific Models Stack Up?

None of the models presented in Chapter V are compatible with the solutions we have presented here. Wolfenstein's parameterization requires

$$\mathbb{H}_{23} \approx -\mathbb{K}_{23} \approx \mathbb{K}_{33}, \quad (385)$$

as seen by examination of equation (269). The first approximate equality is met by all three solutions, (376), (377), and (381), but the second is not met by any of them. The small-angle approximation is merely a special case of the Wolfenstein parameterization, so it is not consistent with the current data either.

Equations (339) and (341) of Chapter V present two possibilities for Zee-model-induced oscillations. Both possibilities predict  ${}^{11}\square_{22} \approx {}^{11}\square_{23}$ , a condition which is not met by any of the above solutions. This equality is very hard to reconcile with both the LSND results and the solar neutrino measurements, but it could become relevant if matter effects enhance the effect of an otherwise small  ${}^{11}\square_{22}$ . And as discussed in Section 2.3.2, we have only examined the Zee mechanism for two limits of coupling constants; our work does not address the applicability of other coupling-constant choices.

The Fritzsch mass matrix model of Section 5.2.1 predicted that for a mass hierarchy, the diagonal elements  ${}^{11}\square_{22}$  and  ${}^{22}\square_{33}$  should be much larger than the other elements. These two boxes are of the same order in solution 2 (377), but they are not significantly larger than the off-diagonal  ${}^{21}\square_{32}$  and  ${}^{12}\square_{33}$ . The reverse mass hierarchy considered in that Section predicts the same two dominant boxes, once we swap the 3 and 1 mass indices to account for the new labeling of mass states, so it is inconsistent with our solutions too. Again, our work does not comment on the more general Fritzsch model, but only on its limits when one mass scale dominates.

Before concluding this Chapter we must remind the Gentle Reader that the solutions derived above assume an energy-independence of the solar neutrino data and the atmospheric neutrino data. Choosing this interpretation allows the fitting of all current data with only three neutrino flavors, but we do not mean to present this choice as the only one possible. Many other excellent analyses of the data, such as those by Fogli and Lisi [57] and those by Cardall and Fuller [58], take different approaches which are equally valid.

The neutrino-oscillation interpretations of all three data sets considered here (solar, atmospheric, and LSND) are still unconfirmed and controversial. If an energy dependence of solar neutrino oscillations is unequivocally demonstrated by future experiments, or if any of the probabilities used here change dramatically (or keep the same mean value with smaller error bars), the solutions we have found will no longer be valid, and another neutrino generation and/or matter effects on oscillations may be implicated. At the present, however, our solution sets fit all of the existing data and provide a demonstration of the use of the boxes.

## CHAPTER VII

### OUTLOOK

Neutrino oscillations address many current physics questions. Observation of them would present the first contradiction of the Standard Model and provide a clue as to the direction that extensions of the Model should take. Understanding what role, if any, oscillations play in the solar neutrino deficit will help refine theories of stellar evolution. And indications of the magnitude of neutrino masses from oscillation experiments would indicate how much neutrinos contribute to dark matter. With approximately 115 low-energy “relic” neutrinos of each flavor occupying every cubic centimeter of space [59], a single neutrino mass on the order of 7 eV (or all neutrino masses summing to 7 eV) provides enough mass to close the universe [12].

Once neutrino oscillations are detected and the boxes and neutrino masses determined, neutrinos may be used to probe the universe. Neutrino oscillations could help determine the density of different regions of the earth [60] and bring information about cosmologically distant objects [47]. Neutrinos can act as a long-wavelength telescope, peering further out in space (and therefore further back in time) than conventional telescopes. The distance for which neutrino telescopes will be sensitive depends on the values of mass-squared differences. This dependence is illustrated in Figure 11, a plot popularized by J. G. Learned. The neutrino telescope AMANDA is already taking data, hoping to use gamma-ray bursters and supernovae to measure neutrino masses [61]. Other neutrino telescopes are under construction and will soon join the hunt.

Neutrino physics has entered a golden age of research. New experiments all over the globe promise an unequaled amount of data, from the sun, the atmosphere, accelerators, supernovae, and other cosmic sources. SuperK in Japan amassed as much data in its first 102 days of running as all of the previous solar neutrino experiments did over their combined lifetimes [62]. Analyzing such refined data requires a consistent, model-independent approach. In this dissertation, we have developed such an approach and then illustrated its use by comparison with the low-statistics data currently available.

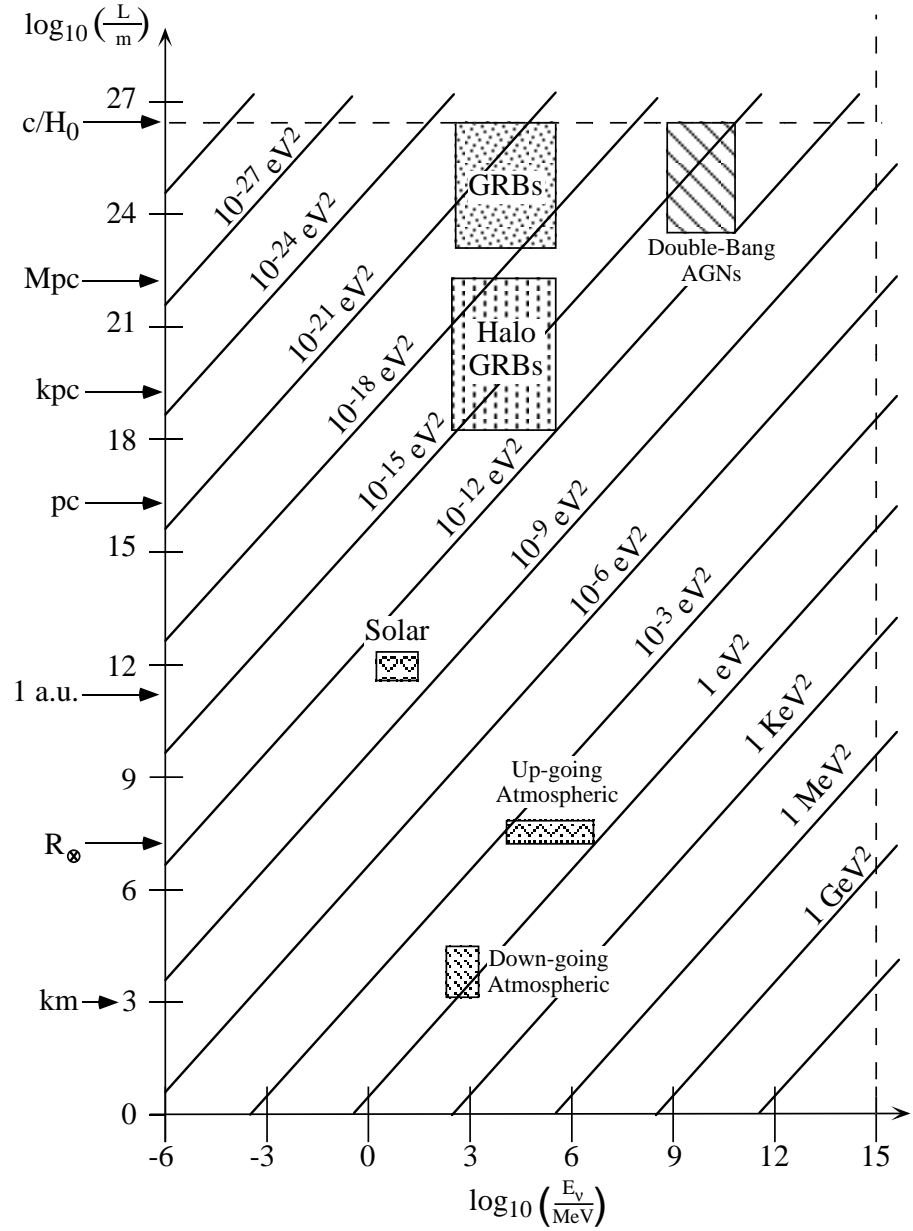


**Figure 11:** Lengths and energies probed by neutrino oscillations for different mass-squared differences, obtained by setting  $\Phi_{ij} = \frac{\pi}{2}$  so that the Earth sits on a maximum of an oscillation length. Lengths of interest are labeled on the vertical axis, with  $R_\odot$  representing the radius of Earth and  $H_0$  representing the present value of the Hubble constant. Shaded regions represent energies and distances typical for the indicated cosmological neutrino source. Included are solar neutrinos, both up- and down-going atmospheric neutrinos, gamma-ray bursters both within the galactic halo and outside our Galaxy, and active galactic nuclei. Double-bang AGNs refer to those AGNs producing tau neutrinos energetic enough to produce a “double-bang” signature in detectors.

## APPENDIX A

### NOTATION KEY

Greek Lorentz indices  $\mu, \nu, \sigma$ , *et cetera* may take the values 0 to 3. Latin Lorentz indices  $a, b$ , *et cetera* refer to the spatial components 1 to 3.

Greek particle indices  $\alpha, \beta, \gamma$ , *et cetera* represent states of definite flavor. Latin particle indices  $i, j, k$ , *et cetera* represent states of definite mass.

We will explicitly write out all *flavor* sums, since repeated flavor indices are not necessarily summed over.

Repeated *Lorentz* indices  $\mu, \nu$ , and  $a$  are always summed over.

$\sum_{i \neq j}$  represents a single sum over the index  $i$ , omitting the term for which  $i = j$ . Sums over both indices will be represented by  $\sum_j \sum_{i \neq j}$ .

In this paper, we use the “west-coast metric” in which  $g_{00} = 1$ ,  $g_{aa} = -1$ , and the other elements are zero.

$e = \sqrt{4\pi\alpha}$  in this paper, where  $\alpha$  here is the fine-structure constant. In standard particle physics units ( $c = \hbar = 1$ ), our  $e$  is the electric charge. In other units it is proportional to the electric charge.

$\gamma^0, \gamma^1, \gamma^2, \gamma^3$ , and  $\gamma_5$  are Dirac *gamma matrices*, discussed in detail in Appendix B.1

$\partial_\mu \equiv \frac{\partial}{\partial x_\mu}$  is the Lorentz-covariant partial derivative.

$\theta_W$  is the Weinberg angle, defined by equation (2).

$P_L = \frac{1-\gamma_5}{2}$  is the left-handed projection operator, and

$P_R = \frac{1+\gamma_5}{2}$  is the right-handed projection operator. They are discussed in detail in Appendix B.3.1.

$\vec{p} \equiv \mathbf{p}$  is the 3-vector portion of the four-vector  $\mathbf{p}$ .

$\mathbf{p}\sigma \equiv \mathbf{p} \cdot \boldsymbol{\sigma}$  is the dot product of the vectors  $\mathbf{p}$  and  $\boldsymbol{\sigma}$ .

$\psi$  is used to denote a generic spinor, or the spinor containing all neutrino states, described below.

$\psi^*$  is a complex-conjugated spinor.

$\psi^\dagger = \psi^{*T}$  is a Hermitian-conjugated spinor.

The symbols  $*$  and  $\dagger$  have the same effects on other objects as they do on spinors.

$\bar{\psi} = \psi^\dagger \gamma^0$  is a Dirac-conjugated spinor.

$\psi = C \bar{\psi}^T$  is a charge-conjugated spinor.

$C = i\gamma^2\gamma^0$  is the charge conjugation operator, discussed in detail in Appendix B.4.

$\nu_{\alpha L}$  is the left-handed active neutrino of flavor  $\alpha = e, \mu, \tau$ .

$\nu_{\alpha R}$  is its CP-conjugate antineutrino of flavor  $\alpha$ ; it is right-handed.

$N_{\alpha R}$  is the right-handed sterile partner to  $\nu_{\alpha L}$ . It has not yet been observed.

$N_{\alpha L}$  is the left-handed sterile partner to  $\nu_{\alpha R}$ . It is also the CP-conjugate of  $N_{\alpha R}$  and has not yet been observed.

$\alpha_L$  is the left-handed charged lepton of flavor  $\alpha$ .

$\alpha_R$  is its right-handed partner.

$\alpha_R$  is the CP-conjugate of  $\alpha_L$ .

$\alpha_L$  is the CP-conjugate of  $\alpha_R$ .

$\psi_{\alpha L} = \begin{pmatrix} \nu_{\alpha L} \\ \alpha_L \end{pmatrix}$  is left-handed lepton doublet of flavor  $\alpha$ .

$\nu_L$  is an  $n_L$ -dimensional vector containing all  $n_L$  active left-handed neutrinos.  $\nu_R$  similarly contains all  $n_L$  of the active right-handed antineutrinos.

$N_R$  is an  $n_R$ -dimensional vector containing all  $n_R$  sterile right-handed neutrinos.  $N_L$  similarly contains all  $n_R$  sterile left-handed antineutrinos.

$\psi$ , in addition to being a generic spinor, represents the  $n$ -dimensional vector containing  $\nu_L, N_R$ , and any additional sterile fields not related to active fields.

$l_{L,R}$  is the 3-dimensional vector containing all three flavors of charged lepton spinors  $\alpha_{L,R}$ .

$\phi_D$  is the Higgs doublet which couples to down-type quarks and charged leptons.

$\tilde{\phi}_D$  is the Higgs doublet which couples to up-type quarks and neutrinos.

## APPENDIX B

### THE DIRAC EQUATION, WAVE FUNCTIONS, AND TRANSFORMATIONS

In this Appendix we review many aspects of field theory as they relate to neutrinos. As in the Introduction, the presentation here is synthesized from many sources. For a more in-depth treatment of field theory and weak-interaction physics, the reader is encouraged to consult any or all of the references [63], [11], [17], [18], [64], [65].

#### B.1 Gamma Matrices

The Dirac gamma matrices  $\gamma^\mu$  are defined by their appearance in the Dirac equation:

$$[i\gamma^\mu \partial_\mu - m] \psi(x) = 0. \quad (386)$$

The spinor  $\psi(x)$  is a four-component spinor, and the gamma matrices are  $4 \times 4$ . For Dirac's equation to give the Klein-Gordon equation when its operation is performed twice, the Dirac matrices must obey the anticommutation relations [11]

$$\gamma^\mu \gamma^\nu + \gamma^\nu \gamma^\mu = 2g_{\mu\nu}, \quad (387)$$

where  $g_{\mu\nu}$  is the metric, defined in Appendix A. Dirac noted that the matrices

$$\gamma^0 = \begin{pmatrix} \mathbb{1} & 0 \\ 0 & \mathbb{1} \end{pmatrix} \quad \text{and} \quad \gamma^a = \begin{pmatrix} 0 & \sigma_a \\ -\sigma_a & 0 \end{pmatrix} \quad (388)$$

satisfy the anticommutation requirement. Each element of the matrices in equation (388) represents a  $2 \times 2$  submatrix;  $\sigma_a$  are the Pauli matrices,

$$\sigma_1 = \begin{pmatrix} 0 & 1 \\ 1 & 0 \end{pmatrix}, \quad \sigma_2 = \begin{pmatrix} 0 & -i \\ i & 0 \end{pmatrix}, \quad \text{and} \quad \sigma_3 = \begin{pmatrix} 1 & 0 \\ 0 & -1 \end{pmatrix}, \quad (389)$$

and  $\mathbb{1}$  is the  $2 \times 2$  unit matrix. The product of the four gamma matrices,  $\gamma_5 \equiv i\gamma^0\gamma^1\gamma^2\gamma^3$ , is useful also. In the above *standard representation* it has the form

$$\gamma_5 = \begin{pmatrix} 0 & \mathbb{1} \\ \mathbb{1} & 0 \end{pmatrix}. \quad (390)$$

The representation of the gamma matrices chosen by Dirac is not unique. If a set of  $\gamma^\mu$  satisfy equation (387), then so will any transformation of that set by an invertible matrix  $A\gamma^\mu A^{-1}$ . Two other popular representations include the *Majorana representation* [12],

$$\begin{aligned} \gamma^0 &= \begin{pmatrix} 0 & \sigma_2 \\ \sigma_2 & 0 \end{pmatrix}, & \gamma^1 &= \begin{pmatrix} i\sigma_3 & 0 \\ 0 & i\sigma_3 \end{pmatrix}, & \gamma^2 &= \begin{pmatrix} 0 & -\sigma_2 \\ \sigma_2 & 0 \end{pmatrix}, \\ \gamma^3 &= \begin{pmatrix} -i\sigma_1 & 0 \\ 0 & -i\sigma_1 \end{pmatrix}, \quad \text{and} \quad \gamma_5 &= \begin{pmatrix} \sigma_2 & 0 \\ 0 & -\sigma_2 \end{pmatrix}, \end{aligned} \quad (391)$$

in which Majorana particles have pure real spinors, and the *chiral representation* [66],

$$\gamma^0 = \begin{pmatrix} 0 & \mathbb{1} \\ \mathbb{1} & 0 \end{pmatrix}, \quad \gamma^a = \begin{pmatrix} 0 & -\sigma_a \\ \sigma_a & 0 \end{pmatrix}, \quad \text{and} \quad \gamma_5 = \begin{pmatrix} \mathbb{1} & 0 \\ 0 & \mathbb{1} \end{pmatrix}. \quad (392)$$

## B.2 Neutrino Wave Functions

Neutrino solutions to the Dirac equation (386) are described by *field operators* of the form [12]

$$\psi(x) = \int \frac{d^3 p}{(2\pi)^{\frac{3}{2}}} \sum_{s=\pm 1/2} [e^{ipx} v_s(p) \mathbf{b}_s^\dagger(\mathbf{p}) + e^{-ipx} u_s(p) \mathbf{a}_s(\mathbf{p})]. \quad (393)$$

$u_s(p)$  and  $v_s(p)$  are single-particle *spinors*, and  $px$  is shorthand for the Lorentz invariant  $p_\mu x^\mu$ . Using the standard representation for the gamma matrices, the spinors have the forms

$$u_s(p) = \sqrt{\frac{E+m}{2E}} \begin{pmatrix} \chi_s \\ \frac{\boldsymbol{\sigma} \cdot \mathbf{p}}{E+m} \chi_s \end{pmatrix}, \quad \text{and} \quad v_s(p) = \sqrt{\frac{E+m}{2E}} \begin{pmatrix} \frac{\boldsymbol{\sigma} \cdot \mathbf{p}}{E+m} \chi_s \\ \chi_s \end{pmatrix}, \quad (394)$$

with

$$\chi_{\frac{1}{2}} = \begin{pmatrix} 1 \\ 0 \end{pmatrix}, \text{ and } \chi_{-\frac{1}{2}} = \begin{pmatrix} 0 \\ 1 \end{pmatrix}. \quad (395)$$

$\mathbf{b}_s^\dagger(\mathbf{p})$  and  $\mathbf{a}_s(\mathbf{p})$  are the appropriate creation operator for antiparticle (negative momentum) fields and the destruction operator of particle(positive momentum) fields.  $\sigma$  are the Pauli matrices, given in equation (389).

For simplicity, we will take the momentum along the  $+\hat{z}$  direction,<sup>1</sup> and the mass to be much smaller than the energy of the neutrino. The quantity  $\frac{\sigma \cdot \mathbf{p}}{E+m}$  appearing in the spinor definitions then becomes

$$\frac{\sigma \cdot \mathbf{p}}{E+m} = \frac{|p|}{E+m} \sigma_3 \approx (1-\epsilon) \sigma_3, \quad (396)$$

where  $\epsilon = \frac{m}{E}$ . Using the standard representation for the gamma matrices, the neutrino wave function now has the form

$$\psi(t, \mathbf{x}) = \int \frac{d^3 p}{(2\pi)^{\frac{3}{2}}} \sqrt{\frac{E+m}{2E}} \begin{pmatrix} (1-\epsilon) e^{ipx} \mathbf{b}_+^\dagger(\mathbf{p}) + e^{-ipx} \mathbf{a}_+(\mathbf{p}) \\ -(1-\epsilon) e^{ipx} \mathbf{b}_-^\dagger(\mathbf{p}) + e^{-ipx} \mathbf{a}_-(\mathbf{p}) \\ e^{ipx} \mathbf{b}_+^\dagger(\mathbf{p}) + (1-\epsilon) e^{-ipx} \mathbf{a}_+(\mathbf{p}) \\ e^{ipx} \mathbf{b}_-^\dagger(\mathbf{p}) - (1-\epsilon) e^{-ipx} \mathbf{a}_-(\mathbf{p}) \end{pmatrix}, \quad (397)$$

where the subscripts  $+$  and  $-$  on the creation and annihilation operators represent the spin states  $+\frac{1}{2}$  and  $-\frac{1}{2}$ , respectively.

If we reflect the coordinate system, the momentum is in the  $-\hat{z}$  direction and the quantity in

---

<sup>1</sup> This choice reflects the convention to quantize spin along the z-axis. When discussing kinematics, we follow the convention to choose  $\mathbf{p}$  along the x-axis, which may at first seem to contradict our first assumption. To be consistent throughout, we could either choose  $\mathbf{p}$  always along the z-axis so  $\mathbf{p} \cdot \mathbf{x} = pz$  in our kinematic discussion, or we could choose to quantize spin along the x-axis and redefine the Pauli matrices so  $\sigma_1$  is diagonal with  $\pm 1$  eigenvalues. Either consistent treatment would yield the same results as ours, so we will stick with our convention-motivated choices, inconsistent though they seem.

equation (396) changes sign. The wave function for the reflected system is

$$\psi(t, -\mathbf{x}) = \int \frac{d^3 p}{(2\pi)^{\frac{3}{2}}} \sqrt{\frac{E+m}{2E}} \begin{pmatrix} -(1-\epsilon)e^{ipx} \mathbf{b}_+^\dagger(-\mathbf{p}) + e^{-ipx} \mathbf{a}_+(-\mathbf{p}) \\ (1-\epsilon)e^{ipx} \mathbf{b}_-^\dagger(-\mathbf{p}) + e^{-ipx} \mathbf{a}_-(-\mathbf{p}) \\ e^{ipx} \mathbf{b}_+^\dagger(-\mathbf{p}) - (1-\epsilon)e^{-ipx} \mathbf{a}_+(-\mathbf{p}) \\ e^{ipx} \mathbf{b}_-^\dagger(-\mathbf{p}) + (1-\epsilon)e^{-ipx} \mathbf{a}_-(-\mathbf{p}) \end{pmatrix}. \quad (398)$$

The exponentials do not change under the transformation because  $x'p' = tE - (-\mathbf{x})(-\mathbf{p}) = xp$ . The differential  $d^3 p$  changes sign, but the limits of the integration change sign too, and those two effects cancel each other.

### B.3 Helicity, Chirality, Parity, and Parity Violation

#### B.3.1 A Review of Handedness

The wave function in equation (397) contains all spin states. We may, however separate the states with right-handed, or positive, spin from those with left-handed, or negative, spin through the helicity projectors  $P'_R$  and  $P'_L$ . The handedness of states is determined by considering the component of spin along the momentum axis. When one puts the right thumb along the direction of momentum, if the fingers of the right hand curl in the direction of the spin, the state has positive helicity. If the spin is instead in the direction of the fingers of the left hand, the state has negative helicity.

The helicity projection operators are given by [10]

$$P'_R = \frac{1}{2} \left( \mathbf{1} + \frac{\Sigma \cdot \mathbf{p}}{|\mathbf{p}|} \right), \quad \text{and} \quad P'_L = \frac{1}{2} \left( \mathbf{1} - \frac{\Sigma \cdot \mathbf{p}}{|\mathbf{p}|} \right), \quad (399)$$

with

$$\Sigma \equiv \begin{pmatrix} \sigma & 0 \\ 0 & \sigma \end{pmatrix} \quad (400)$$

in the standard representation, and they are functions of the momentum and energy [10]:

$$P'_{R,L} = \frac{1}{2} \left( \pm \gamma_5 \frac{E - \beta m_0}{p} \right), \quad (401)$$

where  $\beta$  is the particles velocity in terms of  $c$ . These operators are not manifestly Lorentz-invariant, but in the relativistic limit they become

$$\frac{1}{2}(\pm \gamma_5). \quad (402)$$

The relativistic limits of the helicity projection operators are Lorentz-invariant and are called the *chirality projection operators*,  $P_{R,L}$ :

$$P_R = \frac{1}{2}(+ \gamma_5), \quad \text{and} \quad P_L = \frac{1}{2}(- \gamma_5). \quad (403)$$

The chirality operators have the properties

$$P_R P_R = P_R, \quad P_L P_L = P_L, \quad \text{and} \quad P_L P_R = P_R P_L = 0, \quad (404)$$

which are consistent with their roles of projecting out particular states. The helicity is only the same as the chirality if the particle mass is zero, which means the  $\epsilon$  in the wave function equations becomes zero. We will restrict ourselves to that case here for simplicity. Due to the smallness of the neutrino masses, we also use the words helicity and chirality interchangeably in the text. In the standard basis, the chirality projection operators have the forms

$$P_R = \frac{1}{2} \begin{pmatrix} \mathbb{1} & \mathbb{1} \\ \mathbb{1} & \mathbb{1} \end{pmatrix}, \quad \text{and} \quad P_L = \frac{1}{2} \begin{pmatrix} \mathbb{1} & \mathbb{1} \\ \mathbb{1} & \mathbb{1} \end{pmatrix}. \quad (405)$$

Applying these projections to the wave function of equation (397) and taking  $\epsilon$  to zero, we find

$$P_R\psi(x) = \int \frac{d^3p}{(2\pi)^{\frac{3}{2}}} \sqrt{\frac{E+m}{2E}} \begin{pmatrix} e^{ipx} \mathbf{b}_+^\dagger(\mathbf{p}) + e^{-ipx} \mathbf{a}_+(\mathbf{p}) \\ 0 \\ e^{ipx} \mathbf{b}_+^\dagger(\mathbf{p}) + e^{-ipx} \mathbf{a}_+(\mathbf{p}) \\ 0 \end{pmatrix}, \quad \text{and} \quad (406)$$

$$P_L\psi(x) = \int \frac{d^3p}{(2\pi)^{\frac{3}{2}}} \sqrt{\frac{E+m}{2E}} \begin{pmatrix} 0 \\ -e^{ipx} \mathbf{b}_-^\dagger(\mathbf{p}) + e^{-ipx} \mathbf{a}_-(\mathbf{p}) \\ 0 \\ e^{ipx} \mathbf{b}_-^\dagger(\mathbf{p}) - e^{-ipx} \mathbf{a}_-(\mathbf{p}) \end{pmatrix}. \quad (407)$$

The only states surviving the right-handed projection are those with spin pointing in the same direction as the momentum, and those which survive the left-handed projection have spin pointing in the opposite direction. If we were to apply the projection operators to the reflected wave function of equation (398), the right-handed projection would again choose the spin states aligned with the momentum, but if those would have negative spin since the momentum is negative:

$$P_R\psi(t, -\mathbf{x}) = \int \frac{d^3p}{(2\pi)^{\frac{3}{2}}} \sqrt{\frac{E+m}{2E}} \begin{pmatrix} 0 \\ e^{ipx} \mathbf{b}_-^\dagger(-\mathbf{p}) + e^{-ipx} \mathbf{a}_-(-\mathbf{p}) \\ 0 \\ e^{ipx} \mathbf{b}_-^\dagger(-\mathbf{p}) + e^{-ipx} \mathbf{a}_-(-\mathbf{p}) \end{pmatrix}. \quad (408)$$

Operating on the reflected wave function with  $P_L$  pulls out the positive spin states in a similar manner. One must be especially careful to change the argument of the *original* wave function (397) and form the new wave function (398) *before* using the projection operators. The expression in equation (408) will never fall out of any operation on the wave function in equation (406), since the projection operation has already thrown out the negative spin states in equation (406).

### B.3.2 Parity Transformations

The operation of space reflection is called a *parity transformation*. Two parity operations must return a system to its original state, so the reflected annihilation and creation operators  $\mathbf{a}'_s(-\mathbf{p})$  and  $\mathbf{b}'^\dagger_s(-\mathbf{p})$  may differ from the original fields only by a phase:

$$\mathbf{a}'_s(-\mathbf{p}) = \mathbf{a}_s(-\mathbf{p}) = \eta_a \mathbf{a}_s(\mathbf{p}), \quad \text{and} \quad \mathbf{b}'^\dagger_s(-\mathbf{p}) = \mathbf{b}_s^\dagger(-\mathbf{p}) = \eta_b \mathbf{b}_s^\dagger(\mathbf{p}). \quad (409)$$

The parity-transformed wave function in the new coordinates  $x' = (t, -\mathbf{x})$  and  $p' = (E, -\mathbf{p})$  is then

$$\begin{aligned} \psi(x') &= \int \frac{d^3p}{(2\pi)^{\frac{3}{2}}} \sqrt{\frac{E+m}{2E}} \begin{pmatrix} -(1-\epsilon)e^{ipx} \mathbf{b}'^\dagger_+(-\mathbf{p}) + e^{-ipx} \mathbf{a}'_+(-\mathbf{p}) \\ (1-\epsilon)e^{ipx} \mathbf{b}'^\dagger_-(-\mathbf{p}) + e^{-ipx} \mathbf{a}'_-(-\mathbf{p}) \\ e^{ipx} \mathbf{b}'^\dagger_+(-\mathbf{p}) - (1-\epsilon)e^{-ipx} \mathbf{a}'_+(-\mathbf{p}) \\ e^{ipx} \mathbf{b}'^\dagger_-(-\mathbf{p}) + (1-\epsilon)e^{-ipx} \mathbf{a}'_-(-\mathbf{p}) \end{pmatrix} \\ &= \int \frac{d^3p}{(2\pi)^{\frac{3}{2}}} \sqrt{\frac{E+m}{2E}} \begin{pmatrix} -(1-\epsilon)e^{ipx} \eta_b \mathbf{b}_+^\dagger(\mathbf{p}) + e^{-ipx} \eta_a \mathbf{a}_+(\mathbf{p}) \\ (1-\epsilon)e^{ipx} \eta_b \mathbf{b}_-^\dagger(\mathbf{p}) + e^{-ipx} \eta_a \mathbf{a}_-(\mathbf{p}) \\ e^{ipx} \eta_b \mathbf{b}_+^\dagger(\mathbf{p}) - (1-\epsilon)e^{-ipx} \eta_a \mathbf{a}_+(\mathbf{p}) \\ e^{ipx} \eta_b \mathbf{b}_-^\dagger(\mathbf{p}) + (1-\epsilon)e^{-ipx} \eta_a \mathbf{a}_-(\mathbf{p}) \end{pmatrix} \end{aligned} \quad (410)$$

As mentioned above,  $e^{ip'x'} = e^{ipx}$ .

The transformed wave function should be related to the original wave function of equation (397) by simple matrix operations, so each element of the new wave function should be proportional to the corresponding element of the old wave function. Comparison of equations (410) and (397) reveals that  $\eta_a$  must equal  $-\eta_b$ . Choosing  $\eta_a = 1$ , we have

$$\begin{aligned} \psi(x') &= \int \frac{d^3p}{(2\pi)^{\frac{3}{2}}} \sqrt{\frac{E+m}{2E}} \begin{pmatrix} (1-\epsilon)e^{ipx} \mathbf{b}_+^\dagger(\mathbf{p}) + e^{-ipx} \mathbf{a}_+(\mathbf{p}) \\ -(1-\epsilon)e^{ipx} \mathbf{b}_-^\dagger(\mathbf{p}) + e^{-ipx} \mathbf{a}_-(\mathbf{p}) \\ -e^{ipx} \mathbf{b}_+^\dagger(\mathbf{p}) - (1-\epsilon)e^{-ipx} \mathbf{a}_+(\mathbf{p}) \\ -e^{ipx} \mathbf{b}_-^\dagger(\mathbf{p}) + (1-\epsilon)e^{-ipx} \mathbf{a}_-(\mathbf{p}) \end{pmatrix} \\ &= \gamma^0 \psi(x). \end{aligned} \quad (411)$$

So a parity transformation of a wave function multiplies the wave function by  $\gamma^0$ , and changes the sign of the three-vector position and momentum which also changes the sign on the antiparticle creation operators.

Operating with parity on a state of definite chirality is equivalent to flipping the chirality of the state and using the reflected coordinates. For example, the parity conjugate  $\psi_L(x')$  of a left-handed state  $\psi_L(x) = P_L\psi(x)$  is

$$\begin{aligned}\psi_L(x') &= \gamma^0\psi_L(x) = \gamma^0P_L\psi(x) = \\ &= \int \frac{d^3p}{(2\pi)^{\frac{3}{2}}} \sqrt{\frac{E+m}{2E}} \begin{pmatrix} 0 \\ -e^{ipx}\mathbf{b}_-^\dagger(\mathbf{p}) + e^{-ipx}\mathbf{a}_-(\mathbf{p}) \\ 0 \\ -e^{ipx}\mathbf{b}_-^\dagger(\mathbf{p}) + e^{-ipx}\mathbf{a}_-(\mathbf{p}) \end{pmatrix},\end{aligned}\quad (412)$$

where we have used the result of equation (407). This parity conjugate wave function is identical to the one found in equation (408):

$$\begin{aligned}\psi_R(x') = P_R\psi(x') &= \int \frac{d^3p}{(2\pi)^{\frac{3}{2}}} \sqrt{\frac{E+m}{2E}} \begin{pmatrix} 0 \\ e^{ipx}\mathbf{b}_-^\dagger(-\mathbf{p}) + e^{-ipx}\mathbf{a}_-(-\mathbf{p}) \\ 0 \\ e^{ipx}\mathbf{b}_-^\dagger(-\mathbf{p}) + e^{-ipx}\mathbf{a}_-(-\mathbf{p}) \end{pmatrix} \\ &= \int \frac{d^3p}{(2\pi)^{\frac{3}{2}}} \sqrt{\frac{E+m}{2E}} \begin{pmatrix} 0 \\ e^{ipx}(-\mathbf{b}_-^\dagger(\mathbf{p})) + e^{-ipx}\mathbf{a}_-(\mathbf{p}) \\ 0 \\ e^{ipx}(-\mathbf{b}_-^\dagger(\mathbf{p})) + e^{-ipx}\mathbf{a}_-(\mathbf{p}) \end{pmatrix}.\end{aligned}\quad (413)$$

Thus we may represent the parity conjugate field  $\psi_L(x')$  as  $\psi_R(x')$ .

This chirality flip due to parity may also be seen by considering the properties of the gamma matrices.  $\gamma^0$  commutes with  $\mathbb{1}$  but anticommutes with  $\gamma_5$ , so multiplying a projected state by  $\gamma^0$  changes its chirality:

$$\gamma^0 P_L\psi = P_R\gamma^0\psi, \quad (414)$$

which is a right-handed state. Because of the presence of the matrix  $\gamma^0$  in the Dirac conjugation operation, taking the Dirac conjugate of a particle swaps its chirality:

$$\overline{\psi_{L,R}} = \psi^\dagger P_{L,R}^\dagger \gamma^0 = \psi^\dagger \frac{1 \mp \gamma_5}{2} \gamma^0 = \psi^\dagger \gamma^0 \frac{1 \pm \gamma_5}{2} = \overline{\psi} P_{R,L}. \quad (415)$$

*Ergo* a left-handed outgoing particle is equivalent to a right-handed projection on an incoming particle.

### B.3.3 Parity Violation in Weak Interactions

The weak charged current involves only left-handed particles, so it is explicitly parity-violating. Consider a charged-current two-vertex lepton interaction represented by an effective Lagrangian,  $\mathcal{J}_{CC}^\mu \mathcal{J}_{CC\mu}^\dagger$ , as discussed in Section 1.2. As discussed in Section 3.3, a typical charged-current interaction can be Fierzed to produce an interaction of the form

$$\mathcal{L}_{eff}^{CC} = -\frac{G}{\sqrt{2}} \mathcal{J}_{CC}^\mu \mathcal{J}_{CC\mu}^\dagger = -\frac{G}{\sqrt{2}} [\bar{\nu}_e \gamma^\mu (1 - \gamma_5) \nu_e] [\bar{e} \gamma_\mu (1 - \gamma_5) e]. \quad (103)$$

This coupling explicitly violates parity through the presence of the left-handed projection operator  $P_L$ . If we were to not *a priori* assume the Standard Model form of the Lagrangian, we would need a more general interaction [10]

$$\mathcal{L}_{eff}^{CC} = -\frac{G}{\sqrt{2}} [\bar{\nu}_\alpha \gamma^\mu O^i (C_i - C'_i \gamma_5) \nu_\beta] [\bar{\beta} O_i \alpha], \quad (416)$$

where  $O_i$  can be any of the complete set of couplings: 1(Scalar),  $\gamma_\mu$ (Vector),  $\sigma^{\mu\nu}$ (Tensor),  $\gamma_\mu \gamma_5$ (Axial vector), or  $\gamma_5$ (Pseudoscalar). The expression  $C_i - C'_i \gamma_5$  appears only in the first factor in equation (416). Such an expression could be placed in the second factor as well, but it would not introduce any new freedom in the equation. The coefficients of the S, T, and P couplings must be zero at tree-level to preserve gauge-invariance. Deviations in the A and V couplings from common strength would be evidence of some right-handed current. Experiments measure observables, such as interaction rates and energy distributions, not effective Lagrangians. Michel and Bouchiat [67], [11] showed

that the observable results of an interaction of the form (416) depend only on four so-called *Michel parameters*:  $\rho$ ,  $\eta$ ,  $\xi$ , and  $\delta$ . These parameters are functions of the coefficients  $C_i$  and  $C'_i$ , and they are predicted to be equal to  $\frac{3}{4}$ , 0, 1, and  $\frac{3}{4}$ , respectively, for the Standard Model's completely parity-violating weak current. Experimental measurements yield values consistent with the Standard Model predictions [10]:

$$\begin{aligned}\rho &= 0.7517 \pm 0.0026, \\ \eta &= -0.12 \pm 0.21, \\ \xi &= 0.972 \pm 0.013, \text{ and} \\ \delta &= 0.7551 \pm 0.0085.\end{aligned}\tag{417}$$

Such a marked agreement makes the introduction of right-handed currents in extensions of the Standard Model quite difficult.

#### B.4 Charge Conjugation

In this paper, we will distinguish between a charge-conjugate particle  $\psi$  and an antiparticle. Dirac originally postulated the existence of antiparticles as the negative-energy solutions to the Dirac equation having the same mass and opposite charge as their associated particles. The original Dirac equation was charge-conjugation-invariant, so the term antiparticle became associated with the charge-conjugate state,<sup>2</sup>

$$\bar{\psi}_{L,R} = C \overline{\psi_{R,L}}^T, \tag{418}$$

where  $C$  is the charge-conjugation operator, discussed below. With the discovery of charged current interactions in the late 1950s, however, came the discovery that charge-conjugation and parity are not good symmetries independently. The combination of charge-conjugation with parity, CP, seemed to be a good symmetry, so the new negative-energy solution to the Dirac equation was thought to

---

<sup>2</sup> Our notation here differs from that of reference [14] since they apparently use  $\psi_L$  to represent the charge-conjugate field of the *right-handed* field, while we use it to represent the conjugate of the left-handed field.

have the form

$$(\psi_{L,R}(x'))^{\dagger} = C \overline{\gamma^0 \psi_{L,R}(x)}^T = C \overline{\psi_{R,L}(x')}^T = \psi_{R,L}(x') \quad (419)$$

until the early 1960s. With the study of kaon systems came the discovery that even CP is not conserved exactly. We now believe that CPT is a good symmetry, where the T stands for time reversal. The physical antiparticles therefore correspond to the CPT-conjugate states  $\psi^{\text{pt}}(-x)$ . Because the violation of CP is so small, and could possibly be zero in the lepton sector, we will loosely use the term antineutrino to refer to the CP-conjugate

$$\nu_R \equiv (\nu_L)^{\dagger} = C \overline{\nu_L}^T. \quad (420)$$

Having clarified the terminology, let us return to the definition of the charge-conjugate field in equation (418).  $C$  has the following properties [14]:

$$C^T = C^\dagger = C^{-1} = -C, \quad CC^\dagger = \mathbb{1}, \quad \text{and} \quad C\gamma_\mu^T C^{-1} = -\gamma_\mu. \quad (421)$$

Using Dirac's standard representation of the gamma matrices,  $C$  has the form

$$C = i\gamma^2\gamma^0. \quad (422)$$

This identification of the matrix  $C$  is, however, representation-dependent [12], so care should be used when applying it.

The charge-conjugate  $\psi_{R,L}$  of a field of definite chirality  $\psi_{R,L}$  will be composed of the opposite-chirality field but transform like the original field [65]. For example,

$$\psi_L = C \overline{\psi_R}^T \quad (423)$$

is formed from  $\psi_R$  but transforms as a left-handed field since  $C$  commutes with the projection

operators. In the standard representation,

$$P_{R,L}C = \frac{1 \pm \gamma_5}{2} i\gamma^2\gamma^0 = i\gamma^2 \frac{1 \mp \gamma_5}{2} \gamma^0 = i\gamma^2\gamma^0 \frac{1 \pm \gamma_5}{2} = CP_{R,L}, \quad (424)$$

so the charge-conjugate field  $\psi_L$  has the chirality of the Dirac-conjugate field  $\overline{\psi_R}$ . The latter field is shown to be left-handed in equation (415), so the field  $\psi_L$  transforms as a left-handed field, as claimed above.

Using the properties of  $C$  and the definition (419), we can find an expression for  $\overline{\psi_{L,R}}$

$$\begin{aligned} \overline{\psi_{L,R}} &= \overline{\psi_{L,R}^\dagger \gamma^0} = \left( C \overline{\psi_{R,L}}^T \right)^\dagger \gamma^0 = \psi_{R,L}^T \gamma^{0T\dagger} C^\dagger \gamma^0 = \psi_{R,L}^T C^\dagger C \gamma^0 C^\dagger \gamma^0 \\ &= \psi_{R,L}^T C^\dagger (-\gamma^{0T}) \gamma^0 = -\psi_{R,L}^T C^\dagger. \end{aligned} \quad (425)$$

Applied to the neutrino, we find

$$\overline{\nu_R} = -\nu_L^T C^\dagger. \quad (426)$$

## APPENDIX C

### A MORE REALISTIC TREATMENT OF NEUTRINO OSCILLATIONS

The common treatment of neutrino oscillation makes many sometimes contradictory assumptions, yet manages to arrive at an equation for the transition probability, (93), that is consistent with more realistic treatments to leading order in neutrino masses. These assumptions include (a) **the treatment of neutrinos as plane waves rather than wave packets**, (b) **all neutrino mass states have a common momentum but different energy** (energy is conserved for the interaction, but momentum conservation is ignored), (c) neutrinos are relativistic, so  $t \approx |\mathbf{x}|$ , and (d) again the neutrino is relativistic, so  $E_i - p \approx \frac{m_i^2}{2p}$ . In addition, we define the x-axis to be in the direction of the neutrino three-momentum  $\mathbf{p}_i$ , so  $\mathbf{p}_i \cdot \mathbf{x}_i = p_i x_i$ . This final relationship is merely a definition of the coordinate system, so we do not lose any information making it. Under these assumptions, the phase difference of Chapter III,

$$\Phi_{ij} = \frac{1}{2} [(E_i t_i - E_j t_j) - (\mathbf{p}_i \cdot \mathbf{x}_i - \mathbf{p}_j \cdot \mathbf{x}_j)] \quad (427)$$

becomes

$$\Phi_{ij}^{historic} = \frac{1}{2} [(E_i - p)x - (E_j - p)x] = \frac{m_i^2 - m_j^2}{4p}x. \quad (428)$$

Many authors have addressed the nature of the assumptions (a)-(d). Most notably, the plane-wave approximation (a) is addressed in references [31], [68], [69] and [70]. Reference [71] argues that a replacement of assumption (b) with (b') **all neutrino mass states have a common energy but different momentum** is far more logical for most experiments which measure the distance traveled by a neutrino, not the time taken to travel. When either  $p$  or  $E$  is common to all mass states, the wave-packet treatment yields the traditional  $\phi_{ij}^{historic}$  of equation (428), as will be shown in Section C.1.

Neither of the assumptions (b) or (b') are correct or even preferable, according to Goldman, the author of reference [32]. Goldman's work provides a relativistic treatment of oscillations, conserving both energy and momentum, and points out that (c) and (d) are inconsistent assumptions, since the

difference between  $t$  and  $x$  is, to first order, the same as the difference between  $p$  and  $E$ . Goldman allows different mass states to have both unique energies and unique momenta, but arrives at the common expression (93) to leading order in neutrino masses. We examine his work and extend it to an arbitrary number of neutrino flavors in Section C.2.

### C.1 Neutrinos as Wave-Packets

Nussinov [68] was perhaps the first to examine neutrino oscillations using wave packets rather than plane waves to describe the neutrino states. Kayser extended Nussinov's work in reference [31]. Kayser's work laid the groundwork for many more detailed treatments, such as [70] and [71]. Reference [69] provides a useful summary of the wave-packet approach. The probability for the transition  $\nu_\alpha \rightarrow \nu_\beta$  for wave packets is given by reference [70] to be

$$P_{\nu_\alpha \rightarrow \nu_\beta}(x) = A \sum_i \sum_j \alpha^i \square_{\beta j} e^{i2\Phi_{ij}^{hist} B} C e^{-D-F}. \quad (429)$$

$A$  is a normalization constant,

$$A = \left( \sum_k \frac{|V_{\alpha k}|^2}{|v_k|} \right)^{-1}, \quad (430)$$

where  $v_k$  represents the velocity of the  $k$ th mass state.

$$B = \frac{v_i + v_j}{v_i^2 + v_j^2} - \frac{\langle p_i \rangle - \langle p_j \rangle}{\langle E_i \rangle - \langle E_j \rangle} \quad (431)$$

represents the deviation of the phase from the traditional phase.  $C$  and  $F$  both result from the time-averaging performed in reference [70].

$$C = \sqrt{\frac{2}{v_i^2 + v_j^2}} \quad (432)$$

arises because the probability to find a mass state at a detector is inversely proportional to the speed of the mass state.

$$F = \frac{(\langle E_i \rangle - \langle E_j \rangle)^2}{4\sigma_p^2 (v_i^2 + v_j^2)}, \quad (433)$$

where  $\sigma_p$  is the width of the Gaussian wave packet in momentum space, insures that energy is conserved within the uncertainty of the wave packet [70]. Finally,

$$D = \frac{x^2}{4\sigma_x^2} \frac{(v_i - v_j)^2}{v_i^2 + v_j^2}, \quad (434)$$

where  $\sigma_x$  is the width of the Gaussian wave packet in coordinate space, is a damping factor which accounts for the separation of the mass states as they propagate. As they separate, the overlap decreases and the oscillatory behavior disappears. This behavior gives rise to the definition of a coherence length,

$$L_{ij}^{coh} \equiv 4\sigma_x \sqrt{\frac{v_i^2 + v_j^2}{(v_i - v_j)^2}}. \quad (435)$$

As long as the coherence length is much greater than the size of the wave packet, the different mass states will interfere, and oscillations will occur [70].

In the traditional approach,  $AC = B \approx 1$ , and  $D + F \approx 0$ .

## C.2 Neutrinos in a Relativistically Correct Light

Everything in Section 3.1 is relativistically correct, so we may start with equations (85) and (86):

$$\nu_L(t = 0, x = 0) = \nu_{\alpha L} = \sum_i V_{\alpha i} \nu_{i L}, \quad 85$$

and

$$\nu_L(t, x) = \sum_{i=1}^n V_{\alpha i} \nu_i e^{-i(E_i t_i - p_i x_i)} \equiv \sum_{i=1}^n V_{\alpha i} \nu_i e^{-i\phi_i}, \quad 86$$

The probability for transition  $P_{\nu_\alpha \rightarrow \nu_\beta}(x)$ , as shown in Section 3.2, depends on the phase difference

$$\Phi_{ij} = \frac{1}{2} [(E_i t_i - E_j t_j) - (p_i x_i - p_j x_j)]. \quad (436)$$

To find this phase in terms of the neutrino masses we must consider relativistic kinematics.

The  $p_i$  and  $E_i$  are of course related by  $E_i^2 = p_i^2 + m_i^2$ , and they depend on the other energies and momentum of the process which created the neutrino. For simplicity, we will work in the rest

frame of the parent particle. The invariant mass squared of the parent particle is  $M^2$ , and the decay products other than the neutrino will have total mass squared  $M_f^2$  and momenta summing to  $-\mathbf{p}_i$ .

For oscillations to occur, we must not be able to measure the momenta or energies of the other particles closely enough to distinguish between the different possibilities of  $p_i$ . We also must not be able to resolve  $\Delta t_{ij} \equiv t_i - t_j$  between the arrival times of the different mass states.

Energy conservation for the production of the neutrino requires that

$$M = (E_\nu + E_{other}) = \sqrt{p_i^2 + m_i^2} + \sqrt{p_i^2 + M_f^2}, \quad (437)$$

so

$$\left( M - \sqrt{p_i^2 + m_i^2} \right)^2 = M^2 - 2M\sqrt{p_i^2 + m_i^2} + p_i^2 + m_i^2 = p_i^2 + M_f^2, \quad (438)$$

and

$$E_i = \sqrt{p_i^2 + m_i^2} = \frac{M^2 - M_f^2 + m_i^2}{2M}. \quad (439)$$

We may extract  $p_i$  from this equation:

$$\begin{aligned} p_i^2 &= \frac{\left( M^2 - M_f^2 \right)^2 + 2m_i^2 \left( M^2 - M_f^2 \right) + m_i^4}{4M^2} - \frac{4M^2 m_i^2}{4M^2}, \quad \text{so} \\ p_i &= \sqrt{\frac{\left( M^2 - M_f^2 \right)^2 - 2m_i^2 M^2 - 2m_i^2 M_f^2 + m_i^4}{4M^2}} \\ &= \frac{\left( M^2 - M_f^2 \right)}{2M} \sqrt{1 - \frac{2m_i^2 \left( M^2 + M_f^2 \right)}{\left( M^2 - M_f^2 \right)^2} + \frac{m_i^4}{\left( M^2 - M_f^2 \right)^2}}. \end{aligned} \quad (440)$$

Using the Taylor expansion  $\sqrt{1+x} = 1 + \frac{x}{2} - \frac{x^2}{8} + \dots$  and keeping terms to fourth order in the neutrino mass  $m_i$ , we find

$$\begin{aligned} p_i &= \frac{\left( M^2 - M_f^2 \right)}{2M} \left[ 1 - \frac{1}{2} \frac{2m_i^2 \left( M^2 + M_f^2 \right) + m_i^4}{\left( M^2 - M_f^2 \right)^2} - \frac{m_i^4}{8} \frac{4 \left( M^2 + M_f^2 \right)^2}{\left( M^2 - M_f^2 \right)^4} + \mathcal{O}(m_i^6) \right] \\ &= \frac{\left( M^2 - M_f^2 \right)}{2M} \left[ 1 - \frac{m_i^2 \left( M^2 + M_f^2 \right)}{\left( M^2 - M_f^2 \right)^2} + \frac{m_i^4}{2} \frac{\left( M^2 - M_f^2 \right)^2 - \left( M^2 + M_f^2 \right)^2}{\left( M^2 - M_f^2 \right)^4} + \mathcal{O}(m_i^6) \right] \end{aligned}$$

$$= \frac{(M^2 - M_f^2)}{2M} \left[ 1 - m_i^2 \frac{(M^2 + M_f^2)}{(M^2 - M_f^2)^2} - m_i^4 \frac{2M^2 M_f^2}{(M^2 - M_f^2)^4} + \mathcal{O}(m_i^6) \right] \quad (441)$$

We will later want the differences between two energies and between two momenta:

$$E_i - E_j = \frac{M^2 - M_f^2 + m_i^2}{2M} - \frac{M^2 - M_f^2 + m_j^2}{2M} = \frac{m_i^2 - m_j^2}{2M}, \text{ and} \quad (442)$$

$$\begin{aligned} p_i - p_j &= \frac{(M^2 - M_f^2)}{2M} \left[ 1 - \frac{m_i^2 (M^2 + M_f^2)}{(M^2 - M_f^2)^2} - \frac{m_i^4}{2} \frac{4M^2 M_f^2}{(M^2 - M_f^2)^4} \right. \\ &\quad \left. - 1 + \frac{m_j^2 (M^2 + M_f^2)}{(M^2 - M_f^2)^2} + \frac{m_j^4}{2} \frac{4M^2 M_f^2}{(M^2 - M_f^2)^4} \right] \quad (443) \\ &= \frac{(M^2 - M_f^2)}{2M} \left[ - (m_i^2 - m_j^2) \frac{M^2 + M_f^2}{(M^2 - M_f^2)^2} - (m_i^2 - m_j^2) (m_i^2 + m_j^2) \frac{2M^2 M_f^2}{(M^2 - M_f^2)^4} \right]. \end{aligned}$$

$\Phi_{ij}$  does not, however, depend only on  $E$  and  $p$ ; it also depends on  $x$  and  $t$ , and deciding what values to use for these variables is rather tricky. As pointed out in reference [71], experiments measure the distance  $x$  between the neutrino source and the detector, so all mass states must have traveled the same distance  $x = x_i = x_j$ . One could then find the individual times from the relativistic relation  $t_i = \frac{E_i}{p_i}x$  and arrive at the phase

$$\hat{\Phi}_{ij} = \frac{1}{2} \left[ \left( E_i \frac{E_i}{p_i} - p_i \right) - \left( E_j \frac{E_j}{p_j} - p_j \right) \right] x = \left[ \frac{m_i^2}{p_i} - \frac{m_j^2}{2p_j} \right] x. \quad (444)$$

To leading order in mass-squared, this phase is twice the phase obtained by the traditional approach:

$$\hat{\Phi}_{ij} \approx \frac{m_i^2 - m_j^2}{2p_{ave}} = 2\Phi_{ij}^{historic}, \quad (445)$$

Goldman reproduces the historic phase to leading order in reference [32] by using the average time of travel,

$$\begin{aligned} t_{ave} &= \frac{1}{2} \left( \frac{E_i}{p_i} - \frac{E_j}{p_j} \right) x = \frac{1}{2} \left[ \sqrt{1 + \frac{m_i^2}{p_i^2}} + \sqrt{1 + \frac{m_j^2}{p_j^2}} \right] x \\ &= \frac{1}{2} \left[ 2 + \frac{m_i^2}{2p_i^2} + \frac{m_j^2}{2p_j^2} + \mathcal{O}(m_i^4) \right] x \end{aligned}$$

$$= \left[ 1 + \frac{m_i^2}{4} \frac{4M^2}{(M^2 - M_f^2)^2} + \frac{m_j^2}{4} \frac{4M^2}{(M^2 - M_f^2)^2} + \mathcal{O}(m_i^4) \right] x, \quad (446)$$

for all mass states rather than the individual travel times  $t_i$ . This choice may be justified on the grounds of uncertainty since we cannot resolve between the different travel times if oscillations are to occur. A combined treatment of wave packets and correct relativistic kinematics would of course illustrate the correct phase, but that is a topic for a different paper. In this paper, Gentle Reader, we will stick with Goldman's  $t_{ave}$ .

Now we may calculate  $\Phi_{ij}$  using equations (442), (443), and (446):

$$\begin{aligned} \Phi_{ij} &= \frac{1}{2} [(E_i - E_j) t_{ave} - (p_i - p_j) x] = \frac{1}{2} \left[ (E_i - E_j) \left( 1 + \frac{(m_i^2 + m_j^2) M^2}{(M^2 - M_f^2)^2} \right) - (p_i - p_j) \right] x \\ &= \frac{m_i^2 - m_j^2}{4M} \left[ 1 + \frac{M^2 + M_f^2}{M^2 - M_f^2} + \frac{(m_i^2 + m_j^2) M^2}{(M^2 - M_f^2)^2} + \frac{2M^2 M_f^2 (m_i^2 + m_j^2)}{(M^2 - M_f^2)^3} \right] x \\ &= \frac{m_i^2 - m_j^2}{4M} \left[ \frac{2M^2}{M^2 - M_f^2} + \frac{m_i^2 + m_j^2}{(M^2 - M_f^2)^3} [M^2 (M^2 - M_f^2) + 2M^2 M_f^2] \right] x \\ &= \frac{m_i^2 - m_j^2}{4} \left[ \frac{2M}{M^2 - M_f^2} + \frac{(m_i^2 + m_j^2) M (M^2 + M_f^2)}{(M^2 - M_f^2)^3} \right] x \end{aligned} \quad (447)$$

The first term in the brackets,  $\frac{2M}{M^2 - M_f^2}$  is just the reciprocal of the leading term in all  $p_i$ , so we recover

$$\Phi_{ij} \approx \frac{m_i^2 - m_j^2}{4p} x = \Phi_{ij}^{historic} \quad (448)$$

for small  $m_i$ , as promised above.

## APPENDIX D

### NEUTRINOLESS DOUBLE-BETA DECAY

We demonstrated in Section 4.1 that oscillation experiments will not distinguish Majorana neutrinos from Dirac neutrinos. One experiment which can distinguish between the two types is neutrinoless double-beta decay. As mentioned in the Introduction, neutrinos were first discovered by their role in beta decay:

$$n \rightarrow p + e + \bar{\nu}_e. \quad (449)$$

Double-beta decay is a higher-order process and therefore occurs less often than single beta decay. Figure 12a illustrates a typical double-beta decay interaction. This process is identical to one with only one of the  $\bar{\nu}_e$  going out, and the other outgoing  $\bar{\nu}_e$  being replaced by an incoming  $\nu_e$ , as shown in Figure 12b. If neutrinos are Dirac particles, no transition between  $\bar{\nu}_e$  and  $\nu_e$  may occur, so two distinct neutrinos must participate in double-beta decay. But if neutrinos are Majorana particles,  $\bar{\nu}_e$  and  $\nu_e$  are two spin states of the same particle, so the  $\bar{\nu}_e$  emitted by the top neutron could flip into a  $\nu_e$  and be absorbed by the bottom neutron. This possibility is illustrated in Figure 13.

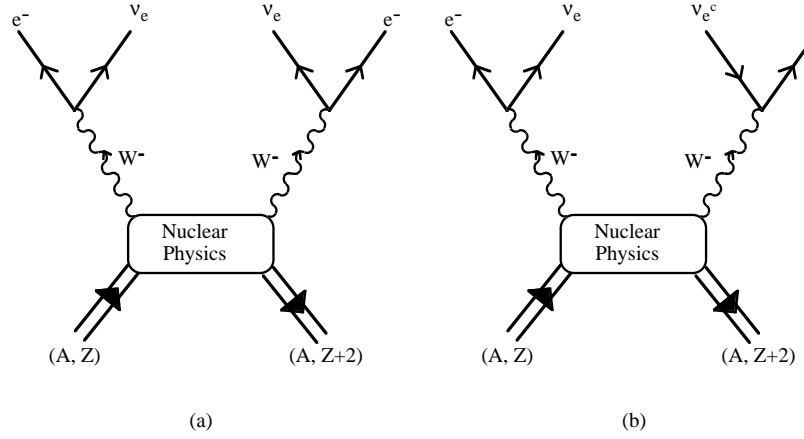


**Figure 12:** A typical double-beta decay process. (a) and (b) are equivalent diagrams by the Feynman rules of particle-antiparticle exchange.

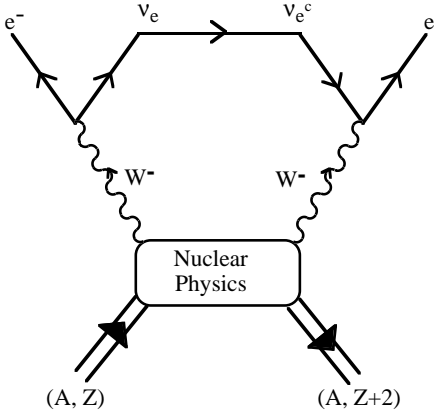


**Figure 13:** Neutrinoless double-beta decay. The outgoing antineutrino flips helicity states to become a neutrino, and is absorbed.

Neutrinoless double beta decay is overwhelmed by single beta decay when the latter is possible, so searches for the neutrinoless decay use nuclei in which the regular beta decay channel is energetically forbidden [10]. The probability that a Majorana neutrino will flip helicity states so it can be absorbed in the neutrinoless process goes as  $(\frac{m}{E})^2$ , which suppresses the neutrinoless channel with respect to the two-neutrino channel. But the neutrinoless process contains only two final-state leptons rather than the four involved in the two-neutrino process, so the neutrinoless channel gets relatively enhanced due to the extra phase-space available. If the neutrino mass is on the order of a few eV, these two effects cancel each other [10].

Other explanations for neutrinoless double-beta decay exist, but those decays caused by neutrino mixing would have a unique final state. If the neutrinoless decay were caused by the exchange of supersymmetric particles with broken R-parity, the final state would contain extra particles in addition to the electrons; if it were due to the production of a Majoran by the two neutrinos, the final state would include a Majoran which would share energy with the electrons [72]. Only the neutrino mixing solution would produce two electrons with equal but opposite momenta in the rest frame of the decay.

The calculation of neutrino masses from neutrinoless double-beta decay involves nuclear matrix elements and is outside the focus of this work. The interested reader may turn to references [10],

[12], and [13] for a more detailed study of neutrinoless double-beta decay.

## APPENDIX E

### A GRAPHICAL REPRESENTATION OF BOXES

Many of the relationships between boxes developed in Chapter IV were originally derived using a graphical representation. In this method, boxes in the numerator of a product are represented by two vertical lines; boxes in the denominator are represented by two horizontal lines. Lines exit the locations of the matrix elements which are not complex conjugated and enter the locations of the complex-conjugated matrix elements. For example, the box  ${}^{11}\square_{22} = V_{11}V_{12}^*V_{22}V_{21}^*$  is represented by a vertical line pointing from  $V_{11}$  to  $V_{21}$  and a vertical line pointing from  $V_{22}$  to  $V_{12}$ , as shown in Figure 14a. The inverse box  $\frac{1}{{}^{11}\square_{22}} = ({}^{11}\square_{22})^{-1}$  is represented by a horizontal line pointing from  $V_{11}$  to  $V_{12}$  and one pointing from  $V_{22}$  to  $V_{21}$ , as shown in Figure 14b. The complex-conjugated box  ${}^{11}\square_{22}^*$  is equal to  ${}^{12}\square_{21}$ , so one just reverses the arrows to complex conjugate a box, as shown in Figure 14c.

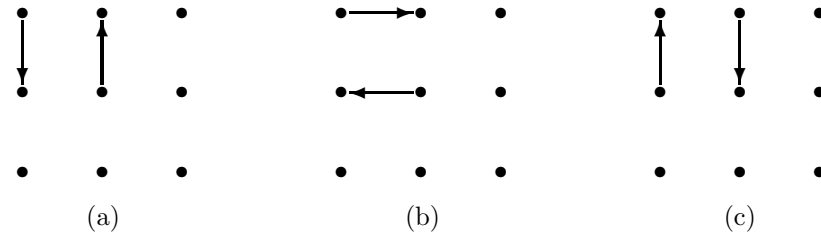


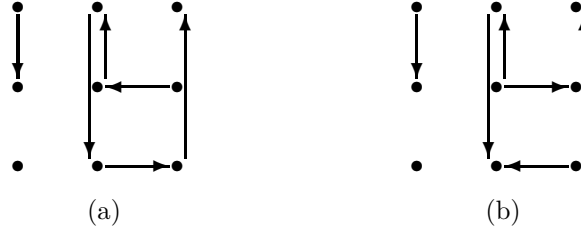
**Figure 14:** The graphical representation for (a)  ${}^{11}\square_{22}$ , (b)  $({}^{11}\square_{22})^{-1}$ , and (c)  ${}^{11}\square_{22}^*$ .

To multiply boxes together graphically, one merely draws the lines corresponding to each factor on the same grid. Horizontal arrows entering or leaving a point cancel out vertical arrows entering or leaving, respectively, that point. Uncanceled arrows entering a point signify the survival of the complex-conjugated matrix element associated with that point. Those leaving a point signify the survival of the ordinary matrix element of that point. Figure 15a represents the product  ${}^{11}\square_{22} {}^{12}\square_{33} ({}^{23}\square_{32})^{-1}$ . The horizontal arrows do not cancel vertical arrows at any point, so no simplification may occur. The upward arrow at  $V_{22}$  represents that element in the numerator. The horizontal arrow represents the element  $V_{22}^*$  in the denominator, which does not cancel. Counting

off the arrows at each vertex, we find the expression

$${}^{11}\square_{22} {}^{12}\square_{33} ({}^{23}\square_{32})^{-1} = \frac{V_{11}V_{12}V_{12}^*V_{13}^*V_{21}^*V_{22}V_{32}^*V_{33}}{V_{22}^*V_{23}V_{32}V_{33}^*}, \quad (450)$$

which agrees with the definitions of boxes.



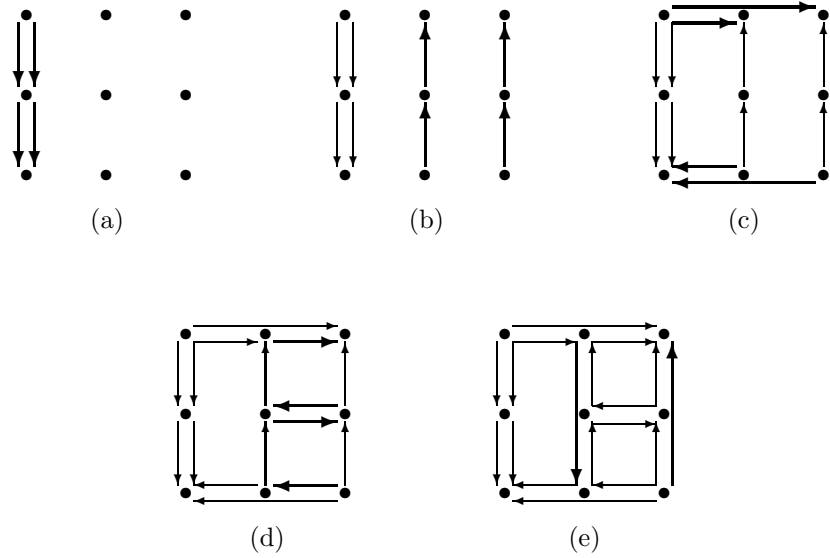
**Figure 15:** The graphical representation for the products a)  ${}^{11}\square_{22} {}^{12}\square_{33} ({}^{23}\square_{32})^{-1}$ , and b)  ${}^{11}\square_{22} {}^{12}\square_{33} ({}^{22}\square_{33})^{-1}$ .

Figure 15b represents  ${}^{11}\square_{22} {}^{12}\square_{33} ({}^{22}\square_{33})^{-1}$ , a product in which some canceling does occur.

Picking out the uncanceled arrows at each vertex, we are left with

$${}^{11}\square_{22} {}^{12}\square_{33} ({}^{22}\square_{33})^{-1} = \frac{V_{11}V_{12}V_{12}^*V_{13}^*V_{21}^*}{V_{23}^*}. \quad (451)$$

The graphical method is a powerful tool for finding relationships between boxes. Consider the degenerate boxes  ${}^{\alpha i}\square_{\alpha i} = |V_{\alpha i}|^4$ . Trying to obtain the equations (143) and (144) presented in Chapter IV without graphs required quite a bit of running down dead ends. Using the graphical method, we need only find a series of arrows which cancel for every point except  $(\alpha, i)$  and leave two incoming and two outgoing vertical arrows at that point. Consider  $|V_{21}|^4$  as an example. We choose to draw all of the arrows involving  $V_{21}$  pointing downward, as shown in Figure 16a. These arrows must be part of boxes, so in Figure 16b we add the arrows to finish those boxes. Next we draw two horizontal boxes in Figure 16c to cancel the extra arrows in the first column of the matrix. This still leaves  $V_{22}$  and  $V_{23}$  with two sets of uncanceled arrows apiece. In Figure 16d we draw two more horizontal boxes to compensate. This adds arrows to our previously clean  $V_{12}$ ,  $V_{13}$ ,  $V_{32}$ , and  $V_{33}$ ; drawing the final vertical box in Figure 16e cancels those. Recapping what we have done, we see that step (b) completes  ${}^{11}\square_{22}$ ,  ${}^{11}\square_{23}$ ,  ${}^{21}\square_{32}$ , and  ${}^{21}\square_{33}$  in the numerator. Step (c) divides



**Figure 16:** The steps to obtaining  $|V_{21}|^4$  as a function of ordered, non-degenerate boxes. The additions in each step are designated by the thicker arrows.

by  ${}^{11}\square_{32}$  and  ${}^{11}\square_{33}$ , and step (d) divides by  ${}^{12}\square_{23}$  and  ${}^{22}\square_{33}$ . Step (e) multiplies by  ${}^{12}\square_{33}$ , leaving only the point  $V_{21}$  with uncanceled arrows. It has two vertical arrows coming in and two leaving, so our graph represents the equation

$$|V_{21}|^4 = \frac{{}^{21}\square_{32} {}^{11}\square_{22} {}^{21}\square_{33} {}^{11}\square_{23} {}^{12}\square_{33}}{{}^{11}\square_{32} {}^{11}\square_{33} {}^{22}\square_{33} {}^{12}\square_{23}} \quad (146)$$

of Chapter IV. Other examples of this representation are included in that Chapter.

## REFERENCES

- [1] Jeremy Bernstein. *The Elusive Neutrino*, Understanding the Atom series. Oak Ridge: United States Atomic Energy Commission/Division of Technical Information, 1969.
- [2] Wolfgang Pauli. Zürich, to a physicists' gathering at Tübingen, December 4, 1930, repr. in *W. Pauli, collected scientific papers Vol. 2*. Eds. R. Kronig and V. Weisskopf. 1313. New York: Interscience, 1964.
- [3] Christine Sutton. *Spaceship Neutrino*. Cambridge: Cambridge University Press, 1992.  
Abraham Pais. *Inward Bound*. New York: Oxford University Press, 1986.
- [4] Frederick Reines and Clyde L. Cowan, Jr. "Free Antineutrino Absorption Cross Section. I. Measurement of the Free Antineutrino Absorption Cross Section by Protons." *Physical Review* 113, no. 1 (1959): 273-279.
- [5] *Structure et propriétés des noyaux atomiques*, Paris: Gauthier-Villars, 1934; F. Perrin, *Comptes Rendus* 197, (1933): 1625.
- [6] Raymond Davis, Jr., Don S. Harmer, and Kenneth C. Hoffman. "Search for neutrinos from the sun." *Physical Review Letters* 20, no. 21 (1968): 1205-1209; K. Lande. In the Proceedings of *Neutrino '96* held in Helsinki, June, 1996, eds. K. Enqvist Huitu and J. Maalampi. Singapore: World Scientific, 1996.
- [7] Kamiokande: K. S. Hirata, *et. al.* "Results from one thousand days of real-time, directional solar neutrino data." *Physical Review Letters*, 65 (1990): 1297-1300; also, SuperKamiokande and Kamiokande: Kenneth K. Young, "First Results From the Super-Kamiokande Experiment." (Paper presented at the annual meeting of the American Physical Society, Washington, D.C., April, 1997). Information available from <http://www.phys.washington.edu/~young/superk/drafts/aps97.html>. Internet. Accessed May 29, 1997.  
SAGE: J. N. Abdurashitov, *et. al.* "Results from SAGE (The Russian-American Gallium solar neutrino Experiment)." *Physics Letters B* 328 (1994): 234-248;  
V.N. Gavrin. In the Proceedings of *Neutrino '96* held in Helsinki, June, 1996, Eds. K. Enqvist Huitu and J. Maalampi. Singapore: World Scientific, 1996.  
GALLEX: Hampel, *et. al.* "GALLEX solar neutrino observations: Results for GALLEX III." *Physics Letters B* 388 (1996): 384-396.
- [8] IMB: R. Becker-Szendy, *et. al.* "Electron- and muon-neutrino content of the atmospheric flux." *Physical Review D* 46 (1992): 3720-3724.  
Kamiokande: K. S. Hirata, *et. al.* "Observation of a small atmospheric  $\nu_\mu/\nu_e$  ratio in Kamiokande." *Physics Letters B* 280 (1992): 146-152; Y. Suzuki. In the Proceedings of *Neutrino '96* held in Helsinki, June, 1996, eds. K. Enqvist Huitu and J. Maalampi. Singapore: World Scientific, 1996.  
Superkamiokande: Their data is not yet published; it was found at the URL of reference [54]
- [9] C. S. Wu, E. Ambler, R. W. Hayward, D. D. Hoppes, and R. P. Hudson. "Experimental Test of Parity Conservation in Beta Decay." *Physical Review* 105 (1957): 1413-1415.
- [10] Walter Greiner and Berndt Müller. *Gauge Theory of Weak Interactions*. Theoretical Physics 5. New York: Springer-Verlag, 1986.
- [11] Otto Nachtmann. *Elementary Particle Physics: Concepts and Phenomena*, trans. A. Lagee and W. Wetzel. Texts and Monographs in Physics. New York: Springer-Verlag, 1990.
- [12] Rabindra N. Mohapatra and Palash B. Pal. *Massive Neutrinos in Physics and Astrophysics*. World Scientific Lecture Notes in Physics Vol. 41. Singapore: World Scientific, 1991.

[13] Chung Wook Kim and Aihud Pevsner. *Neutrinos in Physics and Astrophysics*. Contemporary Concepts in Physics Vol. 8. USA: Harwood Academic Publishers, 1993.

[14] S. M. Bilenky and S. T. Petcov. "Massive neutrinos and neutrino oscillations." *Reviews of Modern Physics* 59, no. 3 (1987): 671-754.

[15] Peter W. Higgs. "Spontaneous Symmetry Breakdown without Massless Bosons." *Physical Review* 145, no. 4, (1966): 1156-1163.

[16] Jeremy Bernstein. "Spontaneous symmetry breaking, gauge theories, the Higgs mechanism, and all that." *Reviews of Modern Physics* 46, no. 1 (1974): 7-48. This review article contains a synopsis of the development of the Higgs mechanism as well as a description of the mechanism itself. Higgs also references the important steps in the mechanism's development in source [15].

[17] F. Mandl and G. Shaw. *Quantum Field Theory*. Chichester: John Wiley and Sons, 1984.

[18] Claude Itzykson. *Quantum Field Theory*. New York: McGraw-Hill, 1980.

[19] Paul Langacker. "Neutrino Mass." In *Testing the Standard Model, Proceedings of the 1990 Theoretical Advanced Study Institute in Elementary Particle Physics* in Boulder, Colorado, June 3-27, 1990, eds. M. Cvetič and P. Langacker. Singapore: World Scientific, 1991.

[20] Majorana, Ettorre, *Il Nuovo Cimento* 14 (1937): 171-184. Trans. S. D. A. Sinclair of the Translations Section of the National Research Council of Canada Library (Technical Translation TT-542).

[21] Boris Kayser. *The Physics of Massive Neutrinos*. World Scientific Lecture Notes in Physics Vol. 25. Singapore: World Scientific, 1989.

[22] G. B. Gelmini and M. Roncadelli. "Left-handed neutrino mass scale and spontaneously broken lepton number." *Physics Letters B* 99 (1981): 411-415.

[23] Howard M. Georgi, Sheldon Lee Glashow, and Shmuel Nussinov. "Unconventional model of neutrino masses." *Nuclear Physics B* 193 (1981): 297-316.

[24] A. Zee. "A theory of lepton number violation and neutrino majorana masses." *Physics Letters B* 93 (1980): 389-393.

[25] Lincoln Wolfenstein. "A theoretical pattern for neutrino oscillations." *Nuclear Physics B* 175 (1980): 93-96.

[26] Alexei Yu. Smirnov and Zhijian Tao. "Neutrinos with ZeeMass Matrix in Vacuum and Matter." *Nuclear Physics B* 426 (1994): 415-433.  
Alexei Yu. Smirnov and Morimitsu Tanimoto. "Is Zee Model the Model of Neutrino Masses?" *Physical Review D* 55 (1997) 1665-1671.

[27] S. T. Petcov. "Remarks on the Zee model of neutrino mixing ( $\mu \rightarrow e + \gamma$ ,  $\nu_H \rightarrow \nu_L + \gamma$ , etc.)." *Physics Letters B* 115, no. 5 (1982), 401-406.

[28] A. Zee. "Charged scalar field and quantum number violations." *Physics Letters B* 161 (1985): 141-145.

[29] M. Fukugita and T. Yanagida "Physics of Neutrinos." In *Physics and Astrophysics of Neutrinos*, ed. M. Fukugita and A. Suzuki, 1-248. New York: Springer-Verlag, 1994.

[30] T. K. Kuo and James Pantaleone. "Neutrino Oscillations in Matter." *Reviews of Modern Physics* Vol 61, No. 4 (1989): pp 937-979.

[31] Boris Kayser. "On the Quantum Mechanics of Neutrino Oscillations." *Physical Review D* 24, no. 1 (1981): 110-116.

[32] T. Goldman. “Source dependence of neutrino oscillations.” Los-Alamos e-print archive number hep-ph/9604357. April, 1996.

[33] Yosef Nir. “The CKM Matrix and  $CP$  Violation.” In *Testing the Standard Model, Proceedings of the 1990 Theoretical Advanced Study Institute in Elementary Particle Physics* in Boulder, Colorado, June 3-27, 1990, eds. M. Cvetič and P. Langacker. Singapore: World Scientific, 1991.

[34] Vernon Barger and Roger Phillip. *Collider Physics*. Redwood City, CA: Addison-Wesley, 1987.

[35] C. Jarlskog. “A Basis Independent Formulation of the Connection Between Quark Mass Matrices,  $CP$  Violation and Experiment.” *Zeitschrift für Physik C - Particles and Fields* 29 (1985): 491-497; C. Jarlskog. “Matrix representation of symmetries in flavor space, invariant functions of mass matrices, and applications.” *Physical Review* 35, no. 5 (1987): 1685-1692.

[36] Dan-di Wu, “Rephasing invariants and  $CP$  violation.” *Physical Review Letters* 33, no. 3 (1986): 860-863.

[37] James D. Bjorken and Isard Dunietz. “Rephasing-invariant parametrizations of generalized Kobayashi-Maskawa matrices.” *Physical Review D* 37, no. 7 (1987): 2109-2118.

[38] Dongsheng Du, Isard Dunietz, and Dan-di Wu. “Systematic study of large  $CP$  violations in decays of neutral  $b$ -flavored mesons.” *Physical Review D* 34, no. 11 (1986): 3414-3427.

[39] Alexander Kusenko and Robert Shrock. “General determination of phases in quark mass matrices.” *Physical Review D* 50, no. 1 (1994): R30-R33; Alexander Kusenko and Robert Shrock. “General determination of phases in leptonic mass matrices.” *Physics Letters B* 323 (1994): 18-24.

[40] Sato, “ $CP$  and T violation test in neutrino oscillation,” Los-Alamos e-print archive number hep-ph/9701306. January, 1997.

[41] Richard F. Arenstorf, Professor of Mathematics, Vanderbilt University. Private communication.

[42] Lincoln Wolfenstein. “Parametrization of the Kobayashi-Maskawa Matrix.” *Physical Review Letters* 51, no. 21 (1983): 1945-1947.

[43] G. L. Fogli, E. Lisi, and G. Scioscia, “ $\overline{\nu}_\mu \leftrightarrow \overline{\nu}_e$  mixing: a analysis of recent indications and implications for neutrino oscillation phenomenology.” Los-Alamos e-print archive number hep-ph/9702298. February, 1997.

[44] Cardall and Fuller. “Can a ‘natural’ three-generation neutrino mixing scheme satisfy everything?” *Physical Review D* 53 (1996): 4424-4429.

[45] Harald Fritzsch. “Quark masses and flavor mixing.” *Nuclear Physics B* 155 (1979): 189-207.

[46] Kaus and Meshkov. “A BCS quark mass matrix.” *Modern Physics Letters A* 3 (1988): 1251-1258. Erratum *ibid*, A 4 (1989): 603-604.

[47] Weiler & Wagner. “A ‘Nu’ Window to Cosmology.” In preparation.

[48] Athanassopoulos, *et. al.* “Evidence for  $\overline{\nu}_\mu \rightarrow \overline{\nu}_e$  Oscillations from the LSND Experiment at LAMPF.” *Physical Review Letters* 77 (1996): 3082-3085.  
Athanassopoulos, *et. al.* “Evidence for Neutrino Oscillations from Muon Decay at Rest.” *Physical Review* 54 (1996): 2685-2708.  
Ian Stancu. “Results from the LSND Experiment at LAMPF.” (Talk given at the Frontiers in Contemporary Physics Conference, Nashville, TN, May 11-16, 1997.)

[49] John N. Bahcall. “Solar Neutrinos. I. Theoretical.” *Physical Review Letters* 12, no. 11 (1964): 300-302; John N. Bahcall and M. H. Pinsonneault; “Solar models with helium and heavy-element diffusion.” *Reviews of Modern Physics* 67 (1995): 781-808; see also reference [50].

[50] John N. Bahcall. *Neutrino Astrophysics*. New York: Cambridge University Press, 1989.

[51] Andy Acker and Sandip Pakvasa. “Three Neutrino Flavors are Enough.” Los-Alamos e-print archive number hep-ph/9611423. November, 1996.

[52] John G. Learned, Sandip Pakvasa, and Thomas J. Weiler. “Neutrino Mass and Mixing Implied by Underground Deficit of Low Energy Moun-Neutrino Events.” *Physics Letters B* 207, no. 1 (1988): 79-85.

[53] W. Frati, T. K. Gaisser, A. K. Mann, and Todor Stanev. “Atmospheric Neutrino Data and Neutrino Oscillations.” *Physical Review B* 48 (1993): 1140-1149; Giles Barr, T. K. Gaisser, and Todor Stanev. “Flux of Atmospheric Neutrinos.” *Physical Review D* 39 (1989): 3532-3534.

[54] Many of these numbers came from the “Ultimate Neutrino Page,” compiled by Juha Peltoniemi and found at <http://neutrino.pc.helsinki.fi/juha/neutrino.html>. Internet. Accessed May 29, 1997.  
 Original references for the solar neutrino data are listed above in references [6] (Homestake) and [7] (the others).  
 The references for atmospheric neutrino experiments are listed in reference [8].  
 Accelerator data are cited in reference [48] above (LSND experiment) and in reference [55] (the others) below.

[55] KARMEN: Klaus Eitel. “Results from the Karmen  $\nu$ -Oscillation Search.” In the Proceedings of the *8th Rencontres de Blois: Neutrinos, Dark Matter, and the Universe*, June 8-12, 1996. Currently available at [http://www-ik1.fzk.de/www/karmen/publist\\_e.html](http://www-ik1.fzk.de/www/karmen/publist_e.html). Internet. Accessed May 29, 1997.  
CHORUS: Paolo Strolin. “CHORUS Status Report.” (Talk given at SPSLC-1997.) Slides available at <http://choruswww.cern.ch/Publications/spslc97.sheets/index.html>. Internet. Accessed May 29, 1997. David Saltzberg. “Status of the Search for  $\nu_\mu \rightarrow \nu_\tau$  Oscillations with the CHORUS Detector.” (Talk given at the *7th International Workshop on Neutrino Telescopes* in Venice, Italy from February 27-March 1, 1996.) Los Alamos e-print archive number hep-ex/9606004.; Jong, *et. al.* “A New Search for  $\nu_\mu - \nu_\tau$  Oscillation.” CERN preprint PPE/93-131 (1993). A scanned version may be found at [http://cedb1.kek.jp/cgi-bin/img\\_index?9310052](http://cedb1.kek.jp/cgi-bin/img_index?9310052). Internet. Accessed May 29, 1997.  
CHARM II Vilain, *et. al.* “Search for muon to electron neutrino oscillations.” *Z. Phys. C* 64 (1994) 539-544.

[56] Takaaki Kajita. “Observation of Atmospheric Neutrinos.” In *Physics and Astrophysics of Neutrinos*, ed. M. Fukugita and A. Suzuki, 559-605. New York: Springer-Verlag, 1994.

[57] G. L. Fogli, E. Lisi, D. Montanino, and G. Scioscia. “Three-flavor atmospheric neutrino anomaly.” *Physical Review D* 55 (1997): 4385-4404; G. L. Fogli and E. Lisi. “Tests of three-flavor mixing in long-baseline neutrino oscillation experiments.” *Physical Review D* 54 (1996): 3667-3670; G. L. Fogli and E. Lisi. “Matter-Enhanced Three-Flavor Oscillations and the Solar Neutrino Problem.” *Physical Review D* 54 (1996): 3667-3670; see also reference [43].

[58] Christian Y. Cardall and George M. Fuller. “Three-generation neutrino mixing and LSND dark matter neutrinos.” *Nuclear Physics Proceedings Supplement* 51 B (1996): 259-263; see also reference [44].

[59] Edward W. Kolb and Michael S. Turner. *The Early Universe*. Redwood City, CA: Addison-Wesley, 1990.

[60] A. De Rujula, S. C. Glashow, R. R. Wilson and G. Charpak. “Neutrino exploration of the Earth.” *Physics Reports* 99 (1983): 341.

[61] Francis Halzen. “Neutrino Astrophysics.” (Talk given at the Frontiers in Contemporary Physics Conference, Nashville, TN, May 11-16, 1997.)

- [62] See the SuperKamiokande reference in [7] above.
- [63] Walter Greiner. *Relativistic Quantum Mechanics: Wave Equations*. Theoretical Physics 5. New York: Springer-Verlag, 1990.
- [64] Steven Weinberg. *The Quantum Theory of Fields I: Foundations*. New York: Cambridge University Press, 1995.  
James D. Bjorken and Sidney D. Drell. *Relativistic Quantum Mechanics*. New York: McGraw-Hill, 1964.  
Peskin and Schroeder. *An Introduction to Quantum Field Theory*. Reading, MA: Addison-Wesley, 1989.
- [65] Pierre Ramond. *Field Theory: A Modern Primer*. Frontiers in Physics Lecture Note Series 51. Reading, MA: Benjamin/Cummings Advanced Book Program, 1981.
- [66] William Rolnick. *The Fundamental Particles and Their Interactions*. New York: Addison-Wesley, 1994.
- [67] Claude Bouchiat and Louis Michel. “Theory of  $\mu$ -Meson Decay with the Hypothesis of Nonconservation of Parity.” *Physical Review* 106 (1957): 170-172.
- [68] S. Nussinov. “Solar neutrinos and neutrino mixing.” *Physics Letters* 63 B, no. 2 (1976): 201-203.
- [69] C. W. Kim. “Neutrino Physics: Fundamentals of Neutrino Oscillations.” (Lectures given at KOSEF-JSPS Winter School on Recent Developments in Particle and Nuclear Theory, Seoul, February 21-28, 1996.) Los Alamos e-print archive number hep-ph/9607391. July, 1996.
- [70] C. Giunti, C. W. Kim, and U. W. Lee. “When do neutrinos really oscillate? Quantum mechanics of neutrino oscillations.” *Physical Review D* 44 (1991): 3635-3639.
- [71] Yuval Grossman and Harry Lipkin. “Flavor Oscillations from a Spatially Localized Source: A Simple General Treatment.” *Physical Review D* 55 (1997) 2760-2767.
- [72] Hiroyasu Ejiri. “Double Beta Decays and Neutrinos.” In *Physics and Astrophysics of Neutrinos*, ed. M. Fukugita and A. Suzuki, 500-519. New York: Springer-Verlag, 1994.